ADVANCED MATERIALS TECHNOLOGIES
www.advmattechnol.de

Green Materials and Technologies for Sustainable Organic Transistors

Fabrizio Torricelli, Ivano Alessandri,* Eleonora Macchia, Irene Vassalini, Marina Maddaloni, and Luisa Torsi**

Intelligent objects, autonomous factories and humans browsing the real world with artificial technology-based capabilities is not the movie set of a new saga but what is going to happen with next-generation electronics and bioelectronics fabricated with emerging materials, technologies, and devices. The emergence of (bio)electronics as a ubiquitous feature of an advanced modern society is posing the challenge of managing an ever-increasing amount of e-waste, also making the recovery more and more difficult. Thus, new design approaches are required considering that a possibly small but significant fraction of mass-scale e-products is inherently impossible to recover. In this perspective, organic materials and technologies can provide important solutions. This review presents and analyses green materials and technologies underpinning the development of sustainable organic transistors, which promise to become key components for Earth-safe widespread electronics and bioelectronics.

1. Introduction

Over the past 60 years, silicon and lately emerging technologies have dramatically pushed the global digitalization economy. The grow rate of technologies, devices and applications has been impressive. New materials, fabrication processes, and hybrid integration approaches were fused with the information technologies. Electronics is permeating our life, significantly augmenting the objects' functionality or even creating new smart objects. Moreover, new-generations flexible, stretchable, and conformable materials and technologies, are further pushing up the demand of wearable, large-area and "invisible" electronics directly integrated in any object or even in the human body.

Along this direction, organic materials and technologies are playing a crucial role, enabling the large-area processing with low-cost industrial techniques, chemically-tunable material properties, mechanical flexibility, softness, and biological compatibility.[1–7] A very wide range of new functional materials, unconventional fabrication processes and device architectures is now available, addressing the needs of a broad palette of application fields, including displays,[8–11] photovoltaics,[12–14] photodetectors,[15,16] physical,[17–19] chemical,[20] and biological sensors,[21,22] analogue and digital electronics,[23–26] robotics,[26] energy harvesters,[27] soft actuators,[28,29] synaptic and neuromorphic computing,[30–33] medical and implantable devices,[34,35] and neural interfaces,[36–39] to name a few. Most of these applications rely on organic transistors. Remarkably, organic transistors combine the signal amplification – typical of transistor architectures – with more specific features tailored for the target application. By the way of example, high-frequency organic transistors can be integrated in ultra-low-cost radio frequency identification tag (RF-ID) tags,[40] smart labels and multi-functional circuits,[41] piezoelectric organic transistors on ultra-flexible surfaces can provide neurorobotics and neuroprosthetic interfaces,[42] synaptic transistors can yield neuromorphic computing,[30] and bioelectronic organic transistors can monitor in-situ cell biology[43] or, when properly endowed with receptors, detect biomarkers with high-sensitivity in point-of-care early diagnostic settings.[44]

The wide range of functionalities offered by organic transistor technologies, often combined with hybrid silicon-organic approaches, are finding increasing exploitation in the present markets and are expected to open even more and new opportunities in the near future, especially considering the fields of medical diagnostics, healthcare, and implantable devices. As a matter of fact, a new era is already on the road. Smart objects are going to become intelligent, factories are going to be autonomous, and humans are going to browse the real world with new artificial technology-based capabilities.[45] Along this direction, implantable brain-computer interface technologies are

F. Torricelli, I. Vassalini, I. Alessandri
Department of Information Engineering
University of Brescia
Brescia 25123, Italy
E-mail: fabrizio.torricelli@unibs.it; ivano.alessandri@unibs.it
E. Macchia
Faculty of Science and Engineering
Åbo Akademi University
Turku 20500, Finland
M. Maddaloni
Department of Mechanical and Industrial Engineering
University of Brescia
Brescia 25123, Italy
L. Torsi
Department of Chemistry
University of Bari "Aldo Moro"
Bari 70125, Italy
E-mail: luisa.torsi@uniba.it
The ORCID identification number(s) for the author(s) of this article can be found under https://doi.org/10.1002/admt.202100445.

DOI: 10.1002/admt.202100445

going to become reality, and they are expected to help the treatment of Alzheimer's, dementia, and spinal cord injuries, giving patients the opportunity to regain their motor sensitivity and capability. A "vision change" is thus going to take place, where the sustainability of our technology-based society becomes part of our developing model. This is critically urgent, considering the climate changes and the heavy environmental footprint of our lifestyle and economy model. An effective solution to such a global issue can come only by a holistic global approach with a paradigm shift of our behavior (awareness and lifestyle), of our governments (education and laws), and of the science (materials, technologies and devices).

Although, to date, organic materials and technologies mainly focused on large-area flexible and/or soft plastic substrates by processing solution-based active materials with quite toxic solvents, there is a huge potential leveraging on the current knowledge and pointing the directions of additive and/or solvent-free manufacturing techniques, for example, printing methods and depositions through shadow masks, synthesis of organic active materials soluble with benign solvents, for example, water, and requiring a low thermal budget for the fabrication, deposition and recycling. We emphasize that this is becoming imperatively more and more important for organic technologies, which target ultra-high volume mass production and hence could significantly contribute to increase the current volumes of electronic waste (e-waste). Here figures are dramatically high: it has been estimated that up to 50 million ton of consumer electronic products are discarded globally every year[46] making e-waste the fastest growing component of the municipal solid waste stream. This is the situation accounting for "conventional" e-waste, substantially based on printed circuit board (PCBs) and electronic devices. Emerging technologies are expected to produce lightweight plastic-based electronics and bioelectronics for disposable applications. Hence, the emerging e-waste is expected to reduce the weight, but its recovery will be even more difficult than current e-waste. A new challenge is thus the development of organic transistor technologies that not only require less energy, less and easy-recyclable materials, as well as less and environment-friendly solvents, but also based on new circular design approaches, where the end-of-life e-product becomes a feedstock for humans and/or nature. The need of such new material and technology design directions is witnessed by plastic oceans (≈10 Mtons of plastic dumped into our oceans every year)[47] and it has been recently further highlighted by the COVID-19 pandemic. Practically, almost everyone had the chance to see masks dispersed in the environment and, considering the endless number of units fabricated and used, this is not so surprisingly. These global lessons clearly teach us that we should design new generations of materials, technologies, and devices considering that a possibly small but significant fraction of mass-scale products is inherently impossible to recover. These new approaches have to minimize the environmental impact making possible, for example, that end-of-life products can feed the Earth instead of polluting.

In this perspective, organic materials and technologies can provide important avenues. This is the background behind this article, that sets out to review green materials and technologies underpinning the development of sustainable organic transistors, key components for future wide-spread electronics and bioelectronics. In **Table 1** some definitions of key concepts related to sustainability and circularity are reported, in order to facilitate the reader.

Table 1. Glossary of some key concepts at the basis of the review.

Term	Definition
Sustainable	Sustainability: "development that meets the needs of the present without compromising the ability of future generations to meet their own needs" (United Nations General Assembly). The concept of "Sustainable" is a recent idea according to which the production of new materials should be obtained by minimizing non-renewable energy consumption, using recycled starting materials (if possible) and limiting the use of toxic and expensive reagents.
Circular approach	Model of production that contrasts with the idea of linear approach or linear economy. A circular approach has as its objective the reduction of waste with the continuous reuse of resources.
Green Chemistry	It is an area of chemistry and chemical engineering focused on the design of products and processes that minimize or eliminate the use and generation of hazardous substances. It aims also on reducing consumption of non-renewable resources and on developing technological approaches for preventing pollution.
Carbon footprint	The amount of carbon dioxide released into the atmosphere, as a result of the activities of a particular individual, organization, or community. In this review we focus on the amount of carbon dioxide released for the fabrication process and materials.
Embodied energy	Sum of all the energy required to produce any goods or services, considered as if that energy was incorporated or "embodied" in the product itself.

We note that with respect to previous reviews[48–53] covering biodegradable materials, bioresorbable materials, natural materials, and green processing for green electronics, here we specifically focus on organic transistors. The analysis presented in this review would like to address the rational design of sustainable organic transistors entirely (or almost entirely) fabricated by components obtained from green sources through green processes, which can be biodegraded, disassembled, and recycled at the end of their life and reintroduced in a circular production of added-value technological products. More in detail, in Section 2 the materials are classified and analyzed considering the essential components of organic transistors. Each class of materials comprises synthetic, natural and natural-inspired green approaches. General considerations on solvents, processing, degradation tests, and embodied energy are drawn in Section 3. Then, Section 4 introduces transistor architectures fabricated with green approaches and the corresponding figures of merits are presented. Integration strategies and fabrication technologies are discussed in Section 5. Finally, in Section 6 these advances are highlighted focusing on application examples accounting for the fields of electronics, bioelectronics, and artificial synaptic functionalities.

2. Green materials for Organic Transistors

Different types of organic transistor (OT) architectures share essentially the same components (**Figure 1**):

i. Substrates
ii. Insulators, ion-gels, and hydrogels
iii. Semiconductors
iv. Conductors

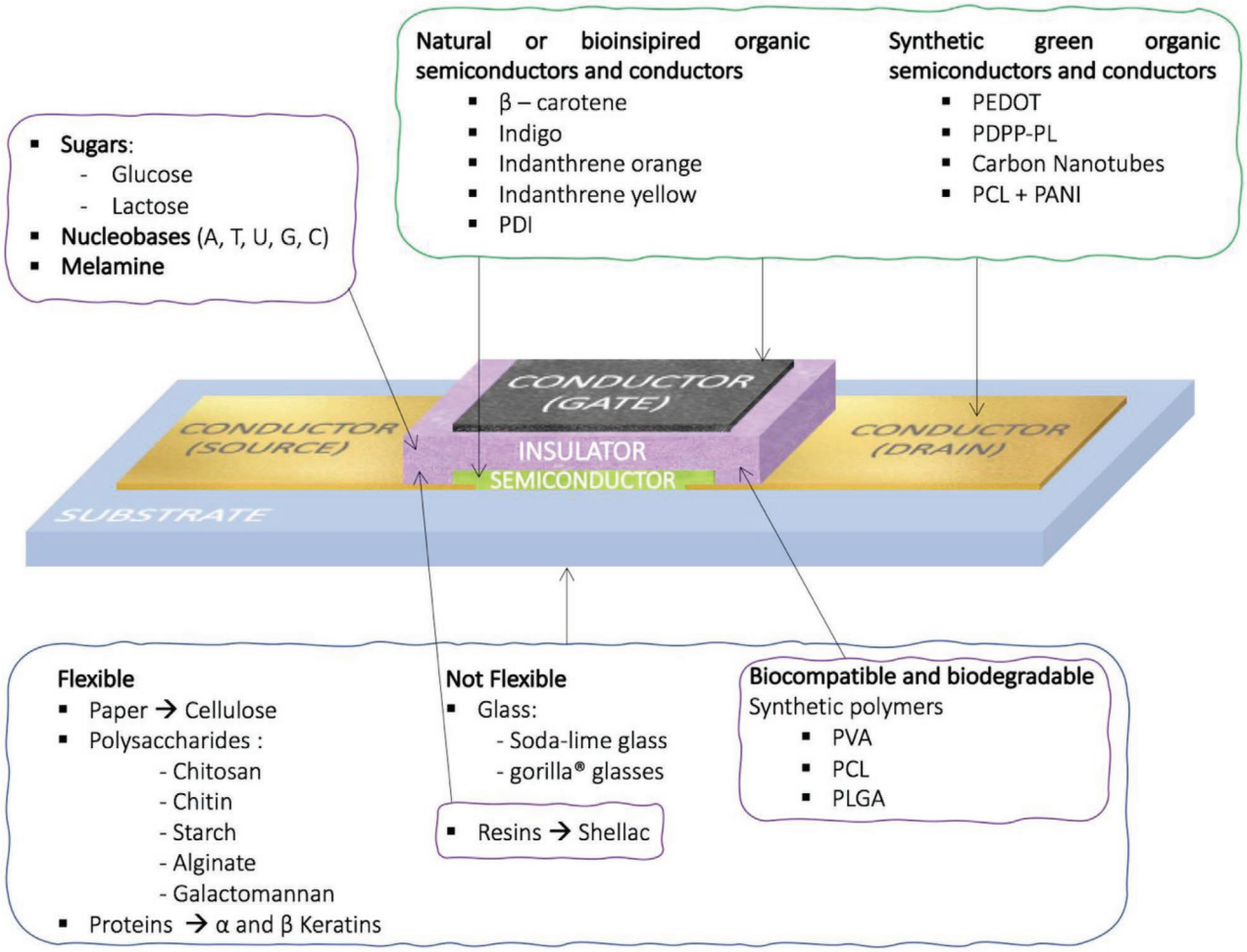

Figure 1. Scheme of the elements of a typical organic transistor and the molecular components described in this section.

In principle, each component could be designed and fabricated according to criteria inspired by green production, zero-waste impact and circular economy. However, the mutual integration of each "green" component into working devices remains a big challenge. To date, the most common configuration is represented by hybrid organic transistor (OT), which are based on the combination of "green" (e.g., the substrate) and "non-green" (e.g., the conductor electrodes) components. In this section we review the materials used in the fabrication of each component, analyzing the state of the art and discussing most of the relevant gaps that should be bridged for enabling an effective future development of green and sustainable OT technologies.

2.1. Substrates and Dielectrics

Substrate represents the most relevant component (>99.5%) in terms of amount of material utilized for OT fabrication. For this reason, the environmental impact of any OT is ultimately determined by the type of substrate. The large majority of substrates utilized so far in production of green OT is based on limited classes of materials, in particular glass and paper. However, an ever-increasing number of alternative substrates, which ensure safe biodegradability and biocompatibility, is going to be developed. In particular, biodegradable synthetic, and natural polymers are intensively investigated.[48,54,55] Most of these materials can be utilized also as dielectric layers for OT gates. Dielectrics play a key role in OT performances as they insulate the gate from the semiconductor and/or the source and drain electrodes, and control charge transport in the semiconductor channels. Ideally, they should be characterized by high permittivity and exhibit good interfacial compatibility with the semiconductor.

Here we discuss only a few examples of materials that have been or could be utilized to fabricate substrates and gate dielectrics (**Figures 2–6**), highlighting the aspects related to their environmental impact.

2.1.1. Non-Flexible Substrates: Glass

Glass is the most widely used material for OT substrates that do not require high flexibility. Common glasses are transparent amorphous solids made of a mixture of silica and other oxides, such as Na_2O and CaO, which are earth abundant. Long tradition and highly developed technology of fabrication make glass available in a rich variety of optical, mechanical, thermal and

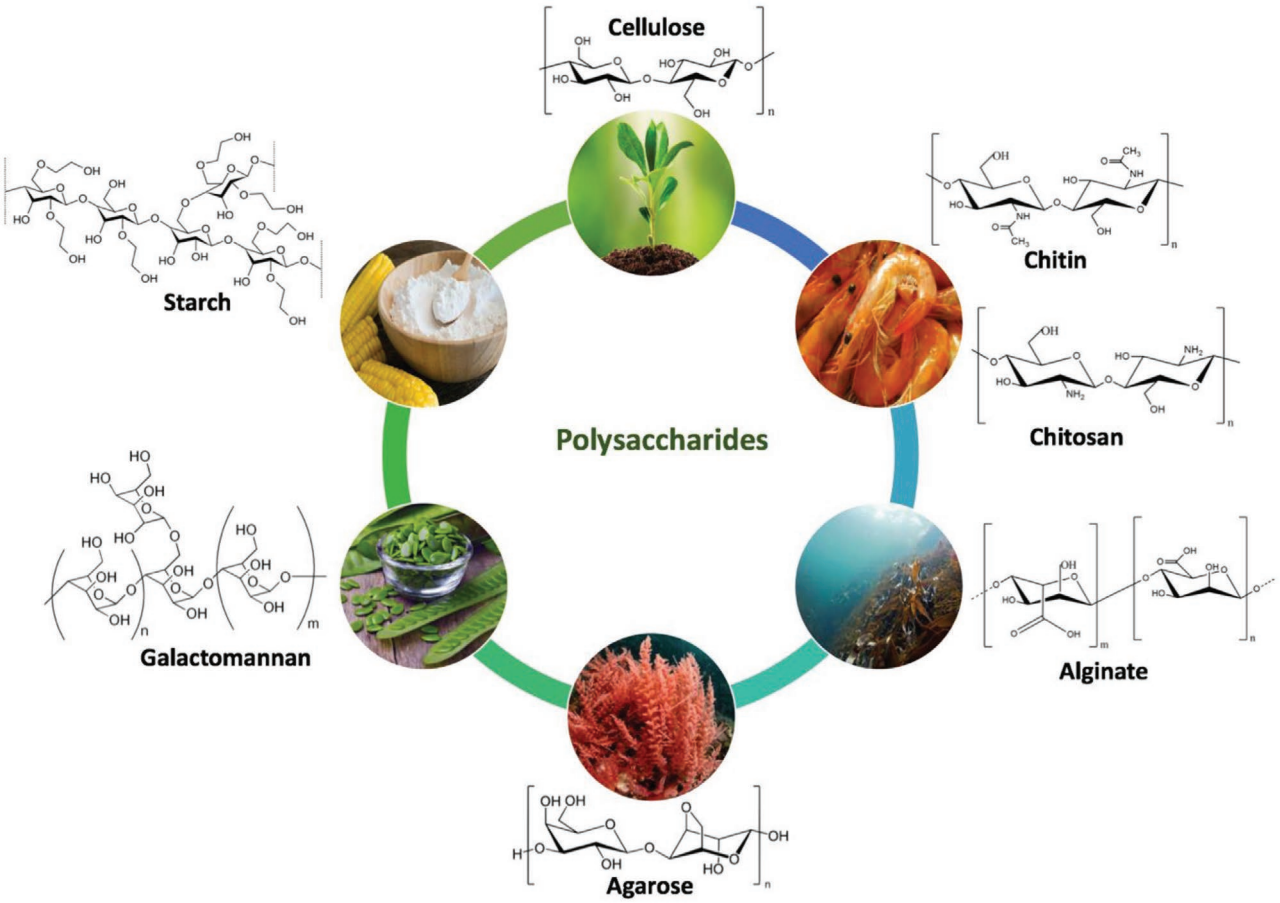

Figure 2. Schematic representation of the main polysaccharides utilized as substrates, dielectric coatings and surface modifiers.

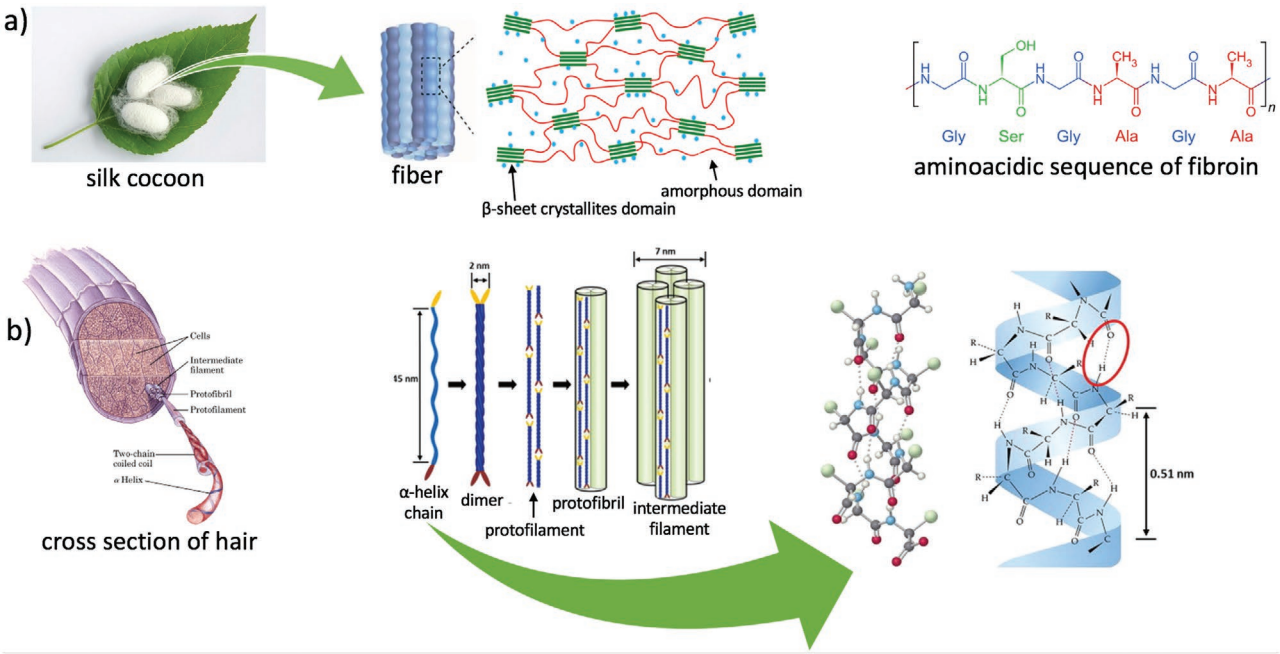

Figure 3. Schematic representation of β-Keratin proteins utilized as substrates and dielectrics: a) silk, and b) keratin.

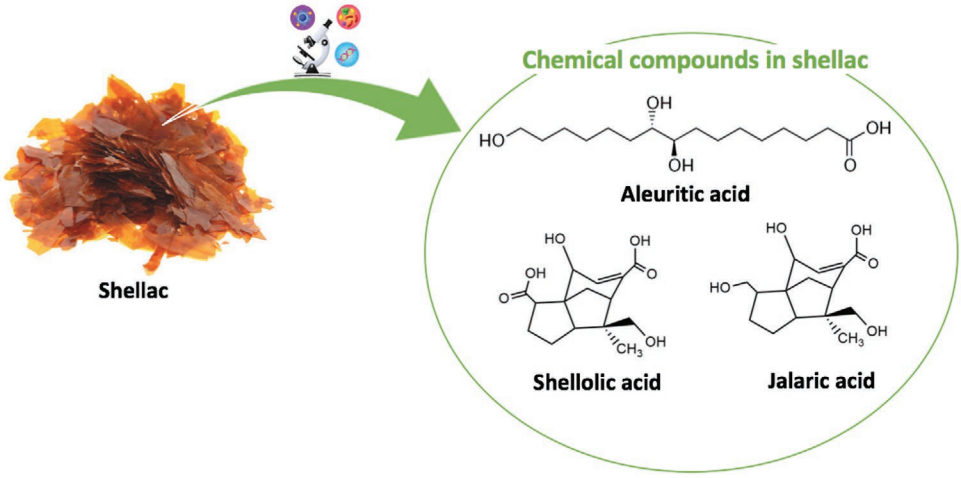

Figure 4. Main components of natural shellac.

electrical properties.[56] In general, the glass slides utilized as substrates for OT are made of soda-lime, which represents over 90% of common glass and is less expensive and more recyclable than the borosilicate counterpart. Soda-lime glasses are characterized by elastic and shear moduli of 71 and 29 GPa, respectively, with a compressive strength around 330 MPa.[57] However, the mechanical properties of glass can be easily tailored and improved if necessary. For example, "gorilla" glasses, developed by replacing sodium with potassium ions in the melting mixture and widely utilized in touchscreens, exhibit a compressive strength of 900 MPa.[58] Although not biodegradable, glass is fully recyclable. Recycling technologies made significant progresses in the last years both in terms of efficiency and low environmental footprint. Nowadays 1 ton of recycled glass save up to 300 Kg of CO_2 emission.[59] Moreover, glass substrates enable the full exploitation of conventional methods that are normally utilized for OT fabrication. The glass surface can be thoroughly cleaned by chemical (e.g., piranha solution, surface etching agents, solvents), and physical (plasma and ozone UV-cleaning) treatments and, if required, easily functionalized with anchoring groups or receptors.

Surface roughness is usually low (< 2nm) and tailorable, which is a key asset for OT fabrication. For example, the Bao's group reported the use of ultra-smooth and ultra-strong ion-exchanged sodium aluminosilicate (NAS) glasses for assisting the growth of organic semiconductor layers. The resulting devices exhibited superior electronic properties in comparison to conventional soda-lime substrates due to the improvement of charge carrier mobility, which took direct advantage of low surface roughness and reduced defect density of the organic molecules grown on NAS substrates.[60] The main difference between NAS and soda-lime glasses mechanical strength relies on the role of alkali ions. In NAS alkali ions enable the charge-stabilization of Al^{3+} ions in a tetrahedral configuration, which reinforces the silicate network. On the other hand, in soda-lime they break the silica network bonds, contributing to the

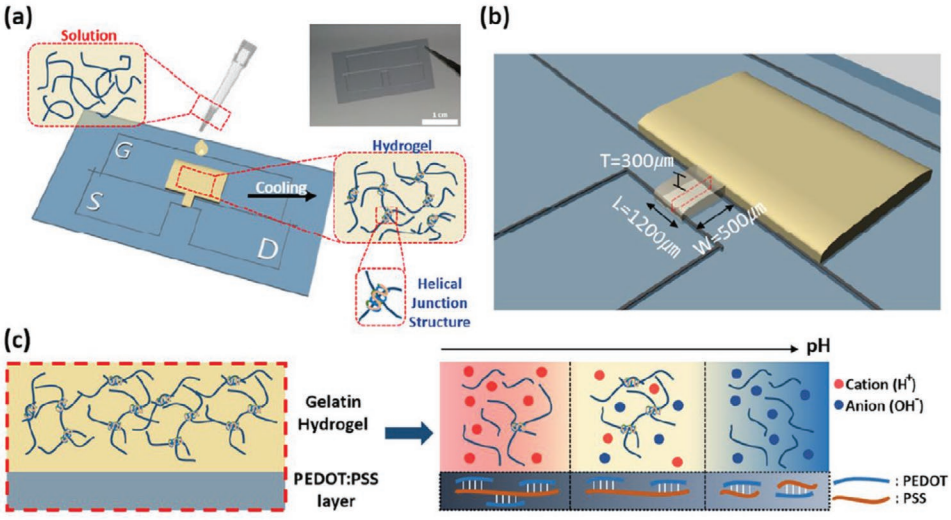

Figure 5. Schematic representation of gelatin electrolyte-based OECT; a) main components; b) geometric parameters; c) the gelatin hydrogel/PEDOT:PSS channel interface and effect of pH on ionic concentration and channel conductivity. Reproduced with permission.[101] Copyright 2018, American Chemical Society

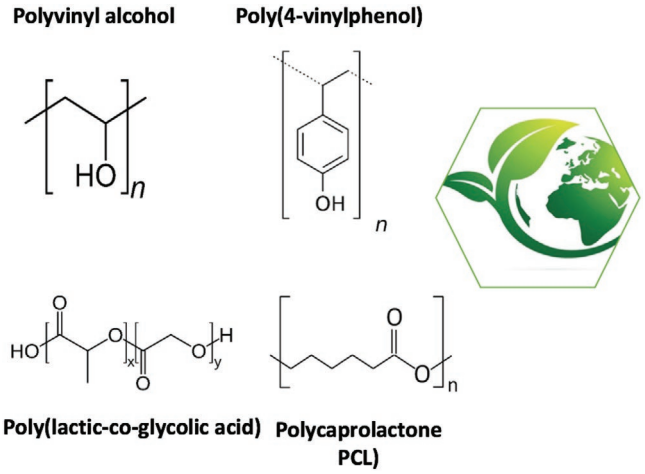

Figure 6. Examples of biodegradable and biocompatible synthetic polymers that have been utilized as substrates and insulators in organic transistor.

formation of non-bridging oxygen sites. Moreover, conductive contacts can be easily deposited on glass substrates with precisely defined patterns through either physical (evaporation, sputtering) or chemical routes. Glass also enables the controlled deposition of semiconductor components through spin or dip coating. In parallel, wettability can also be widely tuned by surface treatments.[61] For all those reasons, glass substrates are often the primary choice whenever new materials or architectures have to be assessed and compared to the existing ones.

2.1.2. Flexible Substrates: Paper

Low cost, flexibility and compatibility with roll-to-roll manufacturing are key hallmarks that made paper intensively investigated for large area electronics.[62,63] Cellulose fibers constituting a paper substrate are usually obtained by wood or other renewable raw materials. Recovery of cellulose fibers from agricultural waste opens further directions towards a more sustainable production of paper for electronics.[64] Moreover, paper substrates can be, at least in principle, fully recycled or biodegraded. However, most of the properties that make paper advantageous in fabrication of energy and information storage devices, sensors and actuators,[65–67] such as high surface roughness and porosity, represent major limitations for the development of thin film transistors, which normally ask for smooth and impermeable surfaces.[63,68–70] Moreover, the presence of impurities and strong dependence of paper resistivity on relative humidity (RH) are possible sources of hysteresis or even irreversibility in the electrical behavior of a printed transistor.[71]

Several options have been explored in order to circumvent those drawbacks. In particular, hydrophobicity and impermeability have been improved by means of functional coatings, made of polymers (e.g., polyethylene, polypropylene, polyurethane, polyvinylalcohol), wax, and combination of smoothening agents with barrier layers such as kaolin and latex.[63,72] However, most of these coatings compromise recyclability and biodegradability of the transistors and, in general, of the whole devices. A valuable support in this regard can be found by drawing inspiration from science and technology of packaging, which actively investigated hydrophobic layers derived from natural polysaccharides, such as modified chitosan or starch.[73–75]

Surface roughness is another major drawback of paper substrates (see **Table 2**). In fact, as the gate dielectric thickness is reduced, the presence of rough surfaces often entails huge gate leakage current, with detrimental effects on the OT performances. At the origin of high roughness of commercial paper is the fact that cellulose fibers are 10–20 µm in size. Smoother surfaces can be obtained by disintegrating cellulose fibers into micro- or nanofibrils. This process is obtained through high-pressure homogenization and give rise to nanocellulose, which is in turn pressed to produce smooth paper. However, the mechanical nanofibrillation of natural cellulose is energy-demanding and can be detrimental for the integrity of nanofibers. On the other hand, 3–4 nm-sized individual nanofibers can be prepared through oxidation mediated by 2,2,6,6-tetramethylpiperidine-1-oxyl radicals (TEMPO), followed by disintegration in water.[76,77] TEMPO-mediated oxidation allows to introduce carboxylate groups on C6 of cellulose fibrils, without altering their pristine crystallinity. Another example of cellulose with promising features for producing OT substrates is that obtained from bacteria like *Acetobacter xylinum*.[78] This type of cellulose does not contain any hemicellulose, lignin or other contaminations and is characterized by high moldability and lower roughness (20-50 nm), which is still too high for many OT application.[79] Moreover, the scalability of this route is still limited.

Table 2 compares the three types of papers described above, summarizing the typical ranges of mechanical properties (maximum loading stress, Young's modulus), surface roughness, porosity and optical transparency in the visible range (550 nm). It can be observed that nanocellulose can tolerate a loading stress which is remarkably higher than that of both bacterial cellulose and conventional paper. In particular, self-standing transparent and flexible nanocellulose substrates are characterized by relatively high tensile strength (200–300 MPa) and elastic moduli (6–7 GPa). Although a value of 114 GPa has been reported for the elastic modulus of bacterial cellulose filaments on the basis of Raman data analysis,[80] the

Table 2. Mechanical properties, average surface roughness, porosity and optical transparency at 550 nm for commercial paper, bacterial-cellulose, and nanocellulose.

	Max loading stress [MPa]	Young's modulus [GPa]	Surface roughness [nm]	Porosity [%]	Optical transparency @550 nm [%]
Traditional paper	6[82]	0.5[82]	5000–10000[82]	50[82]	20[82]
Bacterial cellulose	1.5[79]	114[80]	20–50 [79]	n.a.	85[81]
Nanocellulose	200–400[82]	7.4–14[82]	5[82]	20–40[82]	90[82]

above-discussed limitations associated to bacterial cellulose and its higher average surface roughness make nanocellulose the actual golden standard for the fabrication of OT-grade substrates. On the other hand, the optical transparency at 550 nm of both nano- and bacterial-cellulose, are very similar and in the range of 80–90%.[81] Of course, the mechanical properties and surface morphology of commercial paper exhibit a wide range of values which reflect the rich gamut of paper types that are available. A detailed analysis in this respect has been reported by Osterbacka and co-workers in their seminal review of paper electronics.[63] Direct fabrication of OT on commercial paper would give many obvious practical advantages in many sectors, including secure packaging, food and beverage control, and anticounterfeiting. Overall, several examples of OT fabricated on different types of paper substrates, including photo-, printer-, packing-, nano-, starch-paper, as well as banknotes have been reported. A detailed summary of this research activity have been thoroughly described by Zschieschang and Klauk.[68] The performances reported in most of those examples are still far from those achieved with glass substrates.

2.1.3. Polysaccharides (Chitin, Chitosan, Starch, Galactomannan, Alginate)

Natural polysaccharides are useful not only to modify the surface properties of paper, but also as OT substrates. Figure 2 shows the structural relationships among cellulose and related polysaccharides. Although less investigated than cellulose, most of them can offer unique advantages for green organic electronics. For example, chitin and chitosan are attracting increasing interests in the field. Chitin (poly-β-(1,4)-*N*-acetyl-D-glucosamine) is typically extracted from the exoskeleton of insects, crustaceans and mollusks and can be easily recovered from food-waste. The production of chitin by freshwater and marine arthropods exceeds 10^9 tons per year. Alternatively, it can be recovered also from fungi cell walls.[83] Conventional methods for extracting chitin from food-waste are based on two sequential steps, consisting of demineralization and deproteinization. Chemical demineralization relies on strong acids and high-temperature processes (e.g., HCl 1–2 M, 100 °C, 48 h) to completely remove the mineral components of the exoskeletons. Alternatively, lactic acid bacteria can be utilized for the same purpose, even though the biological route may require several days. Deproteinization is carried out by strong bases (NaOH, 1 M, 3–6 h, 65–100 °C). An additional decolorization process operated through either acetone, H_2O_2, NaClO or organic solvents is necessary to remove natural pigments. Each acid and alkaline attack is interleaved by washing/neutralizing steps, which entail the consumption of significant amounts of water.[83]

Extraction from fungi does not require the demineralization step, however fungal chitin is not pure but complexed with β-glucans, which makes this extraction route unsuitable for practical applications. Alternative approaches are based on the use of deep eutectic solvent (DES) or natural deep eutectic solvents (NADES), which are mixtures of organic molecules (acids, alcohols, amines, amino acids, etc.) that are primary metabolites of plants.[84,85] To date, different types of NADES have been explored, all of them resulting from the combination of choline chloride with organic (lactic, malonic, citric) acids or urea. The use of choline chloride and lactic acid enables direct extraction of chitin at 70 °C, with full recovery of minerals and proteins.[86] Chitin is insoluble in water and has been successfully utilized to fabricate transparent substrates for OLED devices.[87] However, to the best of our knowledge, it has never been explored as a substrate for OTs. On the other hand, chitin deacetylation produces chitosan, which is water soluble because amino groups in C-2 of D-glucosamine bear positive charges. Chitin deacetylation is usually obtained by alkaline (NaOH 40–50%) treatment for 6 h at 107 °C or by enzymatic deacetylation, which proceeds through the hydrolysis of *N*-acetamido bonds. However, the enzymatic route is too expensive and time consuming for practical scaling up.[88]

Chitosan has been exploited in fabrication of substrates for organic field-effect transistor (OFET)[89] or as a coating layer for paper substrates. It can be utilized for a variety of other functions, for example as dielectrics or even proton conductors for synaptic transistors.[90] Moreover, both chitin and chitosan can be combined with natural cross-linking agents, such as citric acid, limonene, genipin, etc., to produce hydrogels, which could be particularly useful for organic electrochemical transistors (OECT).[91] Agarose and alginate can also be exploited in hydrogel formation (see Section 2.1.6). Other examples of (poly) saccharide-based substrates are those made of caramelized sugar and bioplastics derived from potato or corn starch, which are commercialized with the name of Ecoflex by BASF[92] and should not be confused with the homonym siloxane-based elastomer commercialized by SMOOTH-ON[93] that will be introduced in Section 2.1.7.

Recently, galactomannan-based devices have been explored for transient electronics.[94] Galactomannan is a polysaccharide formed by a backbone of mannose units linked with each other by β-1,4-glucosidic bonds with lateral chains made of galactose connected to the mannose backbone through -1,6-glucosidic bonds. Galactomannan is abundant in different botanic species, such as the *Leucaena leucocephala* seed endosperm and can be easily extracted in ethanol, freeze-dried and redispersed in water to form transparent films characterized by good flexibility and mechanical properties, with experimental values of tensile strength and elastic modulus of 47.9 and 48.1 MPa, respectively.[94] Galactomannan is a very interesting materials for substrates because of its full biodegradability in mild conditions. It tolerates ethanol and other organic solvents, but unfortunately it is quickly dissolved in water.

2.1.4. Proteins (Keratins, Hard Gelatin)

Water insoluble proteins are a valuable alternative to polysaccharide-based substrates. In particular, pioneering works by the Kaplan' and Omenetto's groups on silk opened the door to the fabrication of biocompatible and biodegradable electronic devices.[95] The structural part of silk is made of fibroin, a protein consisting of light- (L) and a heavy-(H) chain polypeptides interconnected through disulfide bonds at the C-terminus of the H-chains Each H-chain, which ultimately determines the

mechanical properties of silk fibers, is formed by 12 hydrophobic domains interspersed with 11 hydrophilic domains.[96] The hydrophobic domains form highly ordered crystalline regions through the assembly of β-sheet crystallites, as displayed in Figure 3. Silk fibroin can be extracted from the cocoon of silkworm Bombyx mori L. through a water-based eco-friendly method. Different processes enable to obtain fibroin in form of sponges, films and hydrogels. Films and hydrogels are particularly relevant for OT fabrication. In the case of thin films, the technique utilized for the material deposition plays a key role on the final mechanical properties. Fibroin films prepared by dry-casting are usually affected by poor mechanical properties, whereas spin-coating and layer-by-layer routes enable to achieve products exhibiting remarkable toughness (328 kJ m^{-3}), tensile strength (≈100 MPa) and general robustness, in spite of their extremely reduced (only few nm) thickness.[50,96] These properties, which make fibroin thin films similar or even superior to many synthetic polymers, originate from the direct formation of β-sheets during the coating process. Prolonged immersion in water or exposure to aqueous vapor minimize the natural brittleness of fibroin films. In parallel, silk fibroin solution can be cross-linked and transformed into hydrogels by playing with a variety of parameters (temperature, pH, ions, fiber concentration).

A high content of β-sheets and disulfide bridges is also observed in other keratins (silk itself is classified as a β-Keratin protein). Keratins are the structural proteins that form hair, nails, feathers, horns, claws, hooves in animals. Most of the biological sources of keratin are usually treated as waste and not recycled. In this perspective, recovery and production of keratin from organic and food industry waste could be a promising step towards the sustainable fabrication of OTs. High toughness and chemical resistance can make keratins interesting candidates in the fabrication of transistor substrates. However, most of keratins have been utilized for producing dielectric layers. For example, Singh et al.[97] demonstrated that keratin can be extracted from chicken feathers and utilized as gate dielectric layer for biodegradable OFETs. Extraction is quite complex and time expensive. It consists of a series of washing steps with ether, ethanol and water, drying and subsequent treatment with urea solutions (pH = 10.5) containing L-cysteine as a reducing agent. The solution was stirred in bubbling N_2 for 12 h at 70 °C and repeatedly dialyzed. The overall yield was 33.5%.[97]

Other protein-based dielectric layers have been obtained from gelatin or collagen, which are typically extracted from animal bones and skin, or egg albumen.[50,98–100] Soft gelatin has also been utilized in fabrication of hydrogels for organic electrochemical transistors (see Section 2.1.6).[101]

Table 3 summarizes the main utilization of polysaccharides and proteins in OT and their mechanical properties, which have been discussed in detail in Sections 2.1.3 and 2.1.4. Chitin, silk fibroin and keratin show the highest values of tensile strength and elastic modulus, which makes them more suitable for the fabrication of semirigid substrates. Other polysaccharides and protein-based materials like gelatin and collagen are more suitable as coating layers and components of hydrogels. Notably, all these materials are classified as biodegradable, thus they cannot be recycled. However, materials characterized by high chemical and mechanical stability, like chitin and keratin, can be also recycled and re-used for many cycles. This aspect still needs to be properly investigated in the future and could open the door to inner loops in the cycle of life of OT based on this type of substrates.

2.1.5. Natural Resins (Shellac)

Shellac is a biocompatible, natural resin produced by the female lac bug (*Kerria lacca*) and traditionally used in a variety of applications, as wood finish, varnish agent, sealant, electric insulator, as well as to prevent moisture losses from citrus fruits and masking bad taste of some oral drugs. Shellac is made of different chemicals, including aleuritic, shelloic, and jalaric acids and have been recently employed either as a substrate or as a dielectric (see Figure 4).[109] Baek et al. compared the performances of shellac dielectrics with those of poly(4-vinylphenol) (PVP), a common synthetic polymer dielectric, in OFETs based on donor-acceptor-type organic semiconductors.[110] This study revealed that unlike PVP, the hydroxyl groups of the alcoholic moieties of shellac remain protonated under working conditions. As a result, electron trapping is suppressed, making shellac dielectrics suitable for n-type or ambipolar OFETs. Shellac films can be drop-casted from ethanol solutions and crosslinked below 70 °C. The resulting films are rigid and smooth.[109] However, the dielectric properties can be significantly influenced by the presence of impurities, which

Table 3. Main utilization in organic transistors, mechanical properties, biodegradability and recyclability of various polysaccharides and proteins.

Material	Main utilization in OT	Tensile strength [MPa]	Elastic modulus [GPa]	Biodegradable	Recyclable	References
Chitin	Substrate	3–80	$330–2900 \times 10^{-3}$	Yes	Yes	[102,103]
Chitosan	Substrate, coating layer, hydrogel	1–7	0.8×10^{-3}	Yes	No	[103,104]
Starch	Coating layer hydrogel	1.6–10	$79–205 \times 10^{-3}$	Yes	No	[102,104]
Alginate	Coating layer, hydrogel	28.5	12.9×10^{-3}	Yes	No	[105]
Galactomannan	Substrate, coating layer, hydrogel	48.9	48.1×10^{-3}	Yes	No	[94]
Silkworm silk fibroin	Substrate, coating layer, hydrogel	300–740	10–17	Yes	No	[96]
Keratin	Substrate, coating layer, hydrogel	2–530	0.01–2.5	Yes	Yes	[106]
Gelatin	Coating layer, hydrogel	0.1–0.2	$0.04–0.07 \times 10^{-3}$	Yes	No	[107]
Collagen	Coating layer, hydrogel	0.9–7.4	$1.8–46 \times 10^{-3}$	Yes	No	[108]

are unavoidable in naturally extracted raw materials. Thus, preliminary purification steps could be necessary and should be accounted for in the evaluation of the overall sustainability.

2.1.6. Hydrogels for Electrolyte-Gated and Organic Electrochemical Transistors

Hydrogels are intensively investigated in the field of electrolyte-gated (EGTs) and organic electrochemical transistors (OECTs) (see section 4) because they provide a practical route to exploit the high capacitance typical of liquid electrolytes, yet in form of semisolid materials that are able to entrap water and efficiently transport the ions at low driving voltage. Most of polysaccharides and proteins discussed above can be properly formulated in order to produce non-toxic, biocompatible and biodegradable hydrogels. For example, Jo et al. investigated the use of gelatin hydrogels for fabricating OECTs and their integrated circuits, demonstrating that gelatin can act as a semisolid electrolyte that mediate the gate-to-channel charge injection.[101] In particular, the authors demonstrated that the mobility of charge carriers can be tuned as a function of the hydrogel pH. As shown in Figure 5, gelatin increases their cationic or anionic concentration when the hydrogel pH is maintained in acidic or alkaline conditions, respectively. As a result, the electrical conductivity of the poly(3,4-ethylenedioxythiophene) polystyrene sulfonat (PEDOT:PSS) channels is modulated by the hydrogel pH, which represents a very easy way to control the ion concentration. In comparison to other hydrogels produced by microcrystalline cellulose or synthetic polymers, gelatin can be easily prepared from powder dissolution at 50 °C and the hydrogel pH is controlled by adding common organic acids, such as malic acid, bases like NaOH or neutral salts like NaCl, which represents a major advantage in terms of large-area fabrication and processing. Moreover, these types of hydrogels are particularly suitable for ion sensing, biointegration and edible electronics.

Agarose is another example of green material that can be utilized to prepare hydrogels for electrolyte-gated organic transistors. As shown in Figure 2, agarose is a polysaccharide made of D-galactose and 3,6-anhydro-L-galactopyranose linked by glycosidic bonds. Agarose chains are organized in helical fibers, which are 20–30 nm in size and form extended 3D networks upon gel transition. The hydrogen-bonded gel network is characterized by the presence of channels with sizes ranging from 50 to several hundreds nm. Agarose hydrogels can serve as a constant reservoir of water and enable ion conductivity. Zhang et al. have recently demonstrated the use agarose hydrogels to fabricate hydrogel-gated organic field-effect transistors (HYGOFET) utilized in pressure-sensitive devices. Again, agarose hydrogels play a key role in modulating the current of the organic semiconductor in a reduced (<0.5 V) voltage range.[111]

Cellulose, alginate, chitin, chitosan, and fibroin have also been extensively utilized to fabricate hydrogels. An updated, comprehensive overview on this topic can be found in Mondal et al.[112] We highlight the fact that the field of hydrogels for OT is extremely rich and complex, as these components ask for a synergistic combination of appropriate mechanical and electrical properties, together with non-toxicity, biocompatibility, biodegradation, low cost, and easy processability.

2.1.7. Synthetic Polymers and Encapsulants: Stretchability, Biocompatibility, and Biodegradability

Flexible electronics asks for highly stretchable substrates and materials able to encapsulate and protect the electronic components. A recent review by Li et al.[113] analyzes in detail the mechanical and optical properties, as well as permeability of some of the materials that are commonly utilized for those scopes, such as polydimethylsiloxane (PDMS), Dragon Skin, Ecoflex and hydrogels made by either synthetic (e.g., poly(acrylamide-co-acrylic acid) or natural (e.g., hyaluronic acid) components. All these materials are characterized by an extended cross-linking among the molecular chains that is based on weak interactions. This structural peculiarity makes them more stretchable of other inorganic or hard organic materials. For that reason, they are extensively investigated for planar and conformal 3D applications. The most interesting point is related to their biocompatibility, which makes them suitable for in vivo applications and skin devices. In this regard, the main constrains for the integration of OT and, in general, electronic device with human tissue are represented by elastic modulus and thickness, which should be very small to avoid or minimize any interference with natural motion, and stretchability, which should be high in order to prevent cracks or damages. The analysis of the mechanical properties revealed that these types of materials can be ranked according to the following ideal order: Hydrogels > Dragon Skin > Ecoflex > PDMS. In another recent paper, Skov and co-workers compared the mechanical properties of an extended range of formulation of PDMS and Ecoflex elastomers and blends of both the components, pointing out the superior performances of the latter and the importance of a fine tuning of formulations.[114] We also note that unlike PDMS, Ecoflex and Dragon Skin siloxane-based elastomers, which are biocompatible yet not biodegradable, a variety of hydrogels can be designed and fabricated in order to fulfill this important requirement. Research on biodegradable synthetic polymers has made tremendous progresses in the last years. An excellent overview in this regard has been reported by Bao and co-workers.[115] A variety of synthetic polymers have been tested either as substrates or insulators for organic transistors. Figure 6 shows some examples of the most common synthetic polymers that have been utilized for those applications.

Polyvinyl alcohol (PVA), polycaprolactone (PCL), poly(lactic-*co*-glycolic acid) (PLGA) are only a few examples of polymers that can combine biocompatibility and full degradability in the environment. The design strategy of these polymers is based on the use of monomeric units that participate to physiological or natural cycles. For example, PLGA is formed by lactic and glycolic acids, which are common byproducts of metabolic routes. As the monomers are linked through ester bonds, they can be recovered by simple hydrolysis under mild conditions. PVA is another biocompatible polymer that undergo easy biodegradation and has the key advantage of allowing for a very fine control of crosslinking and swelling by simple adjustment of the formulation.

Biodegradable elastomers based on poly(glycerol sebacate) (PGS) and on poly(glycerol sebacate) acrylate have been proposed for applications in bioelectronic devices, as they can take advantage of esterase enzymes and hydrolysis processes that

normally operate in human body.[116] Other examples of biocompatible and biodegradable polyester is given by poy(diol citrates) that can be obtained by polycondensation of citric acid and linear aliphatic diols. A key asset of polyester elastomers is the easy modulation of the mechanical properties and biodegradability by small adjustment of the synthetic conditions (type of monomers, molar ratio, temperature, crosslinking time, working atmosphere, etc.).[117] For example, in the case of poly-(octanediol-*co*-citrate) an increase of post-polymerization curing at 120 °C from 1 to 6 days results in an increase of the elastic modulus by a factor of nearly three (from 2.84 to 6.44 MPa) and decreases elongation from 253% to 117%. Moreover, the introduction of a second type of crosslinker agents, such as acrylate and fumarate can allow extending the elastic modulus over a wide range (from 7.4 to 75.9 MPa for acrylate- and from 16.4 to 38.3 MPa for fumarate- co-crosslinkers).[118] Most of polyester elastomer investigated for biomedical applications exhibit mechanical properties, in particular flexibility and stretchability, which are comparable or even superior to the silicone-based counterparts. For example, poly(trimethylene carbonate-*co*-D,L-lactide) P(TMC/DLLA) with a 50:50 molar ratio exhibits an elongation of 570%[119] and poly(4-hydroxybutyrate) (PH4B) can reach about 1000%,[120] which is analogous to the values reported for Dragon Skin or some encapsulating hydrogels.

Table 4 compares some of the materials discussed above in terms of mechanical properties (flexibility/stretchability), general applications and possibility of biodegradation or recycling.

We note that the numerical values reported in Table 4 are based on a non-exhaustive selection of data taken from literature, with the aim of providing an immediate, yet approximate, classification of each type of material in view of a given application. On the other hand, as already discussed, each parameter may span over a wide range of values within each class of materials. Moreover, we highlight that the classification of a given material as flexible or nonflexible is based on their most common use. For example, glass is reported to give a reference of non-flexible substrate, even though ultra-thin glass substrates have been utilized in fabrication of displays.[121] Analogous arguments apply for biocompatibility, biodegradability, and recyclability, which have been considered only in general terms and for basic materials. As discussed before, most of these properties can be modified by adding specific co-factors and tuning the formulation of the final materials. In particular, the realm of biodegradable polymers covers an extremely rich palette of possible combinations –whose treatment is well beyond the scope of this work– which open exciting perspectives on the way of sustainability.

2.1.8. Small Molecules (Sugars and Nucleobases)

In their pioneering works on green transistors, Irimia-Vladu and co-workers extensively explored the use of sugars and nucleobases as dielectrics for OFETs (**Figure 7**).[125] Glucose and lactose have similar dielectric constants (6.35 and 6.55 at 1 kHz, respectively), but quite different breakdown fields (1.5 and 4.5 MV cm^{-1}, respectively). Both sugars are biodegradable and can be easily processed in water and DMSO. Spin-coating gives rise to smooth films (roughness: 0.5–1 nm). Glucose was also combined with caffeine to produce all-natural compound-based OFETs with capacitance per unit area of 1.9 nF cm^{-2}. Nucleobases (adenine, guanine, cytosine, thymine) can be extracted from natural sources and utilized as dielectrics, showing low losses and relative permittivity ranging from 2.4 (thymine) to 4.65 (cytosine) at 1 kHz. Cytosine and guanine exhibit the highest breakdown fields of about 3.4 MV cm^{-1} and 3.5 MV cm^{-1}, respectively.

Unlike sugars, the films made of nucleobases are characterized by higher values of surface roughness (3–65 nm), resulting from progressive crystallization. However, in spite of such a relatively high roughness, limited hysteresis was observed. Among other types of organic small molecules utilized as gate dielectrics, melamine has been successfully utilized in combination with C_{60} semiconductors to fabricate OFETs.[125] Melamine can be easily evaporated and, in general, it is suitable for vacuum processing. However, vacuum deposition results in formation of large crystals (size: 350–700nm), which yield high surface roughness (10-60 nm). In the range 10–10^4 Hz the relative permittivity of melamine insulating films is around 4.25. Overall, in comparison to natural biopolymers, biodegradable small molecules have the advantage of highest purity, which is maintained by vacuum processing and allows to counterbalance surface roughness originated from crystallization. The main dielectric properties of the molecules described in this Section are listed in **Table 5**.

Table 4. Synoptic comparison of the mechanical properties and biodegradability/recyclability of the materials discussed in Section 2.1.7.

Material	Tensile strength [MPa]	Elastic modulus [GPa]	Elongation [%]	Biocompatible	Biodegradable	Recyclable	References
glass	41–180	23.8–90.5	2	No	No	Yes	[113]
PDMS	1.1–14.3	$0.4–5 \times 10^{-3}$	93	Yes	No	No	[113]
Dragon Skin	2–3.5	170×10^{-6}	1000	Yes	No	No	[113]
EcoflexTM	0.8–2.4	$20–125 \times 10^{-6}$	164	Yes	No	No	[113]
PCL	20.7–34.5	$0.21–0.34 \times 10^{-3}$	300–500	Yes	Yes	No	[122]
PG/CL	<1	N.A.	250	Yes	Yes	No	[123]
P(TMC/DLLA) 50:50	10	16×10^{-3}	570	Yes	Yes	No	[119]
PGS	0.5	0.282×10^{-3}	267	Yes	Yes	No	[124]
Poly(diol citrates)	1.3–334.8	$0.11–40.8 \times 10^{-3}$	207–405	Yes	Yes	No	[117]
PH4B	50	70×10^{-3}	1000	Yes	Yes	No	[120]

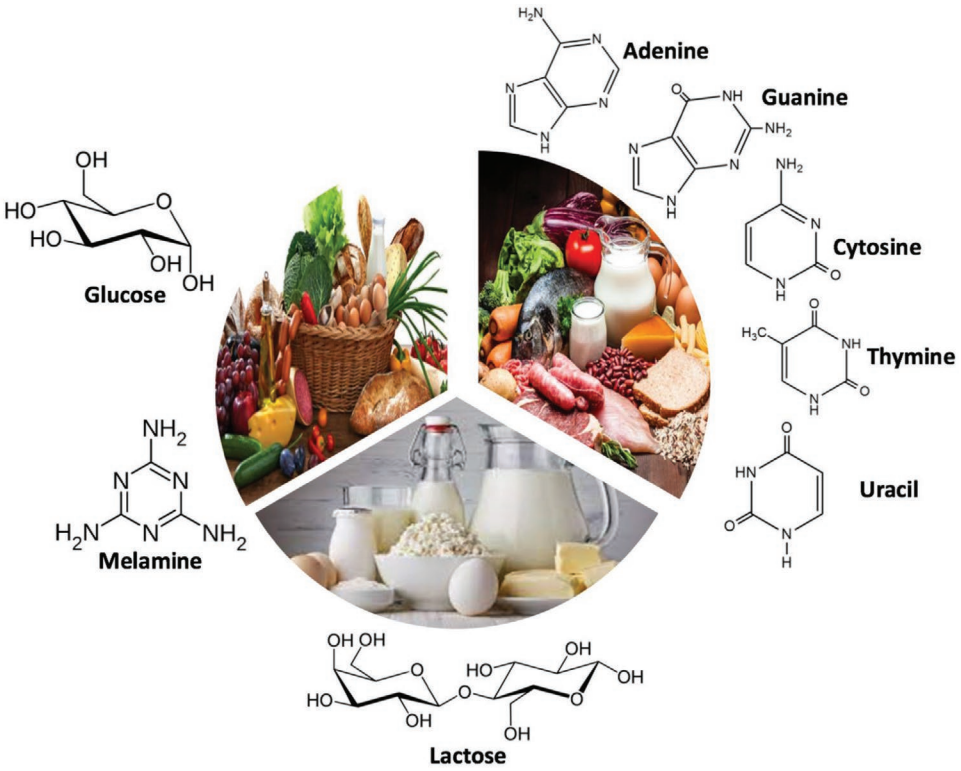

Figure 7. Examples of small molecules utilized as dielectrics.

2.2. Semiconductors and Conductors

At the heart of complementary OT technologies there are p- or n-type organic semiconductors, which are normally made of synthetic compounds, including for example pentacene, rubrene, pyrrole, phtalocyanine, thiophene, aniline, naphthalene- and perylene-diimide units, as well as fullerenes. A few examples of these molecules are shown in **Figure 8**. The extremely rich variety of semiconductors derived from these molecules has been exhaustively reviewed by Facchetti[136] and, more recently, by Quinn et al.[137] Conductive polymers, such as poly(3,4-ethylenedioxythiophene) (PEDOT), can also serve as electrodes or interconnectors. Although most of those molecules are biocompatible, biodegradation is often hampered by the high stability of their C-C bonds. The transition towards green organic semiconductors and conductors featuring low/zero-toxicity, biodegradability or recyclability, can be accomplished through different approaches. On one hand, natural or bioinspired semiconductors and conductors can be either extracted or de novo synthesized according to green chemistry protocols. Alternatively, synthetic organic semiconductors and conductors can be modified with functional groups that promote degradation under mild conditions. Moreover, even though not specifically designed for biodegradability, most of those functional groups are made of "green" units consisting of sugars, amino-acids or esters. A few examples of these approaches are reported below.

Table 5. Dielectric properties of the sugars and nucleobases small molecules.

	Permittivity	Breakdown field [MV cm^{-1}]	Dielectric constant	Surface roughness [nm]
Glucose	n.a.	1.5[125]	6.35[125]	0.5–1[125]
Lactose	n.a.	4.5[125]	6.55[125]	0.5–1[125]
Adenine	4.4-6.3@10-10^5 Hz[126]	1.5[127]	3.85[127]–13.9[127]	3–6.5[125]
Guanine	n.a.	3.5[125]	4.35[127]–9.36[128]	3–6.5[125]
Cytosine	4.65 @ 1 KHz[125]	3.4[125]	17.6[128]	3–6.5[125]
Thymine	2.4 @1 KHz[125]	n.a.	12.5[128]	3–6.5[125]
Melamine	4.25 @ 10–10^4 Hz[125]	n.a.	4.7–10.2[125]	n.a.
Polyvinyl alcohol	7-10 @ 1KHz[129]	n.a.	1.3–11.3[130]	n.a.
Polycaprolactone	4.4 @ 1 KHz[131]	n.a.	3.22[132]	n.a.
Polydimethylsiloxane	2.67[133]	2.5–6.35[134]	2.3–2.8[135]	n.a.

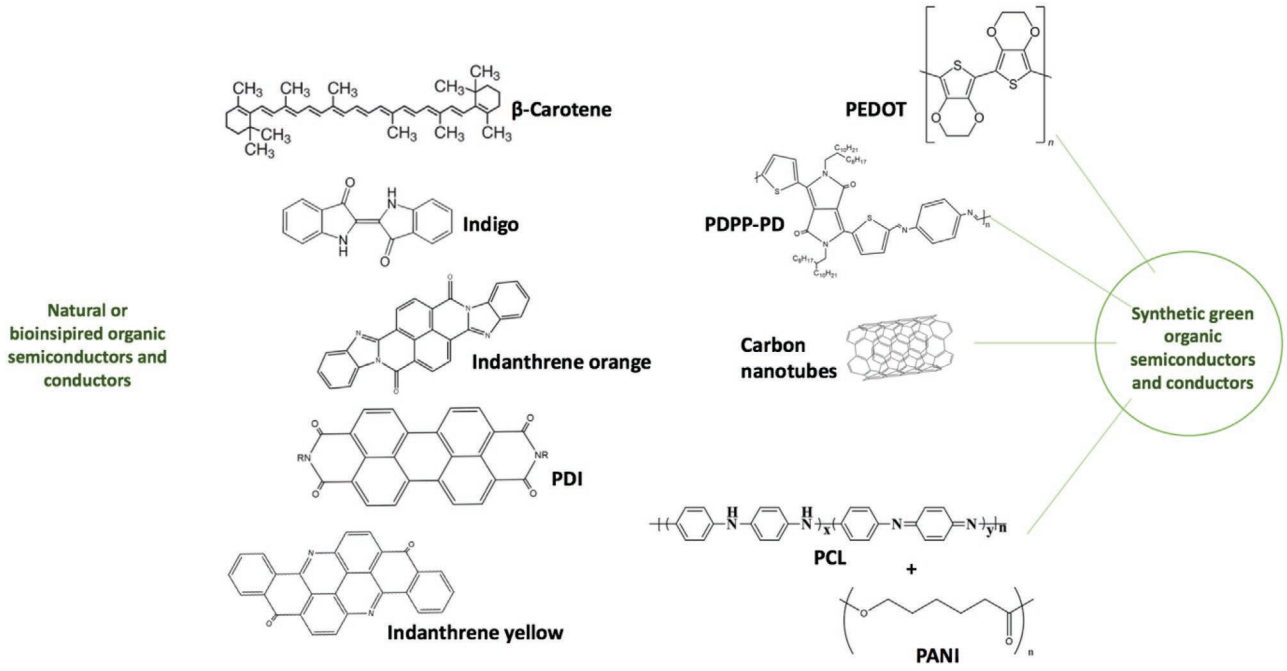

Figure 8. Examples of organic semiconductors and conductors utilized in organic transistors.

2.2.1. Natural or Bioinspired Organic Semiconductors

Nature is an endless source of inspiration also for organic semiconductors. From the simplest natural dyes to complex antenna and redox systems, a number of highly efficient and finely adapted structures can be found. In particular, organic molecules with extended conjugated π–systems can be characterized by good charge transport properties and highest occupied molecular orbital/lowest unoccupied molecular orbital (HOMO/LUMO) energies compatible with hole/electron charge injection or extraction when in contact with metal or conductive electrodes. By the way of example, beta carotene, with a long π-conjugated chain, has been utilized as p-type semiconductor in organic transistors made using glucose and caffeine as dielectrics. The field effect mobility was 4×10^{-4} cm^2 V^{-1} s^{-1}. In parallel, n-type semiconductors obtained from indigo natural dyes were tested in analogous transistors, exhibiting a field effect mobility of 1.5×10^{-4} cm^2 V^{-1} s^{-1}. Indigo dyes deposited on shellac/AlOx substrates can take advantage of their extended planar p systems and redox reversibility for fabricating ambipolar devices with charge carrier mobility of 10^{-2} cm^2 V^{-1} s^{-1}.[125] Figure 8 shows a few examples of bio- or bioinspired molecules utilized as semiconductors for OT. Bioinspired anthraquinone derivatives, such as indanthrene yellow G and indanthrene brilliant orange RF were combined with natural substrates, giving rise to transistors with mobilities ranging from 10^{-2} to 10^{-4} cm^2 V^{-1} s^{-1}.[54] As shown in Figure 8, most of those natural or bioinspired molecules have sites that can play both as acceptors (C=O) and donor/acceptor (-NH, -OH) for hydrogen bonds, which represents a major advantage in view of biodegradability and integration in green devices. Rapid progresses towards fully green organic semiconductors have been obtained using oligo-furans, which can be processed by non-halogenated solvents and are characterized by mobilities around 10^{-2} cm^2 V^{-1} s^{-1}.

2.2.2. Synthetic Green Organic Semiconductors and Conductors

The development of biodegradable semiconductors and conductors is essential not only for the production of environment-friendly OT, but also in view of specific applications, such as edible transistors or skin devices. A smart strategy to endow organic semiconductors with biodegradability is the exploitation of pH-sensitive stability of imine-bonds. Semiconductor molecular units can be linked through imine bonds, which are stable in neutral environment, but undergo rapid acid-catalyzed hydrolysis. This strategy enabled the production of diketopyrrolopyrrole-phenylenediamine (PDPP-PD) semiconductors, which are characterized by high hole mobility (0.12 cm^2 V^{-1} s^{-1}). Moreover, diketopyrrolopyrrole-phenylenediamine can be completely degraded within 30 days in acid solution (pH = 4.6).[48]However, the imide bond breaking releases in solution the individual molecular units, which remain unaltered and could have potential toxicity as they contain benzene rings. This is a general warning for design of biodegradable materials. Molecular degradation or depolymerization can often give rise to molecular species that are more toxic than the pristine material.

The development of green electrodes is a further big challenge for OTs. The type of conductors can be either inorganic or organic. For obvious reasons, platinum and coinage metals (Au, Ag and Cu) cannot be considered as green components. However, the reactivity in air of earth-abundant, environment-friendly metals, such as iron, zinc, or magnesium represents a double-edged sword. On one hand, it allows for easy and relatively fast degradation, which does not release any harmful byproduct. Fe electrodes were dissolved within 1 h at pH 4.6, producing iron ions that can be easily recovered and recycled.[48] Zn and Mg exhibit an analogous behavior, the dissolution rate

being strongly dependent on pH and temperature. In particular, Mg electrodes quickly dissolved (2 min.) in PBS buffer (pH = 7.4) at 37 °C, which are conditions utilized to simulate biologic fluids, whereas it takes 12 h at 25 °C and pH = 10.[48] On the other hand, the high reactivity of non-noble metals can be detrimental for the stability and reliability of organic transistors. Carbon nanotubes (CNTs) can be an alternative approach since when properly functionalized ensure biodegradation. However they pose serious concerns in terms of biocompatibility and toxicity, because of their facilitated penetration through the respiratory systems.[138,139]

Biodegradable and biocompatible synthetic metals could be a solution to this conundrum, although achieving these properties in a single conductive polymer is not trivial. For example, PEDOT:polystyrene sulfonate (PSS) blend, which exhibit high conductivity (up to 4600 S cm^{-1}) and can be easily produced over a large scale, being utilized as both cathode and anode, is biocompatible, yet not biodegradable. A general strategy to improve biodegradation is the infiltration of PEDOT:PSS into biodegradable insulating matrices. Again, as in the case of PDPP-PD semiconductors discussed above, degradation leaves behind non-degradable organic units. However, in this case, the remaining PEDOT units are biocompatible. Alternatively, conductive polymers can be modified by adding non-conjugated chains, such as polyurethane, which ensure polymer disintegration into harmless unit.[48] In a recent example, the biodegradable insulating polymer poly(ε-caprolactone) (PCL) has been mixed with polyaniline (PANI) to produce conductive and biodegradable nanofibrous yarn for smart textiles.[140] The idea at the basis of this approach is that high biodegradability of PCL can be harnessed to drive the overall degradation process, making the devices compostable. PCL degrades at 58 °C with 60% of humidity, however many environmental factors, including soil microorganisms and hydrolytic enzymes, can promote the process. Although not biodegradable, the PANI layer undergoes spontaneous detachment from the PCL surface within four weeks and this separation is directly stimulated by the progressive PCL degradation, which proceeds through water penetration within the PCL cracks. Overall, all these degradation strategies are quite general and offer a variety of solutions for improving a safe self-degradation of the conductive polymers.

3. General Considerations on Solvents, Processing, Degradation Tests, and Embodied Energy

A crucial aspect to be taken into account in the fabrication of green and sustainable OTs is related to the type of solvents utilized for extraction/synthesis of raw materials and their processing to prepare substrates and active layers. Toxic and carcinogenic halogenated and aromatic solvents have been widely employed in traditional processes. In the last years their use has been banned or strongly limited in most of the developed Countries. Ideally, water would be the green solvent par excellence. Common alcohols, ketones, and esters can also be classified as green solvents, because of their low toxicity. However, most of polymers utilized as semiconductors or conductors have nonpolar backbones that limit their solubility in polar green solvents. Thus, finding efficient green alternatives is, in general, not trivial. The Hansen's solubility parameters (HSP), which rely on thermodynamic data and quantification of the intermolecular forces involved in dissolution processes (dispersion, polar, and hydrogen bonding forces) have been used to predict solubility and design efficient solvent blends. Computer-aided methods, based on HSP, enable a rapid screening, which is accurate in the case of small molecules, but can give rise to non-accurate predictions in the case of polymers, because of the uncertainty of polymer length. For this reason, the selection of green solvent is still largely based on empirical approaches. As discussed above in the case of substrate materials, the choice of solvents for extraction of raw materials such as polysaccharides-including cellulose-and proteins is quite limited. HCl, NaOH, and ethanol are commonly used in different extraction steps, but DES and NADES alternatives are reported quite frequently.[83] In both cases, aromatic and halo-aromatic solvents can be avoided.

On the other hand, the choice of green solvents is particularly relevant and challenging in preparation of semiconductors, conductors and insulators. Solution-processed techniques rely on the control of the deposition conditions and solvent evaporation upon drying. The latter step is crucial in the case of blends, as the solvent evaporation rate mediates phase separation and leads structuring of the active layer film, which in turn strongly influences the electrical properties. D. Ho et al. reported a comparative investigation over a wide selection of green solvents to process 6,13-bis(triisopropylsilylethynyl)-pentacene (TIPS-PEN), often utilized as organic semiconductor in OTFTs. This study allowed to sort optimal green solvents, that is, non-harmful solvents having suitable boiling point and viscosity, which enabled to fabricate OFETs with field-effect mobilities comparable or even superior to those achieved by chlorinated or aromatic compounds. The best TIPS-PEN performances were obtained by using isobutyl acetate, which exhibited high mobility 2.6 $cm^2 V^{-1} s^{-1}$ and on/off ratio > 10^4. Very good results were also reported for dimethyl carbonate, anisole, t-amyl methyl ether and isopropyl acetate. Isoamyl acetate, n-amyl acetate and diethyl carbonate were quite promising, however processing should be optimized. The study was then extended to other n- and p-type semiconductors, showing encouraging results in the case of isopropyl acetate and anisole.[141] Other common strategies to improve the solubility and processability of polymer (semi)conductors are based on the introduction of ionic moieties in the lateral size of the hydrophobic polymer chain. As ionic chains limit the stability of the semiconductor to a narrow range of pH, neutral moieties are preferred as side groups. Successful examples are given by 3-(2-(2-(2-methoxyethoxy)ethoxy)ethoxy) ethyl chains that have been linked to polythiophene to achieve P3TEGT polymers, which can be directly processed in water and employed in preparation of OFET devices with hole mobility of 3.5×10^{-5} $cm^2 V^{-1} s^{-1}$. Analogously, other non-ionic polymers such as PPDT2TFBT-A enabled ethanol processing and production of OFET with hole mobility of 1×10^{-2} $cm^2 V^{-1} s^{-1}$.[141]

The fabrication of OT based on multilayered architectures asks for different deposition steps for semiconductor, electrodes, and gate dielectric. For example, OFETs with a top-gate bottom-contact architecture require to deposit the dielectric

layer in the last deposition step. Thus, the employment of a solvent that dissolves the dielectric compound(s), yet does not dissolve the underlying semiconductor, is mandatory. Moreover, in some contexts, such as bulk heterojunctions, it is necessary to achieve interpenetrated phases that are maintained separated at the nanoscale. Although this type of architectures is usually applied for molecular photovoltaic devices, useful lessons can be drawn also for OT fabrication. For example, limonene, a natural molecule extracted from citrus fruit peel, have been exploited as an orthogonal solvent to selectively dissolve fullerene derivatives (PCBM) deposited on poly(3-hexylthiophene) (P3HT) layers. Limonene allows for excellent wetting of P3HT, without inducing its extended dissolution. As a result, PCBM layers can be uniformly spin coated over P3HT layers, yet PCBM/P3HT intermixing is minimized. In addition to its green nature, limonene outperforms dichloromethane and other halogenated solvents utilized for the same scope.[142]

The rich palette of natural or bioinspired compounds that could be used as selective orthogonal solvents, makes that a burgeoning, yet still quite unexplored field, which promises to reach major breakthroughs in the next years. Another major aspect to be considered in design and fabrication of green OT is their degradation. In this regard, we should distinguish between different scenarios. The first one is that of degradation in natural environment. As discussed above, substrate determine over 99.5% of mass of OTs, thus substrate degradation is the main parameter to take into account. Natural environments offer a variety of factors that can promote degradation, such as temperature, solar irradiation, mechanical forces, enzymatic processes, including aerobic and anaerobic reactions, which can be mediated by fungi and bacteria, etc. Although quite heterogenous, the ways to test biodegradation are quite easy to implement. In fact, the degradation of green OTs should be tested directly in real or simulated natural environments. In general, substrates made of naturally derived materials are fully biodegradable. In parallel, anthropic chemical treatments can be applied in order to accelerate degradation and/or recovery and recycling of raw materials. Typical tests are carried out in acidic or alkaline conditions. On the other hand, OT for edible, or transient wearable electronics should be digested, cleared, or bio-resorbed through safe routes and without releasing harmful byproducts. In these cases, simulated biological fluids can be utilized to test biodegradation. The simplest tests are based on PBS solutions reproducing the physiological pH (7.4), with temperature fixed at 37 °C. Under these conditions silk fibroin dissolve in 3 h, whereas keratin films are stable over 7 days, but can be degraded within 15 days by adding protease enzymes.[143]

Closely related to degradation in biological fluids is biocompatibility. Several studies on biocompatibility have been reported for silk fibroin, which was demonstrated to be safe for human skin and does not induce inflammations of cytotoxicity in feline and rat brains.[50,144] Keratin did not show any cytotoxicity.[50] Collagen and PEDOT:gelatin films enabled adhesion and growth of endothelial cells, which could be helpful in view of fabricating OT for in-vivo bioelectronic applications. The use of biocompatible components can also be exploited to prepare composite substrates, as demonstrated in the case of chitin-silk membranes.[50]

Finally, a correct evaluation of the environmental impact of materials and processes involved in fabrication of OTs should take into account the energetic cost and CO_2 footprint. This analysis is often totally neglected in the large majority of scientific papers on this topic, yet it should be taken as a mandatory figure of merit in order to classify a given OT as "green". The most critical issue in evaluating embodied energy is the absence of data related to the cost of extraction of natural materials and integrated evaluation of all the processes and chemicals utilized in the fabrication chain. In general terms, the evaluation of the "embodied energy" should account for the energy invested in the product lifecycle considered as a whole, which includes data for transports, manufacturing and disposal/recycling. For those reasons, an accurate estimate of the energy utilized to produce the components needed to fabricate an OT is not trivial, which represents a relevant part of the great uncertainty in classifying it as "green".

Table 6 reports data extracted from two commercial software tools (OPEN LCA and CES Selector) dedicated to the calculation of embodied energy and CO_2 footprint. Only a very limited portion of the materials described above is reported. No data are available for most of polysaccharides, proteins, small organic molecules, and polymers utilized as dielectrics or (semi)-conductors, as well

Table 6. Embodied energy and carbon footprint values of relevant materials for organic transistors. All data have been extracted from OPEN LCA (Green Delta, version 1.10.3, Berlin, Germany, 2006), except from those of glass and paper, which have been extracted from CES selector (Granta Design, Cambridge Engineering Selector (CES) Software, 2019).

Material	Role in OT	Embodied energy [MJ kg^{-1}]	Carbon footprint [kg kg^{-1}]
Glass	Substrate (non flexible)	37.5–41.5	2.2–2.43
Paper	Substrate (flexible)	49–54	1.11–1.23
PMMA	Substrate, coating, gel	94.91769	3.92416
PVA	Substrate, coating, gel	60.4175	2.8817
Melamine	Small molecule dielectrics	92.28233	5.55856
Glucose (from starch hydrolysis)	Small molecule dielectrics	16.77161	1.17416
Silver	Conductor (not "green")	4692.88268	319.61703
Gold	Conductor (not "green")	645299	61559
Magnesium	Conductor ("green")	286.92285	28.23575
Zinc	Conductor ("green")	30.99322	2.82859

as for biodegradable elastomers that can be applied for stretchable substrates. As discussed above, over 99.5% of the mass of a transistor is given by the substrate, which is expected to have the major impact in defining its sustainability.

Interestingly, we note that embodied energy associated to the production of commercial paper is significantly higher than that needed to fabricate soda-lime glass, whereas the average CO_2 footprint is lower. In general, glass and paper can be classified as sustainable substrates, as the carbon footprint associated to their production is limited and both of them can be recycled, or in worst case scenario, disposed without major environmental concerns. On the other hand, gate dielectric polymers such as PVA or PMMA have a relatively high energetic cost, however their contribution to the OT mass is quite limited. The same arguments apply for conductors. Unfortunately, the absence of data related to conductive polymers restricted the comparison among conventional metals, like silver and gold, whose production is greatly energy consuming and in the case of gold poses serious social concerns, and "greener" metals like magnesium and zinc, can make their way in OT for transient or edible electronics in view of their biocompatibility and reduced carbon footprint. An important aspect in this analysis is related to the role played by solvents utilized for raw material extraction, purification and processing has probably the stronger impact, as already discussed in recent papers on chitin/chitosan[83] and pectin extracted through different routes.[145] This issue is illustrated with an example in **Table 7**, which reports the variability of embodied energy and CO_2 footprint associated to the production of starch. We note a strong dependence on the source of extraction. Using potatoes allows for a remarkable reduction of the impact in comparison to other sources, in particular rice, which is characterized by an embodied energy of the same order of magnitude of that required for silver production (Table 6) and a very strong carbon footprint. This example clearly demonstrates that using materials derived from natural sources is not per se sufficient to ensure their low environmental impact. As a consequence, the classification of a transistor (or, in general, an electronic device) as "green" or "sustainable" should not be based only on the type of materials utilized as components, but requires a deeper analysis of the energetic cost of production. Moreover, this example also highlights the importance of a careful selection of the sources and extraction methods. In this regard, developing strategies that enable extraction and purification of raw natural materials with reduced amount of solvents, such as those based on microwave and sonication-assisted methods,[145,146] could help mitigating the energy impact of OT fabrication.

Table 7. Embodied energy and carbon footprint values of different types of starch, obtained from the manipulation of different natural sources. Data extracted from OPEN LCA (Green Delta, version 1.10.3, Berlin, Germany, 2006).

Source of starch	Embodied energy [MJ kg^{-1}]	Carbon footprint [kg kg^{-1}]
Potato	0.77622	0.12804
Rice	4983.83261	787.55635
Pea protein	9.32064	0.75469
Maize	9.61064	0.92187
Wheat	11.61937	1.13517

Overall, the limited number of available data and the critical issues related to the evaluation of the energy and environmental impact make the production of reliable databases extended to all the materials utilized to fabricate green electronic devices one of the most compelling challenges for the near future.

4. Transistor Architectures and Figures of Merit

Various architectures have been used for the fabrication of organic transistors fabricated with green materials and technologies. The adopted architecture depends on the specific materials, solvents, fabrication technology, and operation conditions. Considering the last 10 years, an overview of the various organic transistor architectures, materials, fabrication technologies and figures of merit is shown in **Table 8**. The comparison shows that the most commonly used OFET architectures are bottom-gate top-contacts (BG-TC).[54,109,110,125,147–155] In this architecture the gate and the insulator are deposited before the semiconductor, reducing the semiconductor sensitivity to the roughness and wettability properties of the substrate. On the other side, the roughness of the substrate could be critical for the integrity of the insulator and planarization layer are used for improving the yield.[54,74,147] Other architectures used for the implementation of green OFETs are the bottom-gate bottom-contacts (BG-BC) and top-gate top-contact (TG-BC) structures.[156–159] BG-BC and TG-BC architectures have found application also for the implementation of ion-gated transistors, including both EGOFETs and OECTs.[69,74,160–162] Since in ion-gated transistors an ionically-conductive and electrically-insulating material is used for the electrostatic coupling of the gate with the channel, a simple yet effective implementation approach commonly used for EGOFETs and OECTs is based on lateral-gate bottom-contact (LG-BC) architecture.[163,164] In this structure the gate and the source and drain electrodes are on the same level.

Table 8 shows that most of the approaches focused on the use or development of substrate materials, including paper, starch paper, cellulose, PLGA, caramelized glucose, ecoflex, hard gelatine capsule, natural resin shellac, and polysaccharide.[54,69,74,109,147,149,150,153,155,156,158,163,164] As mentioned in Section 2.1, various planarization materials, including for example PVA, chitosan, and aurin, were used, especially in the case of paper substrates.[54,74,147] Various works also focused on the development of green materials and approaches for the gate insulator. Several approaches focused on natural materials including guanine, adenine, glucose, caffeine, shellac, almond gum, albumen and melanin.[54,109,110,125,151,159] Other approaches were devoted to the development of naturally degradable gate insulators including for example polymethacrylated tannic acid (PMTA), trimethylsilyl cellulose, Fe-Gelatin, and choline-based ionic liquid embedded in polysaccharide.[149,164] The gate insulator is a key component of a transistor and a large capacitance per unit area (C_i) results in both low-voltage operation and large on-current. When a polarizable gate dielectric is used, the typical C_i ranges from $\approx 1 \times 10^{-9}$ F cm^{-2} to $\approx 700 \times 10^{-9}$ F cm^{-2}, and the best values were achieved with high-performance approaches based on self-assembled monolayers[148,153] When ion-based insulators are adopted, the nanoscale ionic-electronic charge compensation results

Table 8. Overview of the various organic transistor architectures, materials, fabrication technologies and figures of merit, from literature of the last 10 years. The "green" functional layer(s), fabrication technologies and the key features when applied for green and sustainable organic transistors are highlighted. The figures of merit include the field-effect mobility (μ_{FE}), threshold voltage (V_T), maximum operating voltage (V_{MAX}), on-current, on-off current ratio (I_{on}/I_{off}), the subthreshold slope (SS) and the degradation time (t_{DEG}). As regards "fabrication technology", TE stands for Thermal Evaporation, SpCo stands for Spin Coating, SoCa stand for Solvent Casting, IP stands for Ink-jet printing, CVD stands for Chemical Vapor Deposition, RF-S stands for RF-sputtering, SP stands for Spray Pyrolysis, SC stands for Spray Coating, L stands for Lamination and BC stands for Blade Coating.

Transistor architecture	Functional layer	Substrate	Semiconductor	Gate Insulator	Gate, source, drain	Fabrication technology	μ_{FE} [$cm^2 V^{-1} s^{-1}$]	C_i [F cm^{-2}]	V_T [V]	V_{MAX} [V]	I_{on} [A]	I_{on}/I_{off} [.]	SS [V dec^{-1}]	t_{DEC} [h]	Key green-features/Target applications	Ref
OFET BG-TC (n-type)	Substrate, semiconductor, gate insulator	Caramelized glucose	Indanthrene yellow G	Guanine+adenine / Al-adenine-guanine	Al, Au, Au	TE, SpCo	0.012 / 0.015	$5.6\ 10^{-9}$ / $23.4\ 10^{-9}$	10	15 / 15	$1.5\ 10^{-7}$ / $1\ 10^{-6}$	$1.5\ 10^{1}$ / $1\ 10^{3}$	6 / 2.5	N.A.	Biocompatible and biodegradable	[54]
OFET BG-TC (n-type)	Substrate, semiconductor, gate insulator	Caramelized glucose	Indanthrene yellow G	Al/adenine/guanine	Al, Au, Au	TE, SpCo	0.015	$23.4\ 10^{-9}$	5	15	$1\ 10^{-6}$	$1\ 10^{3}$	2.5	N.A.	Biocompatible and biodegradable	[54]
OFET BG-TC (n-type)	Substrate, semiconductor, gate insulator	Biodegradable Ecoflex /aurin	Perylene diimide	Adenine / Al-glucose	Al, Au, Au	TE, SpCo	0.01 / 0.01	$3.1\ 10^{-9}$ / $128.8\ 10^{-9}$	2.5 / 3	20	$1\ 10^{-7}$ / $2\ 10^{-7}$	$1\ 10^{3}$ / $1\ 10^{4}$	2.5 / 1	N.A.	Biodegradable	[54]
OFET BG-TC (n-type)	Substrate, semiconductor, gate insulator	Hard gelatine capsule/aurin	Perylene diimide	Guanine and adenine	Al, Au, Au	TE, SpCo	0.02	$5.1\ 10^{-9}$	10	20	$2\ 10^{-7}$	$1\ 10^{5}$	2.5	N.A.	Edible	[54]
OFET BG-TC (p-type)	Semiconductor, gate insulator	Glass	Beta-carotene	Glucose and caffeine	Al, Au, Au	TE, SpCo	0.0004	$1.9\ 10^{-9}$	−70	−100	$2\ 10^{-8}$	$2\ 10^{3}$	11	N.A.	Environmentally safe devices	[125]
OFET BG-TC (p-type)	Substrate, gate insulator	PLGA	DDFTTF	nPVA	Ag, Au, Au	TE, SpCo	0.21	$5.2\ 10^{-9}$	−15.4	−80	$100\ 10^{-6}$	$5.5\ 10^{3}$	5	1680	Biocompatible and bioresorbable	[150]
OFET BG-TC (n/p-type)	Gate insulator	Glass	C60 / Pentacene	Albumen	ITO, Au, Au	TE, SpCo	0.13 / 0.09	$13.25\ 10^{-9}$	1.5 / −8	−20 / 20	$8\ 10^{-6}$ / $1\ 10^{-6}$	$1\ 10^{4}$ / $1\ 10^{4}$	2 / 2.5	N.A.	Natural dielectric	[151]
OFET BG-TC (n/p-type)	Substrate, gate insulator	Natural resin shellac	C60 / Pentacene	Natural resin shellac	Al, Au, Au	TE, SpCo	0.4 / 0.2	N.A.	3 / −3	15 / −15	$8\ 10^{-6}$ / $5\ 10^{-6}$	$1\ 10^{5}$ / $1\ 10^{3}$	1.5 / 3	N.A.	Biocompatible and sustainable	[109]
OFET BG-TC (n/p-type)	Gate insulator	Glass	C60 / Pentacene	Al_2O_3 + trimethylsilyl cellulose	Al, Al, Au	TE, SpCo	0.70 / 0.22	$65\ 10^{-9}$ / $57\ 10^{-9}$	1.3 / −4.7	13 / −12	$2\ 10^{-5}$ / $2\ 10^{-5}$	$1\ 10^{5}$ / $2\ 10^{5}$	0.3 / 0.2	N.A.	High-performance cellulose dielectrics	[152]
OFET BG-TC (p-type)	Substrate, gate insulator	Cellulose	PDPP-PD	Al_2O_3 + trimethylsilyl cellulose	Fe, Fe, Fe	TE, SpCo	0.12	$280\ 10^{-9}$	−5	−10	$5\ 10^{-6}$	$6\ 10^{4}$	1	720	Disintegrable and biocompatible semiconducting polymers	[153]
OFET BG-TC (p-type)	Gate insulator	Glass	P(CDT-BTZ)	Shellac	Al, Au, Au	TE, SpCo	$1.1\ 10^{-3}$ / $2.7\ 10^{-5}$ / 0.1	N.A.	N.A.	−60	$8\ 10^{-7}$ / $1\ 10^{-8}$ $1\ 10^{-6}$	$1\ 10^{2}$ / ^{5} 102 / $5\ 10^{3}$	20 / 10 / N.A.	N.A.	Natural dielectric	[110]
OFET BG-TC (p-type)	Gate insulator	PVA	Pentacene	PMTA	Al, Au, Au	SoCa, TE, SpCo	0.14	$28\ 10^{-9}$	−6	−20	$4\ 10^{-6}$	$5\ 10^{3}$	4	192	Naturally degradable dielectric	[154]
OFET BG-TC (p-type)	Substrate	Starch paper	Pentacene / DNTT / PTAA	Parylene-C	Ag, Au, Au	TE, CVD	0.37 / 0.36 / 0.013	$3.49\ 10^{-9}$	−21.3 / −15.7 / −13	−40	$5\ 10^{-6}$ / $5\ 10^{-6}$ / $2\ 10^{-7}$	$4.9\ 10^{3}$ / $1.6\ 10^{5}$ / $6.9\ 10^{4}$	N.A.	576	Eco-friendly flexible, transparent and disposable starch paper	[155]
OFET TG-BC (p-type)	Substrate, gate insulator	Paper/starch/ ethylcellulose	P3HT / P3HT:PS	ethylcellulose	Ag, Ag, Ag	IP	$1.97\ 10^{-4}$ / $7.09\ 10^{-3}$	$5.5\ 10^{-9}$	N.A.	−60	$2\ 10^{-8}$ / $7\ 10^{-7}$	$1\ 10^{2}$ / $1\ 10^{4}$	10 / 5	N.A.	Edible and printed	[156]
OFET TG-BC (n-type)	Substrate, gate insulator	Paper/starch/ ethylcellulose	29-DPP-TVT	ethylcellulose	Ag, Ag, Ag	IP	0.15 / 0.08	$5.5\ 10^{-9}$	N.A.	60	$8.31\ 10^{-6}$ / $8\ 10^{-6}$	$1\ 10^{4}$ / $1\ 10^{4}$	5 / 7	N.A.	Edible and printed	[156]

Table 8. Continued.

Transistor architecture	Functional layer	Substrate	Semiconductor	Gate Insulator	Gate, source, drain	Fabrication technology	μ_{FE} [$cm^2\ V^{-1}\ s^{-1}$]	C_i [$F\ cm^{-2}$]	V_T [V]	V_{MAX} [V]	I_{on} [A]	I_{on}/I_{off} [.]	SS [$V\ dec^{-1}$]	t_{DEC} [h]	Key green-features/Target applications	Ref
OFET BG-TC (p/n-type)	Substrate, gate insulator	Polypropylene carbonate	Pentacene / PTCDI-C8	Polypropylene carbonate	ITO, MoO_3-Al, Au	TE, SpCo	0.14 / 0.026	$9.8\ 10^{-9}$	−15.7 / 12.4	−60 / 60	$1\ 10^{-5}$ / $1\ 10^{-6}$	$1\ 10^{5}$ / $1\ 10^{3}$	N.A.	N.A.	Boost consumption of CO_2	[157]
OFET BG-TC (p-type)	Substrate	Paper/PVA	Tips-Pentacene:PS	PVP/HfO_2	Ag, Au, Au	TE, SpCo	0.44	$9.0\ 10^{-9}$	0	−10	$1\ 10^{-6}$	$1\ 10^{5}$	1	NO	Long-term stable operation and shelf-life	[147]
OFET BG-TC (n/p-type)	Substrate	Banknote	N1100 / DNTT	AlOx / SAM	Al, Au, Au	TE	0.15 / 1.12	$700\ 10^{-9}$	1.6 / −1.4	3 / −3	$1\ 10^{-6}$ / $5\ 10^{-6}$	$4\ 10^{6}$ / $1\ 10^{7}$	0.17 / 0.1	N.A.	Low-voltage high-frequency	[148]
OFET BG-TC (p-type)	Substrate, gate insulator	Paper	Pentacene	Fe-Gelatin	Al, Au, Au	RF-S, SpCo	8	N.A.	−1.4	−8	$3\ 10^{-6}$	$5\ 10^{2}$	0.6	N.A.	Biodegradable electronics	[149]
OFET BG-BC (n/p-type)	Substrate	Paper	N1400 / TIPS pentacene	Parylene-C	PEDOT:PSS, PEDOT:PSS, PEDOT:PSS	IP, CVD	0.01 / 0.2	$9\ 10^{-9}$	0.5 / −0.4	4 / −4	$1.2\ 10^{-7}$ / $1.5\ 10^{-6}$	$4\ 10^{2}$ / $6\ 10^{3}$	0.6 / 0.5	N.A.	Printed paper electronics	[158]
OFET BG-BC (p-type)	Gate insulator	Glass	DPPTTT / PMMA	Almond gum	Au, Au, Au	TE, SP, SpCo	0.75	$8\ 10^{-9}$	-0.8	−3	$2\ 10^{-6}$	$1\ 10^{3}$	0.27	N.A.	Biodegradable gate dielectric	[159]
OFET BG-BC (p-type)	Gate insulator	Glass	DPPTT/PMMA	Almond gum	Au, Au, Au	TE, SP, SpCo	0.75	$8\ 10^{-9}$	-0.8	−3	$1\ 10^{-6}$	$1\ 10^{3}$		N.A.	Biocompatible and natural insulator	[159]
EGOFET TG-BC (n-type)	Gate insulator	Silicon	ZnO / P3HT	Cellulose ionogel	Au, Al, Al	TE, SC, L	75 / N.A.	$15\ 10^{-6}$	0.25	1 / −1	$5\ 10^{-3}$ / $1.5\ 10^{-6}$	$5\ 10^{4}$ / $1\ 10^{3}$	0.5 / 0.1	N.A.	Cellulose-based paper electronics	[160]
EGOFET LG-BC (p-type)	Substrate	Paper	P3HT/PLLA	PS:PEO:PS + EMIM:TFSI	Au, Au, Au	TE, SpCo	N.A.	N.A.	0.25	−0.1	$3\ 10^{-5}$	$1\ 10^{3}$	0.25	N.A.	Paper transistors	[163]
EGOFET BG-BC (p-type)	Substrate	Paper/chitosan	P3HT	P(VDF-HFP) + [EMI][TSFA]	Au, Au, Au	TE, SpCo	0.97	$10\ 10^{-6}$	2	−2	$1\ 10^{-3}$	$1\ 10^{4}$	0.4	N.A.	Resusable and enviromentally-safe	[74]
EGOFET TG-BC (p-type)	Substrate, gate insulator	Paper	P3HT/PLLA	Reline / Csorb	Au, Au, Au	TE, SpCo	0.5 / 2	$40\ 10^{-6}$ / $70\ 10^{-6}$	1.25	−0.8	$4\ 10^{-8}$ / $2.4\ 10^{-7}$	$5.7\ 10^{3}$ / $6.9\ 10^{3}$	0.07 / 0.09	N.A.	Enviromentally-friendly	[69]
OECT TG-BC (p-type)	Gate insulator	Glass	PEDOT:PSS	Melanin	Au, Au, Au	TE, SpCo	N.A.	$10.3\ 10^{-3}$	0.9	−1	$2\ 10^{-4}$	$1\ 10^{2}$	0.2	N.A.	Ion-gel for bioelectronics	[161]
OECT TG-BC (p-type)	Gate insulator	Glass	P(DPP-DTT-MS)-PE	P(VDF-HFP) + [EMI][TFSI]	PEDOT:PSS, PEDOT:PSS, PEDOT:PSS	IP, BC	1	$110\ 10^{-6}$	-0.5	−1.2	$7.5\ 10^{-4}$	N.A.	N.A.	N.A.	Green solvents	[162]
OECT LG-BC (p-type)	Substrate, gate insulator	Choline-Based Ionic Liquid and Polysaccharide	P3CPT	Choline-Based Ionic Liquid and Polysaccharide	Au, Au, Au	TE, SpCo	0.98	$40\ 10^{-6}$	N.A.	−2	$4\ 10^{-4}$	$1\ 10^{3}$	0.4	2	Biocompatible and biodegradable	[164]

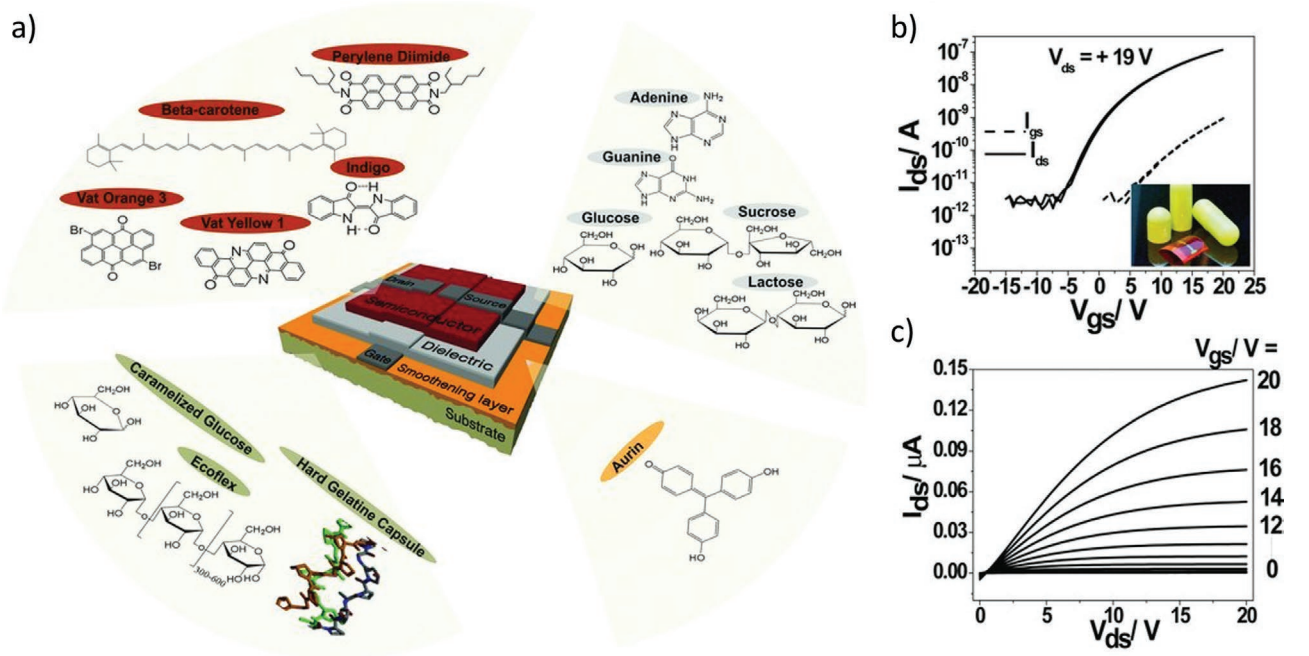

Figure 9. Organic transistors fabricated with natural or natural-inspired materials. a) Bottom-gate top-contact OFET fabricated with various substrate, gate insulator and semiconducting natural or natural-inspired materials. b) Transfer and c) output characteristics of an edible OFET on a hard gelatin capsule substrate. Aurin is used as smoothing layer. The gate dielectric is made of adenine and guanine. The organic semiconductor is perylene diimide. Reproduced with permission.[54] Copyright 2010, Wiley-VCH.

in C_i in the range 1×10^{-6}–100×10^{-6} F cm^{-2}, thus enabling the sub-volt transistor operation.[69,74,161,162,164] Finally, the few approaches addressing the development of green semiconductors include indanthrene yellow G, beta-carotene, PDPP-PD, and P(DPP-DTT-MS)-PE polymers. We note that the development of green organic semiconductor is particularly challenging, and to date the best performance were demonstrated by Bao and co-workers.[153] More in detail, they developed a fully disintegrable and biocompatible polymer transistor with hole field-effect mobility of up to 0.12 cm^2 V^{-1} s^{-1} operating at a negative maximum voltage of –10 V with an on/off current ratio >10^4. Interestingly, BG-TC OFETs were fabricated on ultrathin cellulose (800-nm-thick) biodegradable substrates with iron source and drain electrodes. The transistors were also integrated in unipolar pseudo-CMOS circuit configuration and both inverters and logic gates were demonstrated. The logic circuits were fully disintegrated after 192 h in a pH 4.6 buffer solution, finding relevant application in environment-friendly transient electronics.

The pioneering work by Irimia-Vladu et al. demonstrated a wide set of biocompatible and biodegradable materials for OFETs. As displayed in **Figure 9**, OFETs based on a BG-TC architecture were fabricated with various substrate materials, gate insulators and semiconductors. The use of materials from nature are a key approach for environmentally-safe devices in low-cost, large volume, disposable or throwaway electronic applications, such as in food packaging, plastic bags, and disposable dishware. Figure 9b–c shows the transfer and output characteristics of edible OFET fabricated on a gelatin capsule. A smoothing layer of aurin was used to reduce the roughness of the substrate. Guanine and adenine layers were deposited in vacuum and the organic semiconductor perylene diimide was deposited by spin-coating. Evaporated gold was used for gate, source and drain electrodes. We note that although on one side evaporation is an high-energy budget process, on the other side it is solvent-free when shadow masks are used. The edible OFETs showed a field-effect mobility $\mu = 0.02$ cm^2 V^{-1} s^{-1}, a threshold voltage $V_T = 10$ V and a maximum on-current of 2×10^{-7} A at $V_G = -20$ V. The output characteristics display distinct linear and saturation regions, with flat output current when operating in saturation.

Much larger attention has been paid on paper-based organic transistors. Thanks to its renewable nature, low cost, ubiquity, and flexibility, paper can be a possible alternative to plastic in next-generation flexible electronics.[63,165–167] To date, several researchers have contributed to the development of OFETs on paper substrates and an excellent review by Zschieschang and Klauk specifically covered organic transistors on paper.[68] Along this research direction, Klauk and co-workers demonstrated low-voltage high-frequency operation organic transistors and circuits on commercial and banknote paper substrates. Low-voltage and high-frequency operation are very important features when organic transistors are used in portable applications relying on mobile power supplies and harvesting devices. **Figure 10**a shows the schematic cross-section of the p-type and n-type organic transistors fabricated on banknotes for active anti-counterfeiting or tracking features.[148] The p- and n-channel were fabricated by using dinaphtho[2,3-b:2′,3′-f]thieno[3,2-b]thiophene (DNTT)[168–172] and *N*,*N*′-bis(2,2,3,3,4,4,4)heptafluorobutyl-1,7-dicyano-perylene-(3,4:9,10)-tetracarboxylic diimide (Polyera ActivInk N1100)[173,174] organic semiconductor, respectively. These semiconductors were chosen for

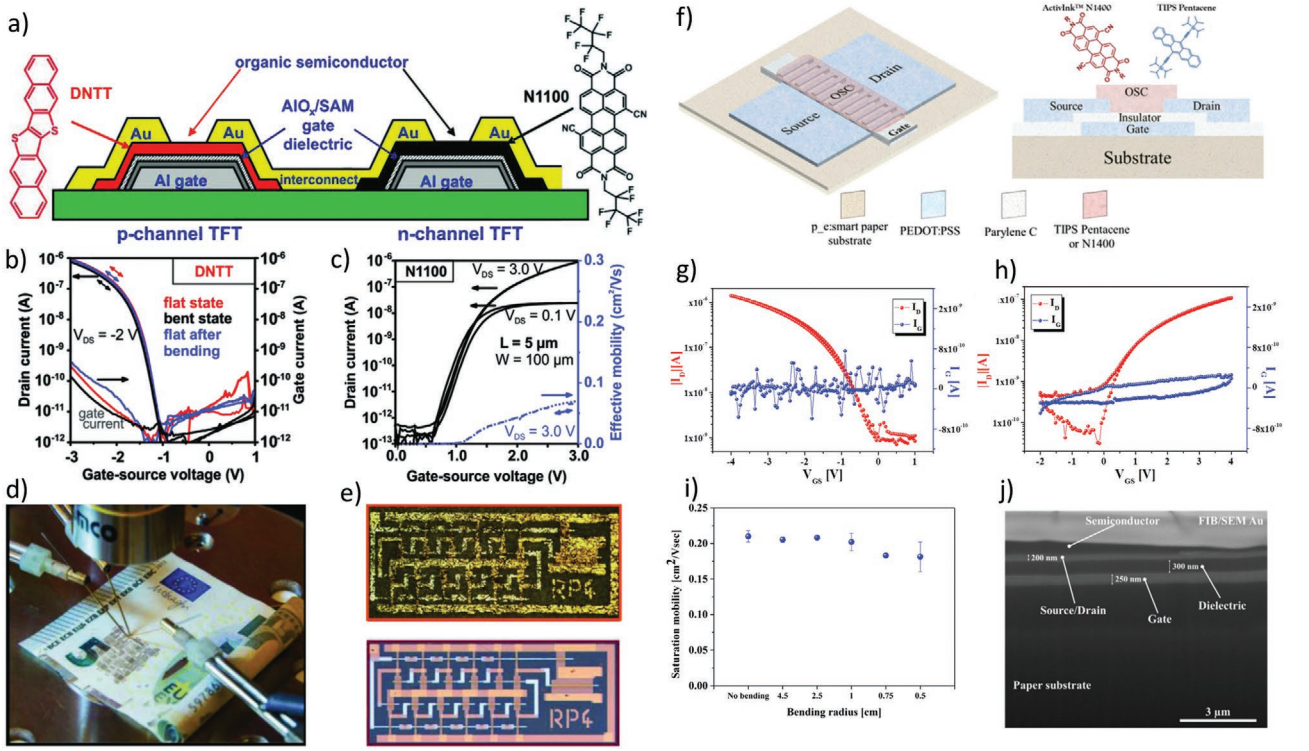

Figure 10. Organic transistors and circuits fabricated on paper substrates. a) Schematic cross-section of p-type (DNTT) and n-type (N1100) BG-TC OFETs connected in an inverter configuration. The Molecular structures of the organic semiconductors DNTT and Polyera ActivInk N1100 are showed. b) Transfer characteristics of a DNTT OFET on a banknote before, during and after bending. The channel length and width are 100 µm and the gate-to-contact overlap is 20 µm. Transfer characteristics of a N1100 OFET on a banknote. c) Transfer characteristics of a N1100 OFET fabricated on a banknote. d) Photograph of OFETs and circuits fabricated a banknote. e) Photographs of unipolar ring oscillators fabricated on a banknote (top) and on plastic PEN foil (bottom). Reproduced with permission from.[148] Copyright 2018, Wiley-VCH. f) Schematic 3D view and cross-section of BG-BC printed OFETs on commercial paper substrate. g) Transfer characteristic and gate leakage current of a p-type TIPS pentancene OFET. h) Transfer characteristic gate leakage current of a n-type ActiveInk N1400 OFET. i) Average saturation mobility of p-OFETs before and during bending at different radius (R = 45, 25, 10, 7.5, and 5 mm). Error bars are the standard deviation. j) FIB-SEM image of an OFET cross-section. The various materials are highlighted. Reproduced with permission.[158] Copyright 2020, Wiley-VCH.

their relatively high carrier mobilities and good shelf-life stability.[175,176] The OFETs were based on a BG-TC architecture and both the metals and the organic semiconductors were thermal evaporated. A high-specific capacitance (C_i) gate insulator was obtained by oxidation of the Al gate and subsequent chemical grafting of alkylphosphonic acid SEM. The transfer characteristics of a DNTT-based OFET fabricated on a banknote is displayed in Figure 10b. The TFT showed a field-effect mobility of 1.1 cm^2 V^{-1} s^{-1}, a threshold voltage of –1.4 V, an on/off current ratio of 10^5, and a subthreshold swing of 0.1 V dec^{-1}. The gate current was below 10^{-9} A, confirming the excellent quality of the oxide/SAM gate dielectric. The stability of the OFET against mechanical deformations of the substrate was investigated by measuring the I_D–V_G characteristics before and after bending, which resulted in a tensile strain of about 3%. No appreciable variations were recorded. The authors investigated the impact of the surface roughness of the substrate by fabricating various organic transistors with the very same materials and process on three different substrates, namely glass (RMS roughness 0.3 nm), PEN (RMS roughness 1 nm), and banknote (RMS roughness 190 nm). The effect of the surface roughness on the carrier mobility was clearly observed since the measured mobilities consistently decreased from 3.6 to 1.1 cm^2 V^{-1} s^{-1} while the gate current consistently increased from 10^{-11} to 3×10^{-10} A, with the increasing the substrate roughness. These effects were attributed to the detrimental impact of the surface roughness on the degree of molecular ordering in the organic semiconductor film and to the density of structural defects in the gate dielectric induced by the surface topology of the substrate.[177] Figure 10c shows the measured I_D–V_G characteristics as function of V_D of n-type OFETs fabricated on banknotes. The OT showed a record field-effect mobility of 0.17 cm^2 V^{-1} s^{-1}, an on/off current ratio of 4×10^5, and a subthreshold swing of 0.17 V dec^{-1}. Unipolar (p-type) and complementary inverters and ring oscillators fabricated on a banknote are displayed in Figure 10d. The ring oscillators enabled to evaluate the switching delay per stage. The best performance, achieved with a minimum channel length of 1 µm and at a supply voltage of 4 V, were 2.5 and 10 µs in the case of unipolar and complementary oscillators on banknotes, respectively, As a comparison, when the circuits were fabricated on PEN substates, the switching delay of unipolar and complementary circuits were 0.58 and 6 μs, respectively. The slightly reduced performance was attributed to the reduced mobility and increased gate current due to the increased surface roughness. Figure 10e shows a comparison between the ring oscillators fabricated on a banknote and on

PEN, demonstrating the strong impact of the surface roughness on the deposited materials. Despite this, circuits operating at few volts and frequencies of several hundred kilohertz directly on paper substrates were demonstrated.

Other alternative approaches for the development of OFETs on paper substrates rely on the use of additive low-temperature fabrication methods. Printing techniques have gained interest for the rapid, precise and reproducible deposition of functional material. In this respect, inkjet printing on paper is very competitive than other approaches. As recently demonstrated by Casula et al. low-voltage all-organic transistors and complementary circuits can be ink-jet printed on commercially available paper substrates.[158] The proposed organic transistors are based on a bottom-gate bottom-contact architecture, as schematically depicted in Figure 10f. More in detail, BG-BC OFETs were fabricated on a 185 μm thick flexible paper substrate with a specific weight of 190 g m^{-2} and a surface coated nonporous primer layer with a surface roughness of about 0.5 nm. OT fabrication was based on two large-area techniques, namely ink-jet printing of electrodes and semiconductors and chemical-vapor-deposition (CVD) of the gate insulator. Gate, source, and drain were fabricated by ink-jet printing the commercially-available biocompatible conductive polymer PEDOT:PSS. Parylene C film was deposited with CVD method obtaining a $C_i = 9 \times 10^{-9}$ F cm^{-2}. P-type OFETs were obtained by ink-jet printing of TIPS pentacene while for n-type OFETs the ActiveInk N1400 was spin-coated. The process required a low thermal budget, with a maximum process temperature of 60 °C. The I_D–V_G characteristics of the fabricated p- and n-type OFETs are displayed in Figure 10g,h, respectively. In both cases the gate leakage current was of the order of 10^{-10} A, which is comparable with the drain off-current. The p-type OFETs showed an average threshold voltage of –0.4 V, a subthreshold slope of 0.5 V dec^{-1}, an on/off current ratio $>10^3$, and a field-effect mobility in saturation regime of 0.2 cm^2 V^{-1} s^{-1}. The n-type OFETs showed comparable parameters, viz. an average threshold voltage of 0.5 V, a subthreshold slope of 0.6 V dec^{-1}, an on/off current ratio $> 10^2$, and a field-effect mobility in saturation regime of 0.01 cm^2 V^{-1} s^{-1}. To assess the device stability under operating conditions, the author measured over 500 double-sweep transfer characteristics and observed a threshold voltage variation limited to a few hundreds of millivolts for the p-type OFETs and about 1 V for the n-type OFETs. The mobility was less affected by the bias stress and it reduced of about 15% and 10% in the case of p-type and n-type OFET, respectively. The OFETs mobility was also monitored as a function of the bending radius and bending cycles. The minimum bending radius was equal to 5 mm and up to 200 bending cycles were performed. The saturation field-effect mobility of both the p-type and n-type OFETs was not affected by the mechanical stress. As displayed in Figure 10i the maximum mobility reduction was less than 10% in the case of p-type OFETs with a bending radius < 7.5 mm. To verify the nanoscale OFET structure, focused-ion beam scanning electron microscopy (FIB-SEM) was performed. A device cross section is shown Figure 10j, where the stacking of various layers composing the device is clearly visible. The FIB-SEM image showed that the deposited materials did not penetrate the substrate and formed a continuous layer, which is fundamental for the development of printed electronics. FIB-SEM analysis also enabled a quantitative evaluation of different layers thicknesses, proving the integrity of the OFET architecture fabricated on commercially available paper substrate.

Another transistor component that is receiving increasingly attention is the gate insulator, especially the class of biomaterial-based insulators. Biomaterials are biodegradable, bioresorbable, biocompatible, typically environmentally friendly, and do not require chemical synthesis. Along this research direction, an interesting approach by Guo and co-workers, proposed the use of chicken albumen dielectrics in OFETs.[151] The albumen was obtained directly from eggs without further extraction. Albumen is composed of 40 proteins and upon irreversible denaturation under thermal processes, the disulfide bonds formed between cysteine groups cross-link the protein molecules. The most significant function of protein disulfide bonds in a dielectric layer of OFETs is the reduction of gate leakage current in albumen film without any additional additives. The authors found that the hydrophobicity of albumen dielectrics was tuned by means of the thermal treatment temperature and an optimized baking procedure was proposed. Upon spin-coating, the albumen films were baked at 100 °C for 10 min, 120 °C for 10 min, and 140 °C for 10 min to ensure the formation of a smooth and dense film for device applications. The proposed OFETs were based on BG-TC architecture, as schematically depicted in **Figure 11**a. OFETs were fabricated on glass substrates and ITO was the gate electrode. Then albumen was spin-coated and properly baked. P- and n-type OFETs were obtained by thermal evaporation through a shadow mask of pentacene and C_{60} organic semiconductors, respectively. Finally, Au source and drain electrodes were evaporated. Figures 11b,c shows the measured forward and backward transfer characteristics of pentacene and C_{60} OFETs with albumen dielectrics. Negligible hysteresis was displayed thanks to natural protein properties, hydrogen-bond inter-changes, and disulfide-bond crosslinking in irreversible thermal denaturation without any additional crosslinking agents. The pentacene- and C_{60} albumen OFETs showed on-currents $> 10^{-6}$ A at the maximum gate voltage $|V_G| = 25$ V, threshold voltages of –8 and 1.5 V, on/off ratio of $\approx 10^4$, and leakage currents of the order of 10^{-10} A. The field-effect mobility of p- and n-type OFETs were 0.09 and 0.13 cm^2 V^{-1} s^{-1}, respectively. Overall, this performance demonstrated that albumen is an excellent dielectric in both pentacene and C_{60} OFETs. The specific capacitance of the albumen dielectrics was thoroughly investigated by means of metal–insulator–metal (MIM) structures. Figure 11d compares the measured capacitance per unit area of albumen dielectrics with PMMA and PS dielectrics. The latter are typical dielectric materials used in OFETs. Investigating the frequency range 10^2–10^6 Hz, at 25 V, the capacitance per unit area of albumen was $>12 \times 10^{-9}$ F cm^{-2}, viz. almost the double of that obtained with PMMA and PS. A relative dielectric constant of albumen in the range 5.3–6.1 was obtained, in agreement with other reports.[178] The larger specific capacitance resulted in a larger driven current, as readily visible by the output characteristics (I_D–V_D) display in the inset of Figure 11d. The influence of environmental conditions on albumen dielectrics was also investigated by storing the MIM devices in nitrogen (relative humidity RH < 0.1%), ambient (RH% = ≈50%), and water vapor (RH > 90%) conditions at room temperature. As displayed in Figure 11e the

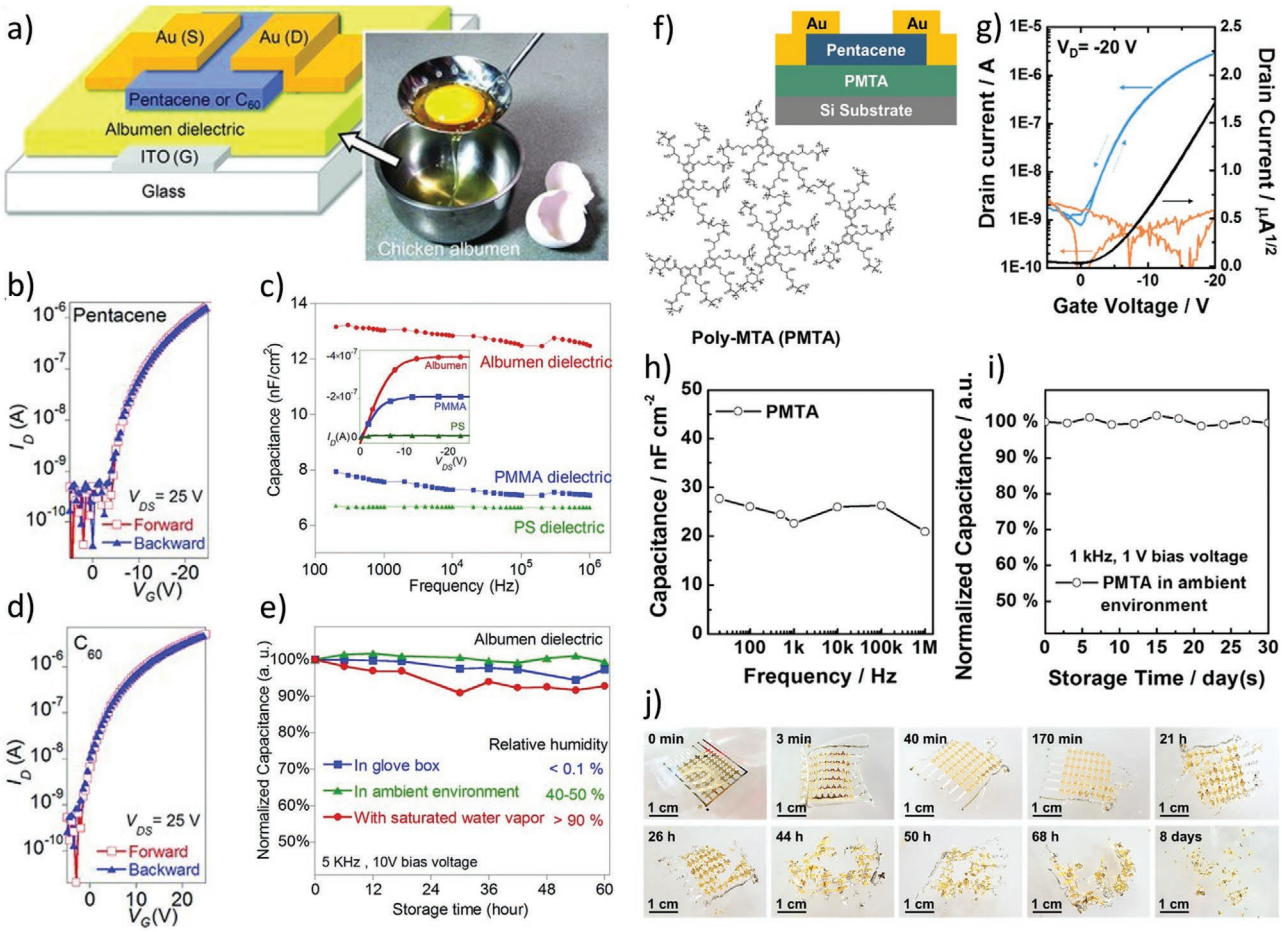

Figure 11. Organic transistors fabricated with naturally degradable gate dielectrics. a) Schematic structure of a BG-TC OFET fabricated with albumen dielectrics. b) Transfer characteristics of a p-type albumen/pentacene OFET. c) Transfer characteristics of a n-type albumen/C_{60} OFET. d) Capacitance-frequency characteristics of albumen, PMMA, and PS MIM devices. Inset: output currents of pentacene OFETs with albumen, PMMA, and PS dielectrics. Reproduced with permission.[151] Copyright 2011, Wiley-VCH. f) Schematic cross-section of poly-MTA (PMTA) and of a BG-TC OFET fabricated with PMTA. g) Drain and gate current as a function of the gate voltage of a p-type pentacene OFET. h) Capacitance-frequency characteristics of PMTA devices. i) Percentage variation of the PMTA capacitance as a function of storage time in ambient environment. j) Degradability test of PMTA/pentacene OFETs on PVA substrates immersed in PBS buffer solution at 35°C. Reproduced with permission.[154] Copyright 2018, Elsevier.

albumen capacitance was stable over 60 h either in nitrogen and ambient. Remarkably, a slightly decrease of <10% was obtained for the MIM devices stored in water vapor conditions. The excellent electrical and stability properties of albumen-based OFETs allowed the fabrication of flexible complementary inverters operating at supply voltages of 15 and 20 V showing static gains of –15.3 and –20, respectively.

More recently, the concept of naturally degradable dielectric materials has been further investigated.[54,69,110,125,149,151,154,156,159–161,164] Along this research direction, Kim and co-workers suggested the poly-methacrylated tannic acid (PMTA), derived from natural tannic acid, as a naturally degradable dielectric material for reducing e-waste.[154] Tannic acid (TA) is abundant in nature, inexpensive, a "green" material that can be degraded by soil bacteria, and it is also edible.[179,180] However, the molecular weight of TA is too small and thus unsuitable for the fabrication of the dense structures needed for robust electrical materials. To overcome this limitation, the authors substituted the abundant hydroxyl groups in TA with methacrylate groups forming the dense structure of PMTA. Interestingly, although methacrylate groups in methacrylated tannic acid (MTA) formed robust bonding, PMTA still contains many ester groups, which can be easily hydrolyzed making PMTA by-products soluble in water.[181]

The BG-TC OFET architecture and the molecular structure of PMTA are displayed in Figure 11f. Gate, source, drain, and semicondutor were deposited by thermal evaporation while PMTA was deposited by spin coating. The measured drain and gate current as a function of the gate voltage are displayed in Figure 11g. The OFETs show a maximum on-current of 3×10^{-6} A at the maximum $V_G = -20$ V, an on-off current ratio $> 10^4$ and the gate leakage current was $< 3 \times 10^{-9}$ A. The forward and backward V_G sweep shows no hysteresis even if no surface treatment of the PMTA layer was used. The maximum field-effect mobility obtained with untreated PMTA layer was 0.14 $cm^2\ V^{-1}\ s^{-1}$ and it increased to 0.23 $cm^2\ V^{-1}\ s^{-1}$ when the PMTA was treated with hexamethyldisilazane (HMDS) SAM. The specific capacitance of a PMTA MIM device as a function

of frequency is displayed in Figure 11h The PMTA capacitance per unit area was in the range 20–28 × 10^{-9} F cm^{-2} and a non-monotonous trend was observed by increasing the frequency from 2 to 10^6 Hz. Moreover, PMTA showed an electrical breakdown strength as high as 5.4 MV cm^{-1}, which is more than the double of that obtained with PMMA, PS and PVP dielectrics (in all cases the MIM thickness was 154 nm). Figure 11i displays the variation of PMTA capacitance measured as a function of time, demonstrating that the capacitance of PMTA dielectric insulators is stably for over 30 days. The degradability test of the OFETs fabricated with PMTA insulating layer on PVA substrates was tested by immersing the devices a PBS solution (pH 7.4) at 35 °C. As displayed Figure 11j the OFETs were fully degraded after 8 days. Further tests in 3.5 wt% NaCl solution at 35 °C (close conditions to seawater) demonstrated fully decomposed OFETs within 19 days. The good stability in ambient environment, the quite fast degradation in salt water conditions and considering that the by-products of PMTA degradation are non-toxic,[182] health risks during waste disposal show good potential for reduction of e-waste.

Very recently, biocompatible and biodegradable organic transistors based on the OECT architecture have been proposed by Kim and co-workers.[164] They developed a solid-state electrolyte composed of levan polysaccharide, a transparent, flexible, and water-soluble biomaterial,[183] and two ions, namely choline and malate. Choline can be found in many plants, eggs, and animals and it is a class of quaternary ammonium compound that can be dissolved in water.[184] Malate contributes to sour taste of fruits.[185] Relevantly, the biocompatible, biodegradable, and solid-state electrolyte was used for both the gate insulator and the substrate of the OECTs. **Figure 12**a shows the schematic 3D view of the lateral-gate bottom-contact (LG-BC) OECT architecture. The Levan-Based Solid-State Electrolyte (LSE) was fabricated by dry casting of a solution mixed with levan and ionic liquid synthesized from choline, malate ions, and evaporating solvent. Dry casted freestanding LSE film showed 98% transmittance in the visible region. The p-type semiconducting polymer poly(3-hexylthiophene), poly[3-(5-carboxypentyl) thiophene-2,5-diyl] (P3CPT) was deposited using transfer method, and Cr/Au electrodes were deposited by thermal evaporator using shadow mask. A 100 µm thick LSE film was used as substrate as well as solid-state electrolyte. We note that the various components of the organic transistor, including the semiconducting polymers based on polythiophene, are biocompatible and can also be used in biological applications.[186–188] The semiconductor polymer was spin-coated on oxygen plasma treated PDMS mold and placed on the LSE film. The semiconducting polymer was transferred on the LSE film by the coated PDMS at 90 °C for 20 min.

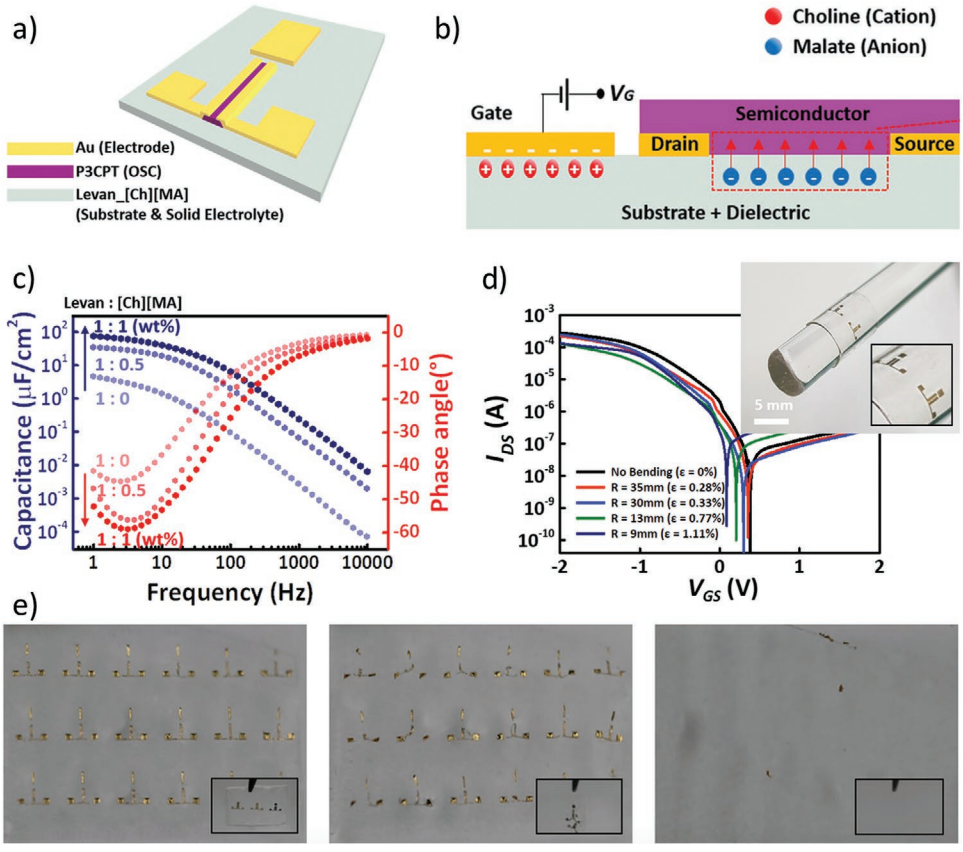

Figure 12. Biocompatible and biodegradable organic ion-gated transistors. a) Schematic 3D view of the LG-BC organic electrochemical transistor (OECT) architecture and relevant materials. b) Simplified cross-section and the working principle of the LG-BC OECT. c) Capacitance per unit area and phase angle as a function of frequency for various Levan: [Choline][Malate] ratios. d) Transfer characteristics as a function of the bending radius. Inset: photograph of the fabricated organic transistors under bending. e) Photographs showing water-solubility when the organic transistors were immersed in deionized water for 0 (left), 30 (middle), and 120 (right) minutes, respectively. Reproduced with permission.[164] Copyright 2020, Wiley-VCH.

The simplified cross-section and the working principle of the organic transistor are displayed in Figure 12b. The transistor gaiting relies on the ion transport within the solid-state electrolyte and the ionic-electronic interaction at the electrolyte/polymer interface.[189–191] Depending on the applied gate voltage, the polymer switches from ion impermeable to ion permeable operation. More in detail, at low gate voltage ($|V_G| < 0.5$ V) the ions cannot penetrate the P3CPT semiconductor and a single-interface electric-double-layer (EDL) is obtained, resembling the EGOFET architecture. By contrast, at high gate voltage ions penetrate the semiconductor and a volumetric EDL is obtained, as in conventional OECT operation. Since ions can drift in the LSE accumulating at the gate/electrolyte and electrolyte/semiconductor interfaces, it is not required that the gate is aligned to the channel. The gate can be placed on the same level of the source and drain and this greatly simplifies the device fabrication. In addition, because of the nanoscale ionic-electronic charge compensation, the gate capacitance per unit area is large, thus allowing low-voltage operation. Electrochemical impedance spectroscopy was used for the characterization of the LSE capacitance per unit area as a function of frequency. A frequency range from 1 to 10^4 Hz was scanned and various Levan: [Choline][Malate] ratios were explored. Figure 12c shows that in all the cases the capacitance per unit area significantly reduced by increasing the frequency. The maximum capacitance was as high as 1×10^{-4} F cm^{-2} and at the maximum frequency it reduced down to 10^{-8} F cm^{-2} considering the best material 1:1 wt% Levan: [Choline][Malate]. Importantly, adding choline-based ionic liquid dramatically increased EDL capacitance of LSE. The more ionic liquid in the LSE, the closer capacitive behavior was observed.

A photograph of the fabricated organic transistors under bending is displayed in the inset of Figure 12d. The impact of the mechanical stress was investigated by measuring the transfer characteristics as a function of the bending radius. Figure 12d shows that without bending (no strain) the maximum on-current was 2×10^{-4} A at the maximum (negative) gate voltage V_G = -2 V and the on-off current ratio was $>10^3$, in agreement with state-of-art OECTs fabricated with conventional photolithographic and printing methods.[192–195] The calculated maximum transconductance was about 2×10^{-3} S at $V_{DS} = -1$ V (OECT channel length and width = 1000 μm). As the degree of cross-linking of the biodegradable LSE increased, the electrolyte and organic transistors on the electrolyte enhanced the reliability of electrical performance against bending. Various electrical characteristics measured as a function of the bending radius and stretching (Figure 12d) demonstrated that the LSE OECTs were robust to the mechanical stress. In addition, biocompatibility and immune response was accurately evaluated by in vivo experiments of OTs implanted subcutaneously into rats. After a natural acute immune response at the initial stage of implantation, over time (5 days), the distribution of macrophages of the M2 phenotype increased and the tissue was remodeled as soon as all the implanted materials were biodegraded. Figure 12e shows dissolution behavior of organic transistor arrays when immersed in deionized water at room temperature. LSE completely dissolved within 2 h. LSE film and semiconducting polymer reacted with water and slowly dissolved, while gold electrodes were dispersed in water or any other bio-solution like buffer solution, cerebrospinal fluid as the substrate dissolved. The excellent biocompatibility and biodegradability properties combined with the mechanical stability and the low-voltage operation, allowed the measurements of ECG signals directly on the organs, as for example the heart of rat, opening opportunities also for implantable and resorbable bioelectronics.

5. Integration Approaches and Technologies

Conventional manufacturing of traditional silicon electronics involves expensive and time-consuming fabrication processes including high-temperature doping, vacuum-based deposition, photolithography, as well as dry/wet etching. In general, biocompatible and biodegradable materials are not compatible with the standard etching processes and several techniques have been utilized to fabricate and pattern green materials. Those techniques can be classified according to three main categories, namely vacuum-based mask deposition, transfer printing, and solution-based printing. So far, conventional vacuum mask-based deposition is the mostly used fabrication scheme. This techniques use shadow masks to define the layout of devices and offer the advantage of avoiding solvent compatibility issues, as typically experienced with photolithographic methods.[196] Many bioresorbable electronics materials have been processed into functional layers by this scheme, as for instance on silk.[197,198] However, vacuum based mask deposition is not applicable to circuits with highly complicated designs due to the limited resolution and possible diffusion of deposited materials. Moreover, the choice of substrates is narrowed because the temperature of substrate should be kept well below its glass transition temperature during the deposition to avoid deformation or degradation.[199]

Using vacuum-based mask deposition techniques, Bao et al. first reported a thin film p-channel 5,50-bis-(7-dodecyl-9H-fluoren-2-yl)-2,20-bithiophene transistor fabricated on a poly(lactic-co-glycolic acid) (PLGA) substrate with a PVA gate dielectric.[199] We note that PLGA has been approved by the US Food and Drug Administration (FDA) and it is widely employed in pharmaceutical, medical, and industrial fields due to its biocompatibility, biodegradability, non-toxicity. The transistors fabricated on PLGA showed a hole mobility of 0.253 cm^2 V^{-1} s^{-1}, similar to the one achieved with an OFETs fabricated with the same semiconductor but on Si substrate, and an on/off ratio of 9.4×10^3.[200] Since then, PLGA has also been utilized in organic electrochemical transistors (OECTs)[201] as well as in water-gated OFET[202] as a biodegradable substrate. Moreover, cellulose has been used as OFET substrate as well.[203] Recently, Bao et al. reported an ultrathin, ultralightweight cellulose substrate for transient electronic applications.[153] **Figure 13**a shows a fully biodegradable and biocompatible BG-TC OFET fabricated on an ultrathin cellulose (800-nm-thick) substrate using vacuum-based mask deposition techniques. More in detail, the gate, source, and drain electrodes were deposited by thermal evaporation through a shadow mask, the Al_2O_3 insulating layer was deposited by atomic-layer-deposition at 150 °C and treated with butylphosphonic acid as the SAM layer, and the synthetized PDPP-PD semiconductor was deposited by

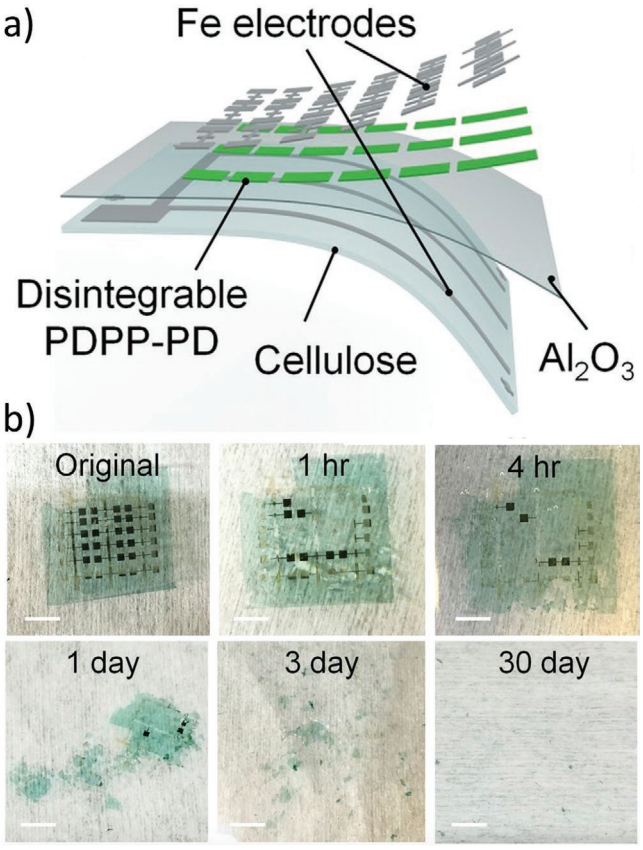

Figure 13. Totally disintegrable electronics fabricated with conventional deposition techniques. a) Schematic of the materials and device structure used for totally disintegrable electronics. The electrodes were deposited by thermal evaporation through a shadow mask, the Al_2O_3 insulating layer was deposited by atomic-layer-deposition and treated with SAM, and the PDPP-PD semiconductor was spin coated. b) Photographs of a device at various stages of disintegration. Scale bars: 5 mm. Reproduced with permission.[153] Copyright 2017, National Academy of Science.

spin coating. In order to realize "green" electronics with zero footprint, a totally disintegrable conjugated polymer was then combined with the biocompatible substrate. In addition, iron was used for the gate and source-drain electrodes instead of gold. The work function of iron (4.8 eV) is close to the HOMO level of the polymer (5.11 eV), making it a good candidate for the replacement of the commonly-used gold. Indeed, although gold is a bio-compatible material widely used in implantable electronics,[54,204] it is not dissolvable.[205] The iron-based devices showed reasonable hole mobilities of 0.12 ± 0.04 cm^2 V^{-1} s^{-1} with on/off ratios $>10^4$. Although operational stability for three days in DI water was demonstrated, the OFETs were rapidly degraded in a pH 4.6 buffer solution containing 1 mg mL^{-1} cellulase. Figure 13b displays the degradation process, showing that iron electrodes degrade rapidly under this condition, typically within 1 h. Considering the other OFET materials, including the conjugated polymer, cellulose substrate, and alumina, they were completely degraded within 30 days. Interestingly, for practical applications the degradation speed of the device could be potentially tuned trough appropriate decomposable encapsulation materials.

Comparatively, the lesser developed solution-based printing techniques, relying on non-vacuum and scalable methods, are a promising route toward the low-cost and facile manufacturing of green organic transistors.[206–208] Remarkably, solution-based digital printing is an additive manufacturing process with significantly reduced material waste compared to the conventional subtractive methods. Among the various printing techniques used for the fabrication of organic transistors, transfer printing – delivering processed and integrated materials from one substrate to another – has found wide application for green electronics and bioelectronics.[209,210] Transfer printing enables to expand the range of processable substrates by sequestering the harsh conditions of conventional fabrication processes (e.g., heating and etching) from the target substrate. Indeed, devices can be temporarily fabricated on conventional substrates such as Si wafers with standard fabrication processes, and then transferred onto biocompatible and biodegradable "green" substrates with the help of sacrificial layer and polydimethylsiloxane (PDMS) stamp. Transfer printing has facilitated the integration of bioresorbable materials on almost any substrate of interest.[156,211]

Recently, Xiang et al. reported carbon nanotube transistors and integrated circuits that can be transferred to arbitrary surfaces. Interestingly, integrated circuit fabrication processes were combined with transfer printing.[211] The transfer-printing fabrication process is illustrated in **Figure 14**a–c. Two transfer approaches, both wet and dry, were developed to meet different application environments. A sacrificial layer was positioned on a silicon wafer (Figure 14a). Sputtered copper (100 nm) was used for the wet etching approach and a spin-coated polyimide was used for the dry etching approach. Silicon dioxide (≈300 nm) was then deposited as a buffering layer via plasma-enhanced chemical vapor deposition (PECVD), and combined with evaporated and thermally oxidized yttrium (10 nm) on its surface. Following substrate preparation, the transistors and integrated circuits were fabricated by photolithography to pattern Ti/Au as the buried-gate electrodes, Ti/Pd/Au as the source–drain contact electrodes, and HfO_2 (20 nm) as the high-k dielectric. A solution-processed semiconducting thin film was dip-coated as the active layer. Notably, hexamethyldisilazane (HMDS) monolayer passivation, which is often used in standard silicon fabrication processes, was utilized before dip-coating the carbon nanotubes thin film. The standard photolithography process yielded wafer-scale integrated circuits. For example, devices were fabricated on a 2-in. wafer, as shown in the inset image of Figure 14a. A transfer technique was then implemented, as depicted in Figure 14b,c. Various types of sacrificial layer were eliminated via different approaches. For wet etching, a thermal release tape was adhered to the devices, and the devices were soaked in a ferric chloride ($FeCl_3$) solution for 3 h to remove the Cu sacrificial layer. After gently rinsing the devices in water and drying them under nitrogen, the devices with tape were pressed against the target substrate on a hot plate to release the tape and complete the process. In the dry etching process, the target substrate was mounted on a PDMS film. The devices, together with polyimide, were first transferred to the target substrate. Next, inductively coupled plasma was applied to eliminate the polyimide, and the target substrate

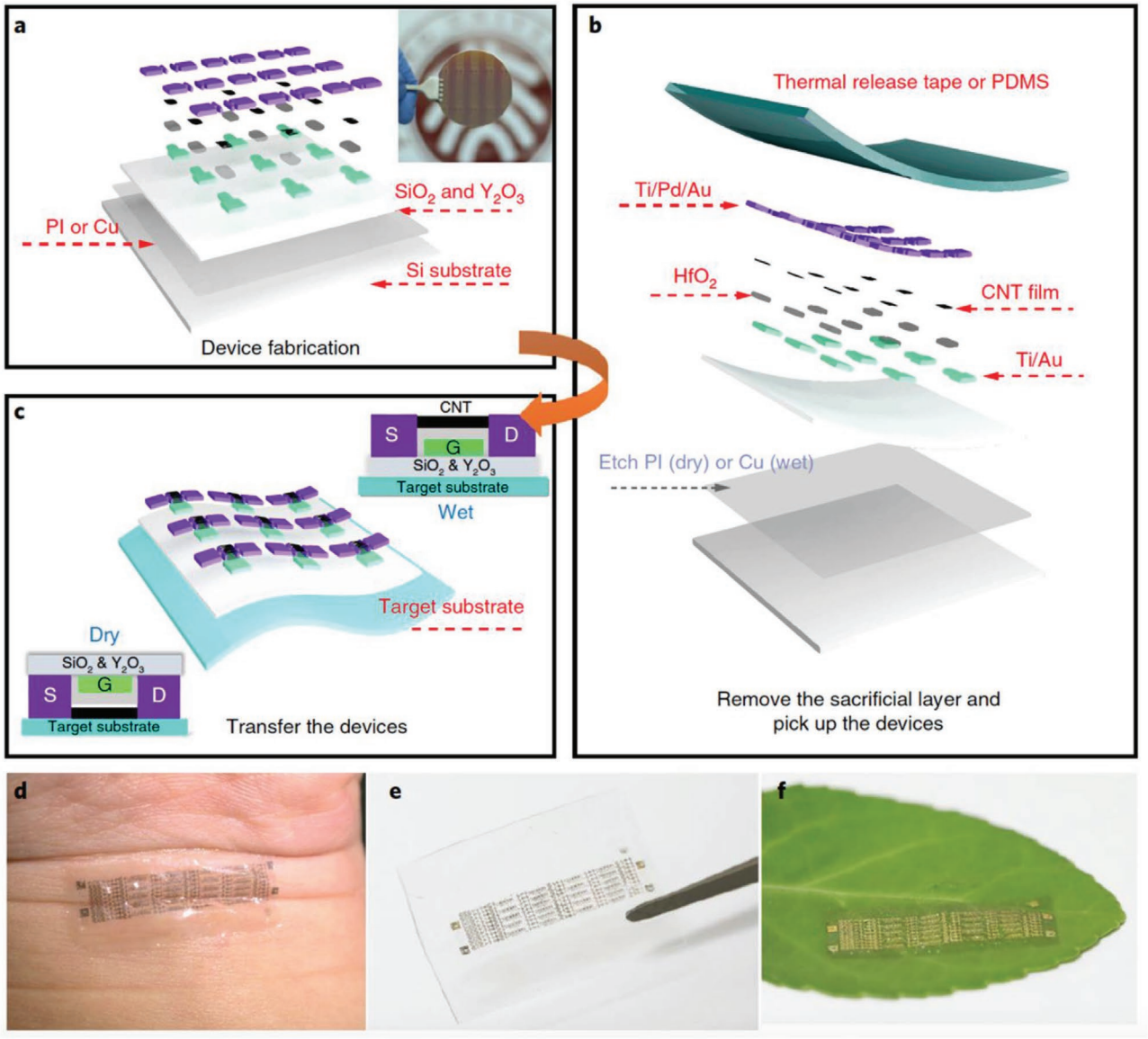

Figure 14. Fabrication process and bio-integration capability. a–c) Schematic illustration of the key transistor fabrication procedures via dry etching or wet etching approaches. The device fabrication was accomplished on a 2-inch wafer, as shown in the inset of panel a. d–f) Photographs showing the bio-integration capability of the electronic devices transferred onto a wrist, biodegradable polymer (PVA) and a plant leaf. Reproduced with permission.[211] Copyright 2018, Springer Nature.

was then gently peeled off the PDMS to complete the procedure. Figure 14d-f shows the bio-integration capability of the fabricated devices with arbitrary nonconventional substrates. The authors demonstrated the operation of the transferred devices and circuits on a curved plant leaf. The transistors on biodegradable flexible substrates showed good reproducibility. When integrated in an inverter circuit topology, the circuits operated at ultralow power consumption, with an off-state current as low as 10^{-13} A μm^{-1}, a subthreshold swing of 0.06 V dec^{-1}, and a static power consumption of 2.5×10^{-13} W. A full adder integrated circuit and a read-only memory operating at a supply voltage as low as 2 V were also demonstrated.

Printing methods, including for example screen-printing, spray-coating, transfer printing, and ink-jet, are applicable to a variety of natural-based, biodegradable and bioresorbable materials and substrates.[212–214] Schematics of common printing techniques are summarized in **Figure 15**.

Template-based printing methods, including screen printing, stencil printing, and microcontact printing, utilize predefined pattern of masks, screens, stencils, or soft stamps. Liquid inks containing functional materials are casted or sprayed onto the whole area of substrates and are selectively deposited according to the predefined pattern. Along this technology direction, an interesting approach combining screen-printing, high precision laser drilling and thermal evaporation was proposed by Peng et al. and a OFET-based 8 × 8 active-matrix array onto standard paper was demonstrated.[216] Interestingly, the authors designed a silver nanoparticles paste used for the fabrication of

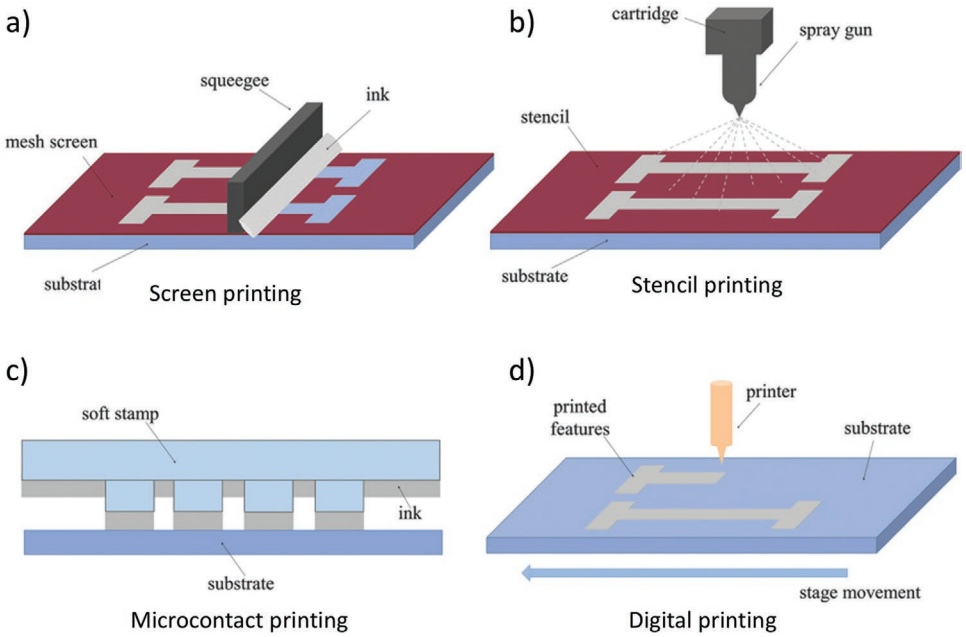

Figure 15. Schematics of common printing techniques: a) screen printing, b) stencil spray printing, c) microcontact printing, and d) digital printing. Reproduced with permission.[215] Copyright 2018, Wiley-VCH.

the gate electrode and for the reduction of the paper substrate. The Ag paste contained silver nanoparticles with a diameter of 300 nm and showed a viscosity of 200 Pa s. This high viscosity was selected o prevent the paste from spreading or being absorbed into the cellulose fiber. The Ag paste did not require post-deposition sintering process and was dried in ambient environment for 2 h, thus minimizing the thermal budget of the process and possible substrate mechanical deformations and stress due to the temperature treatments. The schematic process and the optical and scanning electron microscopy (SEM) images of a mesh are displayed in **Figure 16**a. The electrical conductivity of the single layer screen-printed silver electrode on the paper substrate was measured to be 10^4 S cm^{-1}, which is comparable to other commonly used metal or indium tin oxide (ITO) electrodes. Such a large conductivity on high roughness surface is difficult to achieve by conventional thermal evaporation or magnetron sputtering of a metal thin film. Furthermore, the screen-printed gate electrode can eliminate the need for thick underlying dielectric buffer layers such as PDMS and Cytop on the paper surface. Figure 16b shows that the surface roughness of the bare paper was several micrometers (Figure 16c) and it reduced to around 150 nm after the deposition of the screen-printed Ag gate (Figure 16f). Then, the roughness was further reduced to <50 nm by depositing a parylene-C layer via CVD as gate dielectric. The same Ag paste and different mesh patterns were used to screen-print the source/drain electrodes and electrical interconnects. By optimizing both the screen printer settings and the mesh parameters, the printed electrodes. The schematic cross-section of the BG-TC OFETs as well as the SEM images of the various materials are displayed in Figure 16c–f. OFETs with repeatable 60 µm channel length and nine source/drain fingers were obtained. The OFETs showed a mobility and on/off ratio as high as 0.56 cm^2 V^{-1} s^{-1} and 10^9, respectively.

With the development of additive manufacturing, various digital printing techniques with continuous manufacturing capabilities have been widely investigated. These digital printing techniques, such as inkjet printing,[217,218] aerosol jet printing,[219] and electrohydrodynamic (EHD) printing,[220] employ the movement of motorized stages for patterning. They are mask-less, drop-on-demand processes with high fabrication speed and minimized material waste.[221] The feature size of the digital printing is highly dependent on the diameter of the printing orifice and the printing speed. The smallest feature size achievable by traditional inkjet printing is around 20 µm, although fine features down to the submicron level have been produced with newly developed printing technologies.[222]

Combining printing transfer methods based on commercial tattoo-paper and ink-jet printing, Caironi et al. proposed the integration of biocompatible active electronic devices on edible substrates.[156] Temporary tattoo-paper consists of a sub-micrometric film of ethylcellulose (EC), a cellulose derivative, attached to a paper sheet by means of a sacrificial water-soluble starch/dextrin layer. More in detail, by exploiting tattoo-paper, it was possible to easily and reliably transfer the sub-micrometric EC layer onto many different items. The tattoo-paper was soaked with water that dissolved the starch sacrificial layer, and it was then pressed onto the target object. Finally, the paper sheet was peeled off to release the conformable, hundreds of nanometers thick EC layer. Various sets of p-type and n-type OFETs were presented and characterized onto temporary tattoo-paper, where EC acted both as transferrable substrate and as gate dielectric layer of the OFETs. The OFET electrodes were deposited by inkjet-printing and subsequent sintering of a commercially available silver nanoparticle (AgNP) ink. Importantly, the AgNP biocompatibility with the human body has been recently proved.[223,224] Sintered nanoparticles created a continuous layer of material that hinders phagocytosis, which is a dominant mechanism for

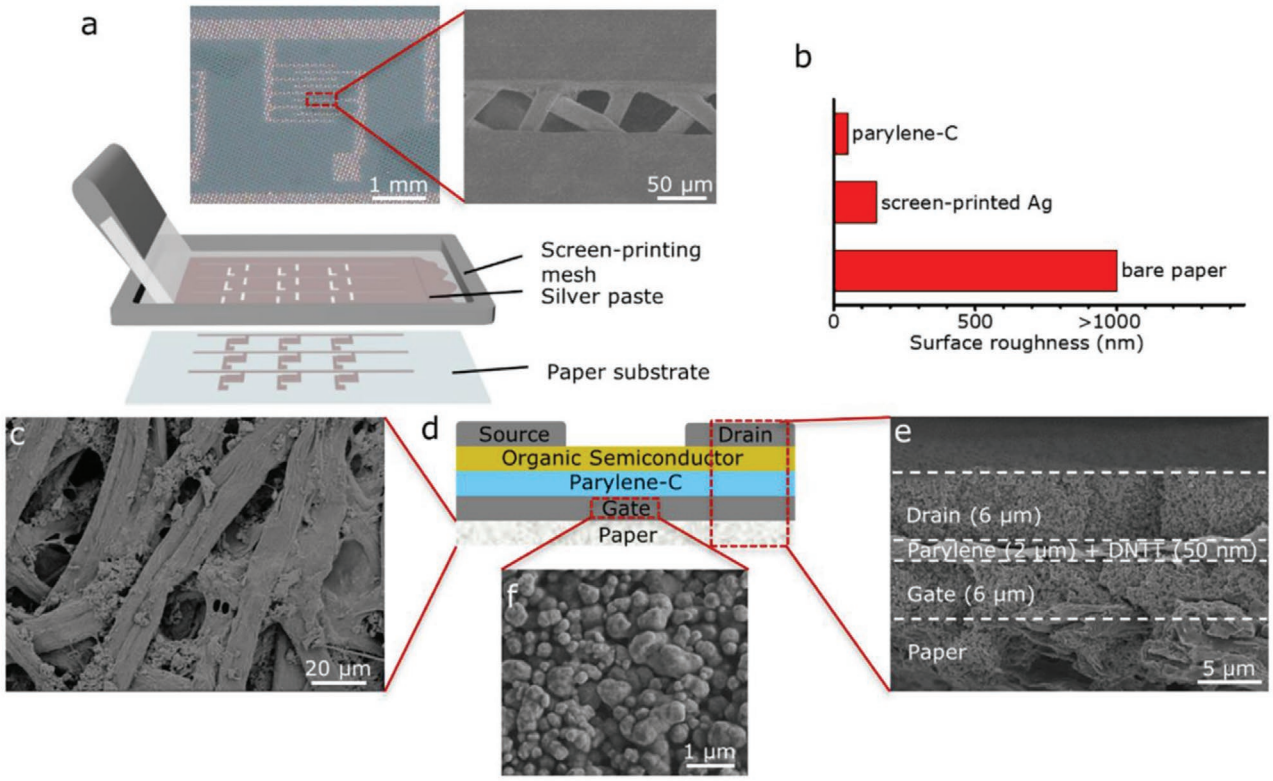

Figure 16. Transistor structures on printer paper. a) Schematic process of the screen-printing approach. Top middle inset shows an optical image of the enlarged source/drain pattern, where the light blue part is covered by emulsion. Top right inset is an SEM image of channel area defined between two fingers. b) Surface roughness (root mean square) after different fabrication processes. c) SEM surface image of the paper substrate. d) Schematic cross sectional structure of the transistor. e) SEM cross sectional image of the transistor under the drain electrode area. f) SEM surface image of the screen-printed gate electrode on paper. Reproduced with permission.[216] Copyright 2014, Springer Nature.

in vitro cytotoxicity.[225] The device fabrication steps are sketched in **Figure 17**a. The silver source and drain electrodes were inkjet-printed and subsequently sintered directly on untreated tattoo-paper. The typical channel width (W) and length (L) of the fabricated OFETs were W ≈ 1000 µm and L ≈ 50 µm. Likewise, the semiconductor was also inkjet-printed, and annealed to remove residual solvent from the film. A separate piece of tattoo-paper was used to laminate a thin EC layer on the device, by exploiting the above mentioned transfer technique. This second EC layer acted as gate dielectric, providing an average gate capacitance of about 5.5×10^{-9} F cm^{-2} at 100 Hz, a value compatible with conventional low-k insulating polymers such as PMMA. As displayed in Figure 17b, at the end of the fabrication process (before transfer) the OFETs have a staggered top-gate bottom-contact configuration, on the top of the tattoo-paper ready for transfer. The latter was achieved by first soaking the entire sample into water to dissolve the starch sacrificial layer, and then by placing it onto the edible substrate and removing the paper. OFETs were transferred on two different types of substrates: a glass microscope slide, serving as a rigid and planar reference, and a pharmaceutical, hard-gelatin capsule (Figure 17c). In order to remove the water in excess after the final transfer without compromising the integrity of the capsules, all samples were left to dry overnight in vacuum at a pressure of about 10 mbar. Overall, the fabrication procedure used scalable printing techniques and the tattoo transfer process. Moreover, four different polymer semiconductors, namely P3HT, 29-DPP-TVT and P(NDI2OD-T2), were tested. This demonstrates the versatility of the transfer procedure and the compatibility with both hole and electron transporting materials, as required by robust complementary logic circuits.[226]

6. Sustainable Organic Transistor Applications

The widespread application of smart electronics has brought to a terrific revolution in human lifestyle, although resulting in the rapidly growing electronic waste and environmental issue. To this end, green and sustainable electronics and bioelectronics have triggered great research interest.[49,53] In addition, biocompatibility and biodegradability allows implanted electronics dissolved or resorbed by the body, greatly reducing the risk of infection by secondary surgery for device removal in clinical applications.[49] Although biodegradable and sustainable electronics are urgently required, the implementation of applications based on green and circular approaches is still in its infancy. One of the most widely explored field of application of sustainable electronic is represented by the realization of electronic circuits, such as inverters and logic gates, which act as the basic backbone of most modern-day electronic devices without using any toxic and expensive materials. In this perspective, all-organic printed circuits fabricated on a commercially available

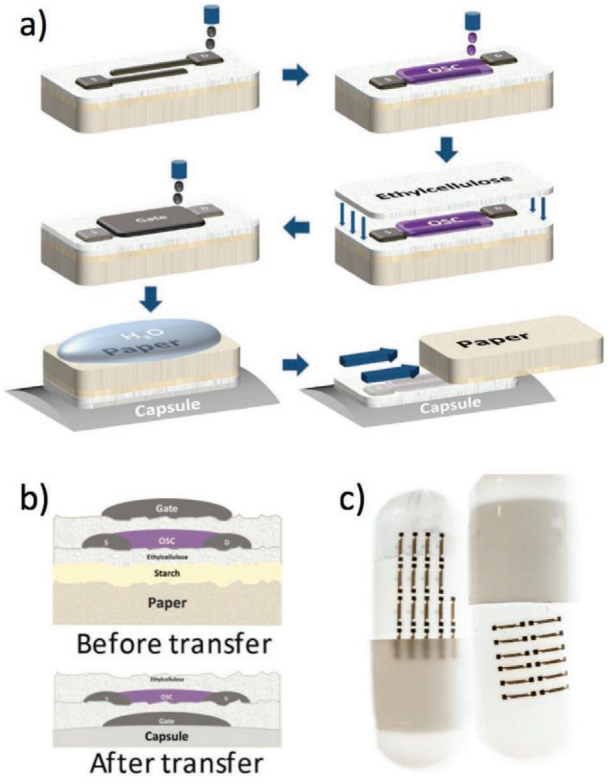

Figure 17. OFET fabrication on tattoo-paper. a) Scheme of the OFET fabrication steps on tattoo-paper substrates. b) OFET structure before after transfer. c) Photograph of a set of silver electrodes transferred on to a pharmaceutical capsule. Reproduced with permission.[156] Copyright 2018, Wiley-VCH.

paper substrate were recently demonstrated.[158] Specifically, complementary organic inverters and logic gates were fabricated by combing inkjet printing and chemical vapor deposition, a mixed technology suitable for up-scalable to industrial size. The complementary inverter is a fundamental building block for both digital and analogue applications.[24] Logic gates are essential components for digital electronics. The OFET architecture and the figures of merit of both p- and n-type inkjet printed transistors were detailed presented in Section 4. **Figure 18**a displays the transfer voltage characteristic V_O–V_I and the corresponding static gain of a complementary inverter printed on commercial paper. The inverter showed a rail-to-rail behavior operating at low voltage (V_{DD} = 5V), with a static gain of about –14 and a transition voltage from V_{DD} to GND close to the ideal point $V_{DD}/2$. The latter is a pre-requisite for a large noise margin. We note that the noise margin is a very relevant parameter in digital applications since it provides a quantitative evaluation of the inverter immunity against input signal variations (noise). According to the "maximum equal criterion", the noise margin can be obtained by mirroring input and output voltages in the transfer curve and by determining the size of the maximum square that fits in the area between the original and the mirrored transfer curve. As shown in Figure 18b, the noise margin results to be 1.4 V which is about 50% of the maximum value $V_{DD}/2$. Starting from basic inverters, logic gates were obtained. Indeed, an inverter is the simplest form of logic gates, that is, the logic NOT. As proof of concept of the proposed technology, complementary NOR, OR, NAND, and AND logic gates were presented. As an example, Figures 18c,d shows the circuit configuration of a NAND and AND logic gates. This logic gates were fabricated by connecting two p-OFETs in parallel (pull-up network) and two n-OFETs in series (pull-down network), as shown in Figure 18c. Similarly, in a NOR gate the pull-up network consists of two p-OFETs in series and the pull-down networks of two n-OFETs in parallel, while the complementary OR gate is obtained by connecting the output of the NOR to the input of an inverter. Typical voltage characteristics of the various logic gates are reported in Figure 18d. The operating voltage was V_{DD} = 5 V, while the two input voltages, A and B, were 5 V for logical 1 and 0 V for logical 0. The fundamental logical operations AND, NAND, OR and NOR were demonstrated, thus proving the great potential of fully-organic printed transistors for the development of low cost, flexible, portable, and easy recyclable electronic products.

Among the fields of application of biodegradable and sustainable electronic proposed so far, remarkable is the case of biosensors for in situ health and food monitoring.[227–236] In this perspective, a biodegradable and biocompatible solid-state LSE OECT (structure and operation described in Section 4) has been recently applied in biomedical applications by electrocardiogram (ECG) recordings on skin of human body and heart of rat.[164] More in detail, **Figure 19**a shows the equivalent circuit used for ECG recording and the fabricated device attached on the skin. Excellent skin adhesion was obtained because the levan polysaccharide substrate and dielectric are based on fructose, which results in soft and sticky ideal properties to create a direct perfect contact with the body. The ECG signal coming from the heart muscular tissue where cell depolarization as ionic influx occurs generates the spread of ionic current to whole body that, in turn, results in a potential gradient on the human body. These potential changes affect measured current from the biodegradable organic transistors by modulating polarization of the electrolyte, when attached on the target surface. The recorded ECG signals from human skin are shown in Figure 19b when V_{GS} = 0 and –1 V with V_{DS} = –1 V. The ECG depicted the typical and periodical spikes with an amplitude of about 0.4 μA similar with heart beat signals from standard ECG equipment. Importantly, there was no remarkable current when the transistor was biased in off state (at V_{GS} = 0 V), because the potential change on the skin was sufficient to generate polarization of the OECT solid-state electrolyte. As a further application example, biodegradable organic transistors were attached to the heart of rat for recording ECG (Figure 19c), settling the same experimental conditions with human skin attachment. As displayed in Figure 19d the ECG measurements shows a maximum peak current of about 15 μA, a larger value with respect to the human skin because of the organic transistor was positioned directly on the organ. In the case of the implanted transistor the biodegradable nature of the electrolyte and substrate eventually resulted in its degradation by body fluids.

Another challenging and emerging field of application of biodegradable and sustainable electronic is represented by neuromorphic devices. In fact, the connectivity of neurons through the synapses is a dynamic metabolic process that plays a crucial role in signal processing and cognitive behaviors. The efficiency

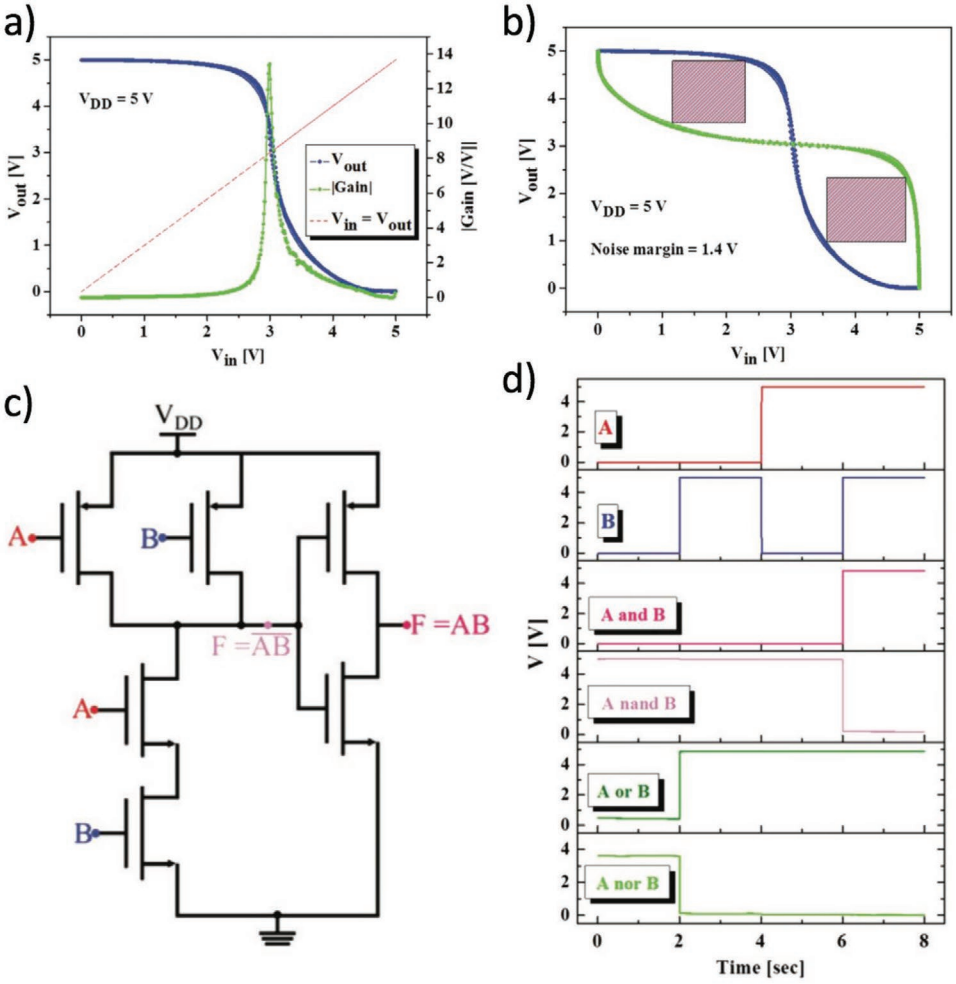

Figure 18. Printed fully-organic complementary circuits on commercial paper. a) Inverter voltage transfer curve and static gain. b) Determination of the noise margin of the inverter. c) Circuit schematic of an AND and NAND logic gates. d) Outputs versus two inputs (A and B) voltage characteristics of AND, NAND, OR, and NOR logic gates. Reproduced with permission.[158] Copyright 2020, Wiley-VCH.

of connection, also referred as synaptic weight, changes with time, which involves learning, memory and various computational tasks of the brain. Such characteristics are called as synaptic plasticity. There are several mechanisms to alter the synaptic weights, including excitatory postsynaptic current (EPSC), short-term plasticity (STP), long-term plasticity (LTP), spike-timing-dependent plasticity (STDP), etc. These mechanisms dominate the synaptic cognitive functions. These configurations make our brain operate in an energy efficient mechanism. Inspired by such brain computation, neuromorphic computing has been proposed, exhibiting advantages of high degree of parallelism, low power consumption, high storage efficiency and good fault-tolerant characteristics.[237] Recently, several kinds of bio-inspired neuromorphic devices have been proposed, demonstrating essential synaptic plasticity behaviors, including two-terminal memristors,[238,239] three-terminal transistors[33,240–242] and multi-terminal transistors.[243,244] In this perspective, organic synaptic transistors with biodegradability and ultraflexibility have been recently realized by exploiting neutral polysaccharides as self-supporting dielectric layers.[245] The fabricated devices were only 200 nm thick allowing bending, folding and conformability to arbitrary-shaped objects. Dextran was used as the dielectric layer and the ultra-flexible and organic biodegradable synaptic transistors emulated the essential synaptic functions, including EPSC, STP, and LTP. Dextran was used as the dielectric layer and a bottom-gate top-contact configuration, that corresponds to the structure of a biological synapse was used (**Figure 20**a). Specifically, the gate voltage pulse is regarded as the presynaptic stimulus, and the current in the conductive channel is analogous to the postsynaptic activity. The mobile proton in the dextran dielectric layer acted as the neurotransmitter and migrates in response to the presynaptic spikes. To assess the synaptic response of the dextran-based devices, the EPSC was measured by applying a presynaptic spike (−5 V) to the gate electrode. Hence, EPSC was triggered when the negative voltage pulse driven the charge carriers toward the DNTT channel. This eventually resulted in a peak current of about 2.5 μA at the end of the pulse (Figure 20b). Subsequently, protons inside the dextran membrane gradually drifted back to the initial positions, and the EPSC decayed back to the initial value within a few seconds. As displayed in Figure 20c, the pulse amplitude dependent EPSC was tested in

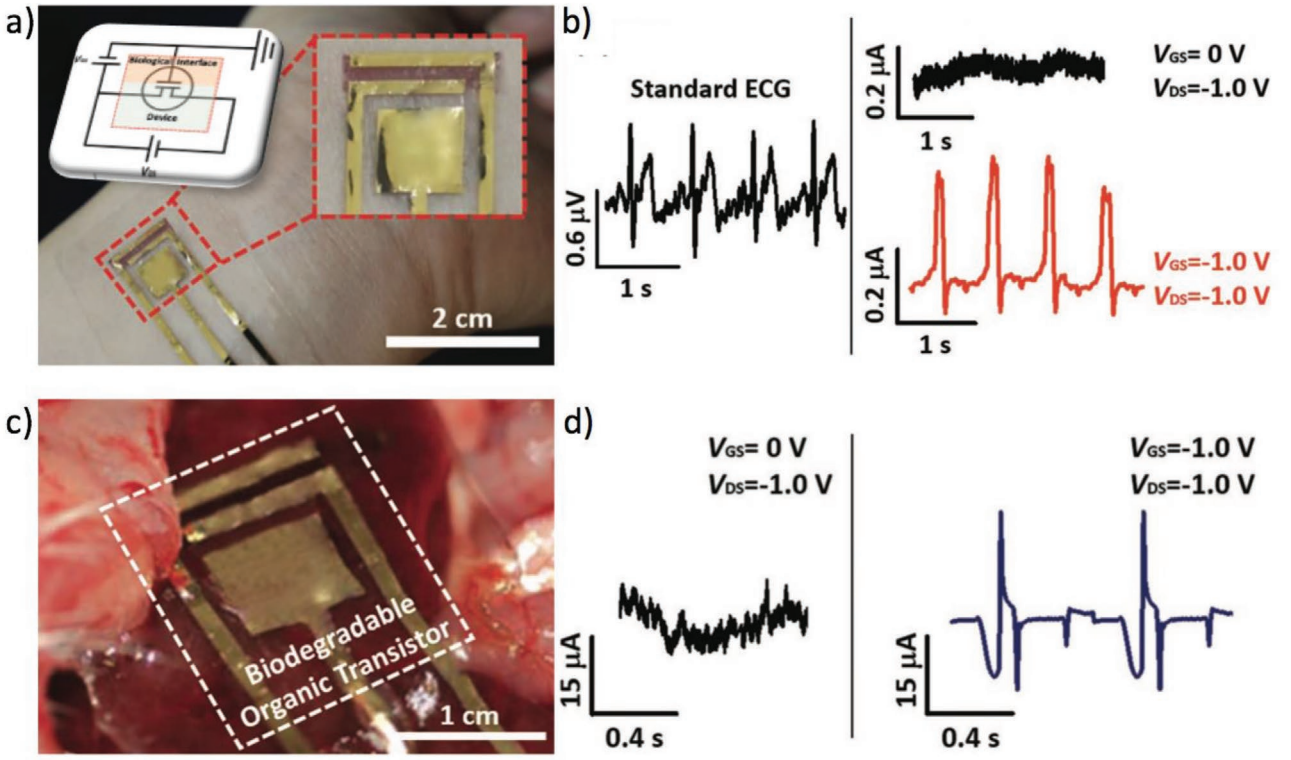

Figure 19. ECG recording with biodegradable organic transistors. a) Photograph of the device on the skin of the human. Inset: equivalent circuit for measurement of ECG signals. b) Recorded ECG signals from the human skin with a standard EGC and the biodegradable OT. c) Photograph of the device on the heart of rat. d) Recorded ECG signals from the heart of rats. Reproduced with permission.[164] Copyright 2020, Wiley-VCH.

the dextran-based synaptic devices in order to further investigate the synaptic response. The maximum (negative) value of EPSC increased from −0.3 to −1.1 μA with the increment of the presynaptic stimuli amplitude (from −2 to −5 V) since an increasing number of protons were attracted towards the gate electrode. This, in turn, increased the time for the protons to diffuse back to the equilibrium positions.

Importantly, the degradation characteristics of the dextran-based synaptic transistors were investigated. The devices were partially buried in the soil to simulate the situation of devices discarded to the natural environment carelessly. As shown in Figure 20d, the disintegration of the synaptic organic transistors array after dripping water was very fast. The transistors completely disappeared after only 15 s. Overall, the reported application examples prove that organic transistors can be a viable route for sustainable and green electronics, bioelectronics and neuromorphic applications.

7. Summary and Outlook

Organic transistor technologies have demonstrated huge advances in the broad field of large-area, flexible, conformable, soft, and lightweight electronics and bioelectronics. Such emerging technologies are enabling a vast number of new applications, where electronic and bioelectronic sensors, circuits, and actuators can be embedded in objects, clothes, and humans. On one side the approaching era of "(bio)electronics everywhere" will positively impact on the progress of our society and economy. On the other side, the emergence of electronics as ubiquitous feature of an advanced modern society is posing the challenge of managing an ever-increasing number of e-waste. In addition, emerging technologies will also enable the ultra-low-cost mass-production of lightweight plastic-based electronics and bioelectronics for disposable applications. Hence, the emerging e-waste is expected to reduce the weight, but the recovery will be even more difficult with respect to current e-waste. Therefore, new sustainability requirements have to be considered for the development of next-generation green organic transistor technologies. Fortunately, organic materials and technologies can offer relevant solutions in this direction, leveraging on both chemical tunability of the synthetic approaches and low-thermal-budget additive techniques.

This review provided a snapshot of current green materials and technologies for the fabrication of sustainable organic transistors. We started considering the class of materials required for the fabrication of the organic transistor main components, namely the substrate, gate insulator, semiconductor, and conducting electrodes. Substrate represents the most relevant component in terms of weight while the impact of functional materials is mainly due to the energy and solvents used for the fabrication. Interestingly, materials used for the substrate are increasingly used also as gate dielectric. At present, the most widely used green materials for substrate and gate dielectric include glass, paper, polysaccharides, proteins, natural resins, hydrogels, synthetic polymers and encapsulants, sugars

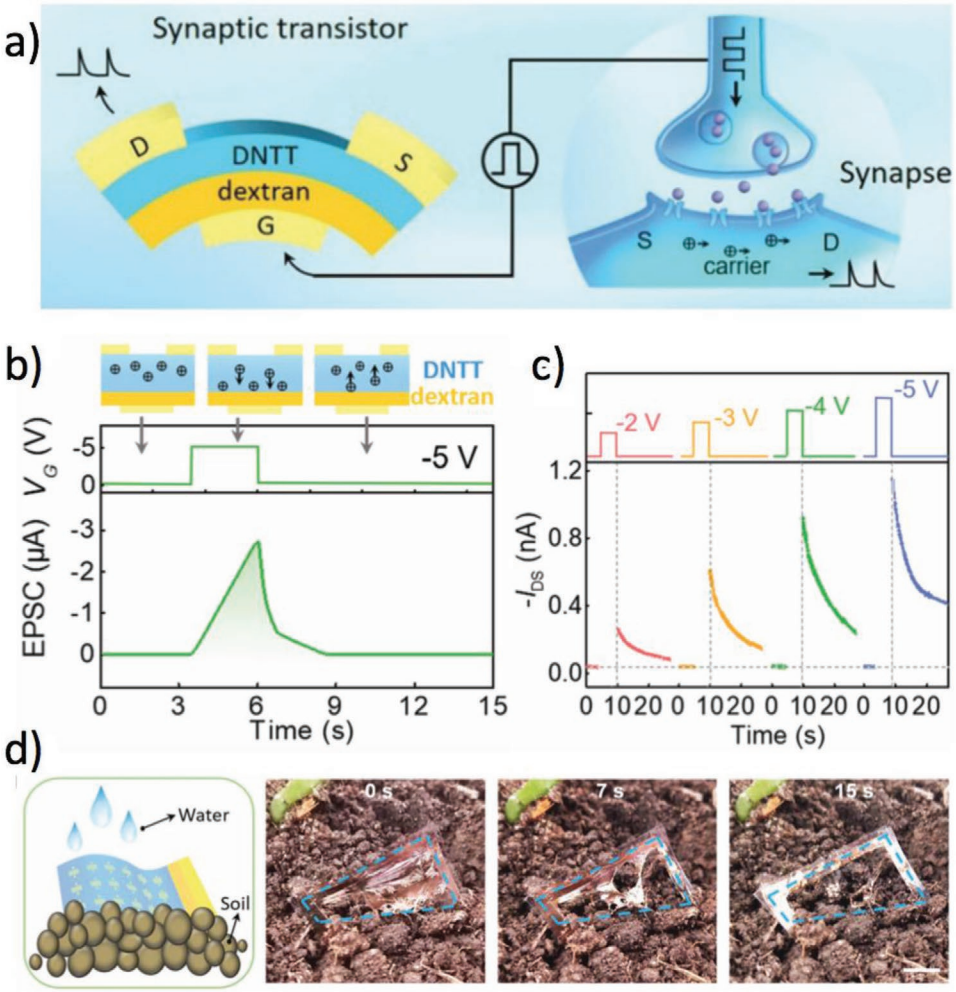

Figure 20. Biodegradable organic synaptic transistors a) Schematic illustration of an artificial synaptic transistor (left) and corresponding biological synapse (right). b) EPSC triggered by presynaptic spikes. Insets show the hole distribution in the semiconductor before (left), during (middle), and after (right) the gate voltage. c) EPSC retention curves at various gate pulses. d) Disintegration process of the self-supporting synaptic organic transistors. Scale bar: 0.4 mm. Reproduced with permission.[245] Copyright 2020, The Royal Society of Chemistry.

and nucleobases. Then, we focused on natural or bioinspired organic semiconductors as well as on synthetic green organic semiconductors and conductors. The overview shows that biodegradable materials and green processed materials are still in their infancy and the transition towards green organic semiconductors and conductors featuring low/zero-toxicity, biodegradability, or recyclability, can be accomplished through different approaches. On one hand, natural, or bioinspired semiconductors and conductors can be either extracted or de novo synthesized according to green chemistry protocols. On the other hand, synthetic organic semiconductors and conductors can be modified with functional groups that promote degradation under mild conditions.

A crucial aspect to be considered in the fabrication of green and sustainable organic transistors is related to the type of solvents utilized for extraction/synthesis of raw materials and their processing to prepare substrates and active layers. Ideally, water would be the green solvent par excellence. Common alcohols, ketones and esters can also be classified as green solvents, because of their low toxicity. However, most of polymers utilized as semiconductors or conductors have nonpolar backbones that limit their solubility in polar green solvents. Finding efficient green alternatives is not trivial and considering that the selection of green solvent is still largely based on empirical approaches, additional and more systematic work is required along this fundamental direction. In this regard, the recent impressive growth in accuracy and prediction capability of machine-learning algorithms and combinatorial approaches could represent a powerful tool for the rapid screening and optimization of extraction and processing protocols.

Moreover, the evaluation of the environmental impact of materials and processes should take into account the energetic cost and CO_2 footprint. Unfortunately, an accurate estimate of the energy utilized to produce the components needed to fabricate an organic transistor is not trivial, and this represents a relevant part of the great uncertainty in classifying it as "green". The most critical issue in evaluating the

embodied energy is the absence of data related to the cost of natural materials extraction and integrated evaluation of all the processes and chemicals utilized in the fabrication chain. For example, no data are available for most of polysaccharides, proteins, small organic molecules and polymers utilized as dielectrics or (semi)-conductors, as well as for biodegradable elastomers that can be applied for stretchable substrates. Interestingly, we note that embodied energy associated to the production of commercial paper is significantly higher than that needed to fabricate soda-lime glass, whereas the average CO_2 footprint is lower. Unfortunately, the absence of data related to conductive polymers restricted the comparison among conventional metals, like silver and gold, whose production is greatly energy consuming. Overall, a great bunch of work is urgently necessary also in this direction.

Focusing on the transistor architectures and figures of merit, we compared and analyzed the research performed in the last 10 years. The most adopted approach is based on the fabrication of conventional organic transistors on green and/or bioresorbable substrates. The bottom-gate bottom-contact architecture is used for reducing the negative impact of the substrate surface roughness on the gate insulator and semiconductor performance. The use of green conductors, for example, Fe instead of Ag or Au, is rarely explored. More ideas and solutions are emerging from ion-gated transistor architectures, which enable to simplify various device constraints, for example, the gate/channel alignment and the insulator thickness, opening possibilities for bioresorbable bioelectronics.

In contrast to the manufacturing of conventional silicon electronics where high-temperature doping, photolithography, and dry/wet etching fabrication processes are used, green approaches ask for low-temperature, minimum waste of material and direct patterning. To date, three main technological approaches were identified as possible paths for a greener fabrication of organic transistors: i) vacuum deposition through shadow mask, ii) transfer printing, and iii) solution-based printing. Although the vacuum mask-based deposition is the most straightforward approach and it was widely used, the operating temperature limits its applicability when low glass transition point substrates are used and the energy budget is a serious point of concern. Comparatively, the lesser developed solution-based printing techniques can be a promising route toward the low-cost and photolithography-free manufacturing. Among printing techniques, transfer printing has found relevant application for green electronics. The main advantage is that transfer printing enables to expand the range of processable substrates by sequestering the harsh conditions of conventional fabrication processes (e.g., heating and etching) from the target substrate. In addition, printing methods, including screen-printing, spray-coating, transfer printing, and ink-jet, have also been applied to a variety of natural-based, biodegradable and bioresorbable materials and substrates. Interestingly, hybrid approaches combining transfer printing methods and ink-jet printing are finding relevant application for edible electronics. The advances of the field are highlighted focusing on application examples accounting for electronic circuits, bioelectronics, and artificial synaptic functionalities.

In a nutshell, we would suggest the following guidelines for the further development of green materials and technologies for sustainable organic transistors:

- Expand the database of synthetic, natural, and biodegradable materials providing optimized functionalities for the specific functions of the various device components.
- Develop systematic studies for the evaluation of the material solubility enabling a wider range of materials processable with benign non-toxic solvents.
- Perform accurate calculations of the overall energy and carbon footprint required for producing the components and devices. This will also enable a clear and fair comparison among the various heterogeneous approaches.
- Develop non-toxic, ultra-low temperature, and solvent-free manufacturing techniques.

Overall, the significant progress achieved in organic materials and technologies is very encouraging and the various research directions already put in place are an excellent springboard for next-generation ubiquitous and sustainable electronics, and bioelectronics.

Acknowledgements

F.T. and I.A. contributed equally to this work.

Conflict of Interest

The authors declare no conflict of interest.

Keywords

green materials, green technologies, sustainable organic transistors

Received: April 15, 2021
Revised: May 21, 2021
Published online: July 28, 2021

[1] E. K. Lee, M. Y. Lee, C. H. Park, H. R. Lee, J. H. Oh, *Adv. Mater.* **2017**, *29*, 1703638.
[2] D. Li, W. Y. Lai, Y. Z. Zhang, W. Huang, *Adv. Mater.* **2018**, *30*, 1704738.
[3] X. Zhao, S. Wang, Y. Ni, Y. Tong, Q. Tang, Y. Liu, *Adv. Sci.* **2021**, *8*, 2004050.
[4] L. V. Kayser, D. J. Lipomi, *Adv. Mater.* **2019**, *31*, 1806133.
[5] M. Ghittorelli, L. Lingstedt, P. Romele, N. I. Crăciun, Z. M. Kovács-Vajna, P. W. M. Blom, F. Torricelli, *Nat. Commun.* **2018**, *9*, 1441.
[6] T. Someya, Z. Bao, G. G. Malliaras, *Nature* **2016**, *540*, 379.
[7] E. Zeglio, A. L. Rutz, T. E. Winkler, G. G. Malliaras, A. Herland, *Adv. Mater.* **2019**, *31*, 1806712.
[8] G. W. Shim, W. Hong, J. H. Cha, J. H. Park, K. J. Lee, S. Y. Choi, *Adv. Mater.* **2020**, *32*, 1907166.
[9] G. Hong, X. Gan, C. Leonhardt, Z. Zhang, J. Seibert, J. M. Busch, S. Bräse, *Adv. Mater.* **2021**, *33*, 2005630.
[10] S. Sudheendran Swayamprabha, D. K. Dubey, R. A. K. Y. Shahnawaz, M. R. Nagar, A. Sharma, F. C. Tung, J. H. Jou, *Adv. Sci.* **2021**, *8*, 2002254.

[11] J. Song, H. Lee, E. G. Jeong, K. C. Choi, S. Yoo, *Adv. Mater.* **2020**, *32*, 1907539.
[12] S. Park, T. Kim, S. Yoon, C. W. Koh, H. Y. Woo, H. J. Son, *Adv. Mater.* **2020**, *32*, 2002217.
[13] P. Meredith, W. Li, A. Armin, *Adv. Energy Mater.* **2020**, *10*, 2001788.
[14] A. Wadsworth, Z. Hamid, J. Kosco, N. Gasparini, I. McCulloch, *Adv. Mater.* **2020**, *32*, 2001763.
[15] H. Ren, J. De Chen, Y. Q. Li, J. X. Tang, *Adv. Sci.* **2021**, *8*, 2002418.
[16] P. C. Y. Chow, T. Someya, *Adv. Mater.* **2020**, *32*, 1902045.
[17] H. Abdolmaleki, P. Kidmose, S. Agarwala, *Adv. Mater.* **2021**, *33*, 2006792.
[18] M. T. Chorsi, E. J. Curry, H. T. Chorsi, R. Das, J. Baroody, P. K. Purohit, H. Ilies, T. D. Nguyen, *Adv. Mater.* **2019**, *31*, 1802084.
[19] Y. S. Rim, S. H. Bae, H. Chen, N. De Marco, Y. Yang, *Adv. Mater.* **2016**, *28*, 4415.
[20] M. Woellner, S. Hausdorf, N. Klein, P. Mueller, M. W. Smith, S. Kaskel, *Adv. Mater.* **2018**, *30*, 1704679.
[21] R. A. Picca, K. Manoli, E. Macchia, L. Sarcina, C. Di Franco, N. Cioffi, D. Blasi, R. Österbacka, F. Torricelli, G. Scamarcio, L. Torsi, *Adv. Funct. Mater.* **2020**, *30*, 1904513.
[22] E. MacChia, R. A. Picca, K. Manoli, C. Di Franco, D. Blasi, L. Sarcina, N. Ditaranto, N. Cioffi, R. Österbacka, G. Scamarcio, F. Torricelli, L. Torsi, *Mater. Horiz.* **2020**, *7*, 999.
[23] Z. Luo, B. Peng, J. Zeng, Z. Yu, Y. Zhao, J. Xie, R. Lan, Z. Ma, L. Pan, K. Cao, Y. Lu, D. He, H. Ning, W. Meng, Y. Yang, X. Chen, W. Li, J. Wang, D. Pan, X. Tu, W. Huo, X. Huang, D. Shi, L. Li, M. Liu, Y. Shi, X. Feng, P. K. L. Chan, X. Wang, *Nat. Commun.* **2021**, *12*, 1982.
[24] T. Leydecker, Z. M. Wang, F. Torricelli, E. Orgiu, *Chem. Soc. Rev.* **2020**, *49*, 7627.
[25] M. Ghittorelli, T. Lenz, H. Sharifi Dehsari, D. Zhao, K. Asadi, P. W. M. Blom, Z. M. Kovács-Vajna, D. M. De Leeuw, F. Torricelli, *Nat. Commun.* **2017**, *8*, 2.
[26] F. Torricelli, L. Colalongo, D. Raiteri, Z. M. Kovács-Vajna, E. Cantatore, *Nat. Commun.* **2016**, *7*, 10550.
[27] F. R. Fan, W. Tang, Z. L. Wang, *Adv. Mater.* **2016**, *28*, 4283.
[28] D. P. Karothu, J. M. Halabi, L. Li, A. Colin-Molina, B. Rodríguez-Molina, P. Naumov, *Adv. Mater.* **2020**, *32*, 2070160.
[29] H. K. Bisoyi, A. M. Urbas, Q. Li, *Adv. Opt. Mater.* **2018**, *6*, 1800458.
[30] Y. Van De Burgt, A. Melianas, S. T. Keene, G. Malliaras, A. Salleo, *Nat. Electron.* **2018**, *1*, 386.
[31] Y. Yang, X. Zhao, C. Zhang, Y. Tong, J. Hu, H. Zhang, M. Yang, X. Ye, S. Wang, Z. Sun, Q. Tang, Y. Liu, *Adv. Funct. Mater.* **2020**, *30*, 2006271.
[32] H. Wang, M. Yang, Q. Tang, X. Zhao, Y. Tong, Y. Liu, *Adv. Funct. Mater.* **2019**, *29*, 1901107.
[33] P. Gkoupidenis, N. Schaefer, B. Garlan, G. G. Malliaras, *Adv. Mater.* **2015**, *27*, 7176.
[34] Y. Lee, J. Y. Oh, T. R. Kim, X. Gu, Y. Kim, G. J. N. Wang, H. C. Wu, R. Pfattner, J. W. F. To, T. Katsumata, D. Son, J. Kang, J. R. Matthews, W. Niu, M. He, R. Sinclair, Y. Cui, J. B. H. Tok, T. W. Lee, Z. Bao, *Adv. Mater.* **2018**, *30*, 1704401.
[35] J. Reeder, M. Kaltenbrunner, T. Ware, D. Arreaga-Salas, A. Avendano-Bolivar, T. Yokota, Y. Inoue, M. Sekino, W. Voit, T. Sekitani, T. Someya, *Adv. Mater.* **2014**, *26*, 4967.
[36] Y. Wu, Q. Zhang, H. Wang, M. Wang, *Mater. Chem. Front.* **2020**, *4*, 3444.
[37] C. Sung, W. Jeon, K. S. Nam, Y. Kim, H. Butt, S. Park, *J. Mater. Chem. B* **2020**, *8*, 6624.
[38] S. M. Won, L. Cai, P. Gutruf, J. A. Rogers, *Nat. Biomed. Eng.* **2021**, https://doi.org/10.1038/s41551-021-00683-3.
[39] P. Fattahi, G. Yang, G. Kim, M. R. Abidian, *Adv. Mater.* **2014**, *26*, 1846.
[40] E. Cantatore, T. C. T. Geuns, A. F. A. Gruijthuijsen, G. H. Gelinck, S. Drews, D. M. De Leeuw, *Dig. Tech. Pap. – IEEE Int. Solid-State Circuits Conf.* **2006**, *42*, 84.
[41] R. A. Street, T. N. Ng, D. E. Schwartz, G. L. Whiting, J. P. Lu, R. D. Bringans, J. Veres, *Proc. IEEE* **2015**, *103*, 607.
[42] Y. Kim, A. Chortos, W. Xu, Y. Liu, J. Y. Oh, D. Son, J. Kang, A. M. Foudeh, C. Zhu, Y. Lee, S. Niu, J. Liu, R. Pfattner, Z. Bao, T.-W. Lee, *Science* **2018**, *360*, 998.
[43] K. Lieberth, M. Brückner, F. Torricelli, V. Mailänder, *Adv. Mater. Technol.* **2021**, *6*, 2000940.
[44] E. Macchia, K. Manoli, B. Holzer, C. Di Franco, M. Ghittorelli, F. Torricelli, D. Alberga, G. F. Mangiatordi, G. Palazzo, G. Scamarcio, L. Torsi, *Nat. Commun.* **2018**, *9*, 3223.
[45] M. Berggren, D. T. Simon, D. Nilsson, P. Dyreklev, P. Norberg, S. Nordlinder, P. A. Ersman, G. Gustafsson, J. J. Wikner, J. Hederén, H. Hentzell, *Adv. Mater.* **2016**, *28*, 1911.
[46] Greenpeace, The E-waste Problem, https://www.greenpeace.org/usa/toxics/green-electronics/, accessed: April 2021.
[47] *Plastic Oceans, Plastic pollution facts*, https://plasticoceans.org, accessed: April 2021.
[48] W. Li, Q. Liu, Y. Zhang, C. Li, Z. He, W. C. H. Choy, P. J. Low, P. Sonar, A. K. K. Kyaw, *Adv. Mater.* **2020**, *32*, 2001591.
[49] P. Wang, M. Hu, H. Wang, Z. Chen, Y. Feng, J. Wang, W. Ling, Y. Huang, *Adv. Sci.* **2020**, *7*, 2001116.
[50] S. Pradhan, A. K. Brooks, V. K. Yadavalli, *Mater. Today Bio* **2020**, *7*, 100065.
[51] S. K. Kang, J. Koo, Y. K. Lee, J. A. Rogers, *Acc. Chem. Res.* **2018**, *51*, 988.
[52] M. Gao, C. C. Shih, S. Y. Pan, C. C. Chueh, W. C. Chen, *J. Mater. Chem. A* **2018**, *6*, 20546.
[53] M. Irimia-Vladu, *Chem. Soc. Rev.* **2014**, *43*, 588.
[54] M. Irimia-Vladu, P. A. Troshin, M. Reisinger, L. Shmygleva, Y. Kanbur, G. Schwabegger, M. Bodea, R. Schwödiauer, A. Mumyatov, J. W. Fergus, V. F. Razumov, H. Sitter, N. S. Sariciftci, S. Bauer, *Adv. Funct. Mater.* **2010**, *20*, 4069.
[55] H. Tran, V. R. Feig, K. Liu, H. C. Wu, R. Chen, J. Xu, K. Deisseroth, Z. Bao, *ACS Cent. Sci.* **2019**, *5*, 1884.
[56] M. Sołtys, A. Górny, J. Pisarska, W. A. Pisarski, *J. Non. Cryst. Solids* **2018**, 498.
[57] Schott AG, *Technical Glasses, Physical and Technical Properties*, Carbon Neutral Print Production, Mainz, Germany **2014**.
[58] Corning, "Corning Gorilla Glass 4 Product Information," www.corninggorillaglass.com, accessed: April, 2021.
[59] R. Lebullenger, F. O. Mear, G. Recycling, in *Springer Handb. Glas.*, (Eds: J.D. Musgraves, J. Hu, L. Calvez), Springer International Publishing, Switzerland, **2019**, pp. 1353.
[60] D. Käfer, M. He, J. Li, M. S. Pambianchi, J. Feng, J. C. Mauro, Z. Bao, *Adv. Funct. Mater.* **2013**, *23*, 3233.
[61] C. Haensch, S. Hoeppener, U. S. Schubert, *Chem. Soc. Rev.* **2010**, *39*, 2323.
[62] A. C. Siegel, S. T. Phillips, M. D. Dickey, N. Lu, Z. Suo, G. M. Whitesides, *Adv. Funct. Mater.* **2010**, *20*, 28.
[63] D. Tobjörk, R. Österbacka, *Adv. Mater.* **2011**, *23*, 1935.
[64] J. Tao, Z. Fang, Q. Zhang, W. Bao, M. Zhu, Y. Yao, Y. Wang, J. Dai, A. Zhang, C. Leng, D. Henderson, Z. Wang, L. Hu, *Adv. Electron. Mater.* **2017**, *3*, 1600539.
[65] L. Hu, J. W. Choi, Y. Yang, S. Jeong, F. L.a Mantia, L. F. Cui, Y. Cui, *Proc. Natl. Acad. Sci. USA* **2009**, *106*, 21490.
[66] R. H. Tang, L. N. Liu, S. F. Zhang, X. C. He, X. J. Li, F. Xu, Y. H. Ni, F. Li, *Microchim. Acta* **2019**, *186*, 521.
[67] I. Vassalini, I. Alessandri, *ACS Appl. Mater. Interfaces* **2015**, *7*, 28708.
[68] U. Zschieschang, H. Klauk, *J. Mater. Chem. C* **2019**, *7*, 5522.
[69] F. Pettersson, T. Remonen, D. Adekanye, Y. Zhang, C. E. Wilén, R. Österbacka, *ChemPhysChem* **2015**, *16*, 1286.
[70] R. Martins, D. Gaspar, M. J. Mendes, L. Pereira, J. Martins, P. Bahubalindruni, P. Barquinha, E. Fortunato, *Appl. Mater. Today* **2018**, *12*, 402.

[71] G. A. Baum, *Handbook of Physical Testing of Paper. 2: Theory*, 2nd ed., Routledge, Oxfordshire, England, **2002**.
[72] R. Bollström, A. Määttänen, D. Tobjörk, P. Ihalainen, N. Kaihovirta, R. Österbacka, J. Peltonen, M. Toivakka, *Org. Electron.* **2009**, *10*, 1020.
[73] N. Bordenave, S. Grelier, F. Pichavant, V. Coma, *J. Agric. Food Chem.* **2007**, *55*, 9479.
[74] C. Qian, J. Sun, J. Yang, Y. Gao, *RSC Adv.* **2015**, *5*, 14567.
[75] H. Li, Y. Qi, Y. Zhao, J. Chi, S. Cheng, *Prog. Org. Coatings* **2019**, *135*, 213.
[76] A. Isogai, T. Saito, H. Fukuzumi, *Nanoscale* **2011**, *3*, 71.
[77] S. Dai, Y. Chu, D. Liu, F. Cao, X. Wu, J. Zhou, B. Zhou, Y. Chen, J. Huang, *Nat. Commun.* **2018**, *9*, 2737.
[78] J. Shah, R. M. Brown, *Appl. Microbiol. Biotechnol.* **2005**, *66*, 352.
[79] B. A. McKenna, D. Mikkelsen, J. B. Wehr, M. J. Gidley, N. W. Menzies, *Cellulose* **2009**, *16*, 1047.
[80] Y. C. Hsieh, H. Yano, M. Nogi, S. J. Eichhorn, *Cellulose* **2008**, *15*, 507.
[81] Z. Li, J. Qiu, C. Pei, *Cellulose* **2016**, *23*, 2449.
[82] J. Huang, H. Zhu, Y. Chen, C. Preston, K. Rohrbach, J. Cumings, L. Hu, *ACS Nano* **2013**, *7*, 2106.
[83] M. Maddaloni, I. Vassalini, I. Alessandri, *Sustainable Chem.* **2020**, *1*, 325.
[84] Q. Zhang, K. De Oliveira Vigier, S. Royer, F. Jérôme, *Chem. Soc. Rev.* **2012**, *41*, 7108.
[85] P. S. Saravana, T. C. Ho, S. J. Chae, Y. J. Cho, J. S. Park, H. J. Lee, B. S. Chun, *Carbohydr. Polym.* **2018**, *195*, 622.
[86] C. Chang, S. Chen, L. Zhang, *J. Mater. Chem.* **2011**, *21*, 3865.
[87] X. Zhang, M. Rolandi, *J. Mater. Chem. B* **2017**, *5*, 2547.
[88] O. C. Agboh, Y. Qin, *Polym. Adv. Technol.* **1997**, *8*, 355.
[89] C. Rullyani, M. Ramesh, C. F. Sung, H. C. Lin, C. W. Chu, *Org. Electron.* **2018**, *54*, 154.
[90] G. Wu, J. Zhang, X. Wan, Y. Yang, S. Jiang, *J. Mater. Chem. C* **2014**, *2*, 6249.
[91] J. R. Du, L. H. Hsu, E. S. Xiao, X. Guo, Y. Zhang, X. Feng, *Sep. Purif. Technol.* **2020**, *244*, 116843.
[92] Basf, ww2.basf.us/businesses/plasticportal/ksc_ecoflex_biodegradable_plastic_literature.htm, accessed: April 2021.
[93] Smooth On, www.smooth-on.com, accessed: April 2021.
[94] N. Yi, Z. Cheng, L. Yang, G. Edelman, C. Xue, Y. Ma, H. Zhu, H. Cheng, *ACS Appl. Mater. Interfaces* **2018**, *10*, 36664.
[95] H. Tao, M. A. Brenckle, M. Yang, J. Zhang, M. Liu, S. M. Siebert, R. D. Averitt, M. S. Mannoor, M. C. McAlpine, J. A. Rogers, D. L. Kaplan, F. G. Omenetto, *Adv. Mater.* **2012**, *24*, 1067.
[96] L. D. Koh, Y. Cheng, C. P. Teng, Y. W. Khin, X. J. Loh, S. Y. Tee, M. Low, E. Ye, H. D. Yu, Y. W. Zhang, M. Y. Han, *Prog. Polym. Sci.* **2015**, *46*, 86.
[97] R. Singh, Y. T. Lin, F. H. Ko, *Macromol. Mater. Eng.* **2018**, *303*, 1700468.
[98] X. He, J. Zhang, W. Wang, W. Xuan, X. Wang, Q. Zhang, C. G. Smith, J. Luo, *ACS Appl. Mater. Interfaces* **2016**, *8*, 10954.
[99] Y. Zeng, B. Sun, H. Y. Yu, X. Wang, H. Peng, Y. Chen, S. Zhu, S. Mao, W. Hou, *Mater. Today Chem.* **2019**, *13*, 18.
[100] M. Irimia-Vladu, N. S. Sariciftci, S. Bauer, *J. Mater. Chem.* **2011**, *21*, 1350.
[101] Y. J. Jo, K. Y. Kwon, Z. U. Khan, X. Crispin, T. Il Kim, *ACS Appl. Mater. Interfaces* **2018**, *10*, 39083.
[102] A. A. Badwan, I. Rashid, M. M. H. Al Omari, F. H. Darras, *Mar. Drugs* **2015**, *13*, 1519.
[103] K. K. Gadgey, A. Bahekar, *Int. J. Mech. Eng. Technol.* **2017**, *8*, 220.
[104] C. L. Luchese, J. M. F. Pavoni, N. Z. dos Santos, L. K. Quines, L. D. Pollo, J. C. Spada, I. C. Tessaro, *J. Food Sci. Technol.* **2018**, *55*, 2963.
[105] S. Y. Park, W. J. Kim, J. B. Choi, S. Kim, *Int. J. Precis. Eng. Manuf.* **2018**, *19*, 129.
[106] B. Wang, W. Yang, J. McKittrick, M. A. Meyers, *Prog. Mater. Sci.* **2016**, *76*, 229.
[107] Q. Xing, K. Yates, C. Vogt, Z. Qian, M. C. Frost, F. Zhao, *Sci. Rep.* **2014**, *4*, 4706.
[108] A. L. Kwansa, R. De Vita, J. W. Freeman, *Biophys. Chem.* **2016**, *214*, 1.
[109] M. Irimia-Vladu, E. D. Głowacki, G. Schwabegger, L. Leonat, H. Z. Akpinar, H. Sitter, S. Bauer, N. S. Sariciftci, *Green Chem.* **2013**, *15*, 1473.
[110] S. W. Baek, J. W. Ha, M. Yoon, D. H. Hwang, J. Lee, *ACS Appl. Mater. Interfaces* **2018**, *10*, 18948.
[111] Q. Zhang, F. Leonardi, R. Pfattner, M. Mas-Torrent, *Adv. Mater. Interfaces* **2019**, *6*, 1900719.
[112] S. Mondal, S. Das, A. K. Nandi, *Soft Matter* **2020**, *16*, 1404.
[113] H. Li, Y. Ma, Y. Huang, *Mater. Horiz.* **2021**, *8*, 383.
[114] J. Vaicekauskaite, P. Mazurek, S. Vudayagiri, A. L. Skov, *J. Mater. Chem. C* **2020**, *8*, 1273.
[115] V. R. Feig, H. Tran, Z. Bao, *ACS Cent. Sci.* **2018**, *4*, 337.
[116] L. S. Nair, C. T. Laurencin, *Prog. Polym. Sci.* **2007**, *32*, 762.
[117] M. C. Serrano, E. J. Chung, G. A. Ameer, *Adv. Funct. Mater.* **2010**, *20*, 1920.
[118] H. Zhao, G. A. Ameer, *J. Appl. Polym. Sci.* **2009**, *114*, 1464.
[119] A. P. Pêgo, A. A. Poot, D. W. Grijpma, J. Feijen, *J. Controlled Release* **2003**, *87*, 69.
[120] D. P. Martin, S. F. Williams, *Biochem. Eng. J.* **2003**, *16*, 97.
[121] S. M. Garner, *Flexible Glass: Enabling Thin, Lightweight, and Flexible Electronics*, Wiley, Hoboken, NJ **2017**.
[122] J. Yang, D. Motlagh, A. R. Webb, G. A. Ameer, *Tissue Eng.* **2005**, *11*, 1876.
[123] S. H. Lee, B. S. Kim, S. H. Kim, S. W. Choi, S. I. Jeong, I. K. Kwon, S. W. Kang, J. Nikolovski, D. J. Mooney, Y. K. Han, Y. H. Kim, *J. Biomed. Mater. Res. – Part A* **2003**, *66*, 29.
[124] Y. Wang, Y. M. Kim, R. Langer, *J. Biomed. Mater. Res. – Part A* **2003**, *66*, 192.
[125] M. Irimia-Vladu, P. A. Troshin, M. Reisinger, G. Schwabegger, M. Ullah, R. Schwoediauer, A. Mumyatov, M. Bodea, J. W. Fergus, V. F. Razumov, H. Sitter, S. Bauer, N. S. Sariciftci, *Org. Electron.* **2010**, *11*, 1974.
[126] V. Baumruk, J. Kocka, J. Kristofik, E. Subertovà, *Czechoslov. J. Phys. B* **1985**, *35*, 670.
[127] A. D. Williams, *DNA-Nucleobase Guanine as Passivation /Gate Dielectric Layer for Flexible GFET-Based Sensor Applications*, Wright State University, August, 2015. https://etd.ohiolink.edu/apexprod/rws_etd/send_file/send?accession=wright1440775088&disposition=inline, accessed: April 2021.
[128] M. B. Da Silva, T. S. Francisco, F. F. Maia, E. W. S. Caetano, U. L. Fulco, E. L. Albuquerque, V. N. Freire, *Phys. Rev. B* **2017**, *96*, 085206.
[129] R. Nangia, N. K. Shukla, A. Sharma, *IOP Conf. Ser. Mater. Sci. Eng.* **2017**, *225*, 012044.
[130] M. Aslam, M. A. Kalyar, Z. A. Raza, *Polym. Eng. Sci.* **2018**, *58*, 2119.
[131] V. J. Hegde, O. Gallot-Lavallee, L. Heux, *Proc. 2016 IEEE Int. Conf. Dielectr. ICD 2016* **2016**, *1*, 293.
[132] S. M. Aguilar, J. D. Sheat, M. A. Al-Joumayly, B. D. Van Veen, N. Behdad, S. C. Hagness, *IEEE Trans. Biomed. Eng.* **2012**, *59*, 627.
[133] S. Bilent, T. H. N. Dinh, E. Martincic, P. Y. Joubert, *Sensors* **2019**, *19*, 1968.
[134] A. P. Gerratt, S. Bergbreiter, *J. Micromech. Microeng.* **2013**, *23*, 067001.
[135] J. E. Mark, *Polymer Data Handbook*, Oxford University Press, New York **1999**.
[136] A. Facchetti, *Mater. Today* **2007**, *10*, 28.
[137] J. T. E. Quinn, J. Zhu, X. Li, J. Wang, Y. Li, *J. Mater. Chem. C* **2017**, *5*, 8654.
[138] N. Kobayashi, H. Izumi, Y. Morimoto, *J. Occup. Health* **2017**, *59*, 394.

[139] A. P. Francis, T. Devasena, *Toxicol. Ind. Health* **2018**, *34*, 200.
[140] V. T. Weerasinghe, D. G. K. Dissanayake, W. P. T. D. Perera, N. D. Tissera, R. N. Wijesena, N. D. Wanasekara, *RSC Adv.* **2020**, *10*, 32875.
[141] D. Ho, J. Lee, S. Park, Y. Park, K. Cho, F. Campana, D. Lanari, A. Facchetti, S. Y. Seo, C. Kim, A. Marrocchi, L. Vaccaro, *J. Mater. Chem. C* **2020**, *8*, 5786.
[142] M. Lamarche, M. T. Dang, J. Lefebvre, J. D. Wuest, S. Roorda, *ACS Sustainable Chem. Eng.* **2017**, *5*, 5994.
[143] H.-Y. Wang, Y.-Q. Zhang, Z.-G. Wei, *Crit. Rev. Biotechnol.* **2021**, *41*, 406.
[144] M. Xu, Y. Jiang, S. Pradhan, V. K. Yadavalli, *Front. Mater.* **2019**, *6*, 331.
[145] L. Benassi, I. Alessandri, I. Vassalini, *Molecules* **2021**, *26*, 1766.
[146] F. Chemat, M. A. Vian, G. Cravotto, *Int. J. Mol. Sci.* **2012**, *13*, 8615.
[147] V. Raghuwanshi, D. Bharti, A. K. Mahato, I. Varun, S. P. Tiwari, *ACS Appl. Mater. Interfaces* **2019**, *11*, 8357.
[148] U. Kraft, T. Zaki, F. Letzkus, J. N. Burghartz, E. Weber, B. Murmann, H. Klauk, *Adv. Electron. Mater.* **2019**, *5*, 1800453.
[149] C. J. Lee, Y. C. Chang, L. W. Wang, Y. H. Wang, *IEEE Electron Device Lett.* **2019**, *40*, 236.
[150] C. J. Bettinger, Z. Bao, *Adv. Mater.* **2010**, *22*, 651.
[151] J. W. Chang, C. G. Wang, C. Y. Huang, T. D.a Tsai, T. F. Guo, T. C. Wen, *Adv. Mater.* **2011**, *23*, 4077.
[152] A. Petritz, A. Wolfberger, A. Fian, T. Griesser, M. Irimia-Vladu, B. Stadlober, *Adv. Mater.* **2015**, *27*, 7645.
[153] T. Lei, M. Guan, J. Liu, H. C. Lin, R. Pfattner, L. Shaw, A. F. McGuire, T. C. Huang, L. Shao, K. T. Cheng, J. B. H. Tok, Z. Bao, *Proc. Natl. Acad. Sci. USA* **2017**, *114*, 5107.
[154] E. Shin, J. Yoo, G. Yoo, Y. J. Kim, Y. S. Kim, *Chem. Eng. J.* **2019**, *358*, 170.
[155] H. Jeong, S. Baek, S. Han, H. Jang, S. H. Kim, H. S. Lee, *Adv. Funct. Mater.* **2018**, *28*, 1704433.
[156] G. E. Bonacchini, C. Bossio, F. Greco, V. Mattoli, Y. H. Kim, G. Lanzani, M. Caironi, *Adv. Mater.* **2018**, *30*, 1706091.
[157] C. Rullyani, C. F. Sung, H. C. Lin, C. W. Chu, *Sci. Rep.* **2018**, *8*, 8146.
[158] G. Casula, S. Lai, L. Matino, F. Santoro, A. Bonfiglio, P. Cosseddu, *Adv. Electron. Mater.* **2020**, *6*, 1901027.
[159] M. Seck, N. Mohammadian, A. K. Diallo, S. Faraji, M. Erouel, N. Bouguila, D. Ndiaye, K. Khirouni, L. A. Majewski, *Org. Electron.* **2020**, *83*, 105735.
[160] S. Thiemann, S. J. Sachnov, F. Pettersson, R. Bollström, R. Österbacka, P. Wasserscheid, J. Zaumseil, *Adv. Funct. Mater.* **2014**, *24*, 625.
[161] M. Sheliakina, A. B. Mostert, P. Meredith, *Mater. Horiz.* **2018**, *5*, 256.
[162] B. Schmatz, A. W. Lang, J. R. Reynolds, *Adv. Funct. Mater.* **2019**, *29*, 1905266.
[163] F. Pettersson, R. Österbacka, J. Koskela, A. Kilpelä, T. Remonen, Y. Zhang, S. Inkinen, C. E. Wilén, R. Bollström, M. Toivakka, A. Määttänen, P. Ihalainen, J. Peltonen, *MRS Commun.* **2014**, *4*, 51.
[164] Y. J. Jo, H. Kim, J. Ok, Y. J. Shin, J. H. Shin, T. H. Kim, Y. Jung, T. il Kim, *Adv. Funct. Mater.* **2020**, *30*, 1909707.
[165] R. Martins, A. Nathan, R. Barros, L. Pereira, P. Barquinha, N. Correia, R. Costa, A. Ahnood, I. Ferreira, E. Fortunato, *Adv. Mater.* **2011**, *23*, 4491.
[166] Y. Lin, D. Gritsenko, Q. Liu, X. Lu, J. Xu, *ACS Appl. Mater. Interfaces* **2016**, *8*, 20501.
[167] Y. Zhang, L. Zhang, K. Cui, S. Ge, X. Cheng, M. Yan, J. Yu, H. Liu, *Adv. Mater.* **2018**, *30*, 1801588.
[168] U. Kraft, M. Sejfić, M. J. Kang, K. Takimiya, T. Zaki, F. Letzkus, J. N. Burghartz, E. Weber, H. Klauk, *Adv. Mater.* **2015**, *27*, 207.
[169] T. Yamamoto, K. Takimiya, *J. Am. Chem. Soc.* **2007**, *129*, 2224.
[170] F. Ante, D. Kälblein, T. Zaki, U. Zschieschang, K. Takimiya, M. Ikeda, T. Sekitani, T. Someya, J. N. Burghartz, K. Kern, H. Klauk, *Small* **2012**, *8*, 73.
[171] U. Kraft, K. Takimiya, M. J. Kang, R. Rödel, F. Letzkus, J. N. Burghartz, E. Weber, H. Klauk, *Org. Electron.* **2016**, *35*, 33.
[172] W. Xie, K. Willa, Y. Wu, R. Häusermann, K. Takimiya, B. Batlogg, C. D. Frisbie, *Adv. Mater.* **2013**, *25*, 3478.
[173] B. A. Jones, M. J. Ahrens, M. H. Yoon, A. Facchetti, T. J. Marks, M. R. Wasielewski, *Angew. Chemie – Int. Ed.* **2004**, *43*, 6363.
[174] J. Soeda, T. Uemura, Y. Mizuno, A. Nakao, Y. Nakazawa, A. Facchetti, J. Takeya, *Adv. Mater.* **2011**, *23*, 3681.
[175] U. Zschieschang, F. Ante, D. Kälblein, T. Yamamoto, K. Takimiya, H. Kuwabara, M. Ikeda, T. Sekitani, T. Someya, J. B. Nimoth, H. Klauk, *Org. Electron.* **2011**, *12*, 1370.
[176] U. Zschieschang, H. Klauk, *Org. Electron.* **2015**, *25*, 340.
[177] R. Rödel, F. Letzkus, T. Zaki, J. N. Burghartz, U. Kraft, U. Zschieschang, K. Kern, H. Klauk, *Appl. Phys. Lett.* **2013**, *102*, 233303.
[178] J. W. Chang, W. L. Hsu, C. Y. Wu, T. F. Guo, T. C. Wen, *Org. Electron.* **2010**, *11*, 1613.
[179] A. E. Hagerman, *J. Chem. Ecol.* **1987**, *13*, 437.
[180] K. Kim, M. Shin, M. Y. Koh, J. H. Ryu, M. S. Lee, S. Hong, H. Lee, *Adv. Funct. Mater.* **2015**, *25*, 2402.
[181] M. Shin, J. H. Ryu, J. P. Park, K. Kim, J. W. Yang, H. Lee, *Adv. Funct. Mater.* **2015**, *25*, 1270.
[182] E. Asadi, M. Abdouss, R. M. Leblanc, N. Ezzati, J. N. Wilson, S. Azodi-Deilami, *RSC Adv.* **2016**, *6*, 37308.
[183] K. Y. Kwon, J. S. Lee, G. J. Ko, S. H. Sunwoo, S. Lee, Y. J. Jo, C. H. Choi, S. W. Hwang, T. il Kim, *Small* **2018**, *14*, 1801332.
[184] H. Chen, L. Peng, M. Pérez De Nanclares, M. P. Trudeau, D. Yao, Z. Cheng, P. E. Urriola, L. T. Mydland, G. C. Shurson, M. Overland, C. Chen, *J. Agric. Food Chem.* **2019**, *67*, 7748.
[185] J. Švarc-Gajić, V. Cerdà, S. Clavijo, R. Suárez, P. Mašković, A. Cvetanović, C. Delerue-Matos, A. P. Carvalho, V. Novakov, *J. Chem. Technol. Biotechnol.* **2018**, *93*, 1627.
[186] T. M. S. K. Pathiranage, D. S. Dissanayake, C. N. Niermann, Y. Ren, M. C. Biewer, M. C. Stefan, *J. Polym. Sci. Part A Polym. Chem.* **2017**, *55*, 3327.
[187] E. W. C. Chan, D. Bennet, P. Baek, D. Barker, S. Kim, J. Travas-Sejdic, *Biomacromolecules* **2018**, *19*, 1456.
[188] A. J. Hackett, J. Malmström, J. Travas-Sejdic, *Prog. Polym. Sci.* **2017**, *70*, 18.
[189] S. Cotrone, D. Cafagna, S. Cometa, E. De Giglio, M. Magliulo, L. Torsi, L. Sabbatini, *Anal. Bioanal. Chem.* **2012**, *402*, 1799.
[190] A. Laiho, L. Herlogsson, R. Forchheimer, X. Crispin, M. Berggren, *Proc. Natl. Acad. Sci. USA* **2011**, *108*, 15069.
[191] T. Fujimoto, K. Awaga, *Phys. Chem. Chem. Phys.* **2013**, *15*, 8983.
[192] D. Khodagholy, J. Rivnay, M. Sessolo, M. Gurfinkel, P. Leleux, L. H. Jimison, E. Stavrinidou, T. Herve, S. Sanaur, R. M. Owens, G. G. Malliaras, *Nat. Commun.* **2013**, *4*, 2133.
[193] J. Rivnay, P. Leleux, M. Sessolo, D. Khodagholy, T. Hervé, M. Fiocchi, G. G. Malliaras, *Adv. Mater.* **2013**, *25*, 7010.
[194] P. Romele, M. Ghittorelli, Z. M. Kovács-Vajna, F. Torricelli, *Nat. Commun.* **2019**, *10*, 3044.
[195] P. Romele, P. Gkoupidenis, D. A. Koutsouras, K. Lieberth, Z. M. Kovács-Vajna, P. W. M. Blom, F. Torricelli, *Nat. Commun.* **2020**, *11*, 3743.
[196] Y. Gao, Y. Zhang, X. Wang, K. Sim, J. Liu, J. Chen, X. Feng, H. Xu, C. Yu, *Sci. Adv.* **2017**, *3*, e1701222.
[197] C. Dagdeviren, S. W. Hwang, Y. Su, S. Kim, H. Cheng, O. Gur, R. Haney, F. G. Omenetto, Y. Huang, J. A. Rogers, *Small* **2013**, *9*, 3398.
[198] S. W. Hwang, S. K. Kang, X. Huang, M. A. Brenckle, F. G. Omenetto, J. A. Rogers, *Adv. Mater.* **2015**, *27*, 47.
[199] H. Cheng, *J. Mater. Res.* **2016**, *31*, 2549.
[200] M. E. Roberts, S. C. B. Mannsfeld, N. Queraltó, C. Reese, J. Locklin, W. Knoll, Z. Bao, *Proc. Natl. Acad. Sci. USA* **2008**, *105*, 12134.

[201] A. Campana, T. Cramer, D. T. Simon, M. Berggren, F. Biscarini, *Adv. Mater.* **2014**, *26*, 3874.
[202] A. Campana, T. Cramer, P. Greco, G. Foschi, M. Murgia, F. Biscarini, *Appl. Phys. Lett.* **2013**, *103*, 073302.
[203] Y. H. Jung, T. H. Chang, H. Zhang, C. Yao, Q. Zheng, V. W. Yang, H. Mi, M. Kim, S. J. Cho, D. W. Park, H. Jiang, J. Lee, Y. Qiu, W. Zhou, Z. Cai, S. Gong, Z. Ma, *Nat. Commun.* **2015**, *6*, 7170.
[204] D. H. Kim, J. Viventi, J. J. Amsden, J. Xiao, L. Vigeland, Y. S. Kim, J. A. Blanco, B. Panilaitis, E. S. Frechette, D. Contreras, D. L. Kaplan, F. G. Omenetto, Y. Huang, K. C. Hwang, M. R. Zakin, B. Litt, J. A. Rogers, *Nat. Mater.* **2010**, *9*, 511.
[205] L. Yin, H. Cheng, S. Mao, R. Haasch, Y. Liu, X. Xie, S. W. Hwang, H. Jain, S. K. Kang, Y. Su, R. Li, Y. Huang, J. A. Rogers, *Adv. Funct. Mater.* **2014**, *24*, 645.
[206] X. Huang, Y. Liu, S. W. Hwang, S. K. Kang, D. Patnaik, J. F. Cortes, J. A. Rogers, *Adv. Mater.* **2014**, *26*, 7371.
[207] B. K. Mahajan, X. Yu, W. Shou, H. Pan, X. Huang, *Small* **2017**, *13*, 1700065.
[208] W. Shou, B. K. Mahajan, B. Ludwig, X. Yu, J. Staggs, X. Huang, H. Pan, *Adv. Mater.* **2017**, *29*, 1700172.
[209] L. Song, L. Ci, W. Gao, P. M. Ajayan, *ACS Nano* **2009**, *3*, 1353.
[210] A. Carlson, A. M. Bowen, Y. Huang, R. G. Nuzzo, J. A. Rogers, *Adv. Mater.* **2012**, *24*, 5284.
[211] L. Xiang, H. Zhang, G. Dong, D. Zhong, J. Han, X. Liang, Z. Zhang, L. M. Peng, Y. Hu, *Nat. Electron.* **2018**, *1*, 237.
[212] A. S. Sharova, F. Melloni, G. Lanzani, C. J. Bettinger, M. Caironi, *Adv. Mater. Technol.* **2021**, *6*, 2000757.
[213] G. Mattana, A. Loi, M. Woytasik, M. Barbaro, V. Noël, B. Piro, *Adv. Mater. Technol.* **2017**, *2*, 1700063.
[214] M. Berggren, D. Nilsson, N. D. Robinson, *Nat. Mater.* **2007**, *6*, 3.
[215] X. Yu, W. Shou, B. K. Mahajan, X. Huang, H. Pan, *Adv. Mater.* **2018**, *30*, 1707624.
[216] B. Peng, X. Ren, Z. Wang, X. Wang, R. C. Roberts, P. K. L. Chan, *Sci. Rep.* **2014**, *4*, 6430.
[217] K. Y. Mitra, A. Willert, R. Chandru, R. R. Baumann, R. Zichner, *Adv. Eng. Mater.* **2020**, *22*, 2000547.
[218] N. Kaihovirta, T. Mäkelä, X. He, C. J. Wikman, C. E. Wilén, R. Österbacka, *Org. Electron.* **2010**, *11*, 1207.
[219] C. S. Jones, X. Lu, M. Renn, M. Stroder, W. S. Shih, *Microelectron. Eng.* **2010**, *87*, 434.
[220] J. U. Park, M. Hardy, S. J. Kang, K. Barton, K. Adair, D. K. Mukhopadhyay, C. Y. Lee, M. S. Strano, A. G. Alleyne, J. G. Georgiadis, P. M. Ferreira, J. A. Rogers, *Nat. Mater.* **2007**, *6*, 782.
[221] X. Yu, B. K. Mahajan, W. Shou, H. Pan, *Micromachines* **2017**, *8*, 7.
[222] B. Zhang, J. He, X. Li, F. Xu, D. Li, *Nanoscale* **2016**, *8*, 15376.
[223] C. J. Bettinger, *Trends Biotechnol.* **2015**, *33*, 575.
[224] M. Van Der Zande, R. J. Vandebriel, E. Van Doren, E. Kramer, Z. Herrera Rivera, C. S. Serrano-Rojero, E. R. Gremmer, J. Mast, R. J. B. Peters, P. C. H. Hollman, P. J. M. Hendriksen, H. J. P. Marvin, A. A. C. M. Peijnenburg, H. Bouwmeester, *ACS Nano* **2012**, *6*, 7427.
[225] A. Zucca, C. Cipriani, Sudha, S. T. , D. Ricci, V. Mattoli, F. Greco, *Adv. Healthcare Mater.* **2015**, *4*, 983.
[226] B. Crone, A. Dodabalapur, Y. Y. Lin, R. W. Filas, Z. Bao, A. LaDuca, R. Sarpeshkar, H. E. Katz, W. Li, *Nature* **2000**, *403*, 521.
[227] D. Son, J. Kang, O. Vardoulis, Y. Kim, N. Matsuhisa, J. Y. Oh, J. W. To, J. Mun, T. Katsumata, Y. Liu, A. F. McGuire, M. Krason, F. Molina-Lopez, J. Ham, U. Kraft, Y. Lee, Y. Yun, J. B. H. Tok, Z. Bao, *Nat. Nanotechnol.* **2018**, *13*, 1057.
[228] K. K. Kim, S. Hong, H. M. Cho, J. Lee, Y. D. Suh, J. Ham, S. H. Ko, *Nano Lett.* **2015**, *15*, 5240.
[229] X. Wang, Z. Liu, T. Zhang, *Small* **2017**, *13*, 1602790.
[230] R. Rahimi, M. Ochoa, A. Tamayol, S. Khalili, A. Khademhosseini, B. Ziaie, *ACS Appl. Mater. Interfaces* **2017**, *9*, 9015.
[231] C. Yan, W. Deng, L. Jin, T. Yang, Z. Wang, X. Chu, H. Su, J. Chen, W. Yang, *ACS Appl. Mater. Interfaces* **2018**, *10*, 41070.
[232] S. K. Sailapu, E. Macchia, I. Merino-Jimenez, J. P. Esquivel, L. Sarcina, G. Scamarcio, S. D. Minteer, L. Torsi, N. Sabate, *Biosens. Bioelectron.* **2020**, *156*, 112103.
[233] Y. Yang, W. Gao, *Chem. Soc. Rev.* **2019**, *48*, 1465.
[234] K. Y. Chun, Y. J. Son, E. S. Jeon, S. Lee, C. S. Han, *Adv. Mater.* **2018**, *30*, 1706299.
[235] S. Y. Oh, S. Y. Hong, Y. R. Jeong, J. Yun, H. Park, S. W. Jin, G. Lee, J. H. Oh, H. Lee, S. S. Lee, J. S. Ha, *ACS Appl. Mater. Interfaces* **2018**, *10*, 13729.
[236] T. Dinh, H. P. Phan, T. K. Nguyen, A. Qamar, P. Woodfield, Y. Zhu, N. T. Nguyen, D. V. Dao, *J. Phys. D. Appl. Phys.* **2017**, *50*, 215401.
[237] J. Wen, L. Q. Zhu, H. F. Qi, Z. Y. Ren, F. Wang, H. Xiao, *Org. Electron.* **2020**, *82*, 105782.
[238] S. Kim, C. Du, P. Sheridan, W. Ma, S. Choi, W. D. Lu, *Nano Lett.* **2015**, *15*, 2203.
[239] Z. Xiao, J. Huang, *Adv. Electron. Mater.* **2016**, *2*, 1600100.
[240] W. Hu, J. Jiang, D. Xie, S. Wang, K. Bi, H. Duan, J. Yang, J. He, *Nanoscale* **2018**, *10*, 14893.
[241] D. G. Seo, Y. Lee, G. T. Go, M. Pei, S. Jung, Y. H. Jeong, W. Lee, H. L. Park, S. W. Kim, H. Yang, C. Yang, T. W. Lee, *Nano Energy* **2019**, *65*, 104035.
[242] H. Shim, K. Sim, F. Ershad, P. Yang, A. Thukral, Z. Rao, H. J. Kim, Y. Liu, X. Wang, G. Gu, L. Gao, X. Wang, Y. Chai, C. Yu, *Sci. Adv.* **2019**, *5*, eaax4961.
[243] P. Gkoupidenis, D. A. Koutsouras, G. G. Malliaras, *Nat. Commun.* **2017**, *8*, 15448.
[244] D. A. Koutsouras, M. H. Amiri, P. W. M. Blom, F. Torricelli, K. Asadi, P. Gkoupidenis, *Adv. Funct. Mater.* **2021**, *31*, 2011013.
[245] Y. Yang, X. Zhao, S. Wang, C. Zhang, H. Sun, F. Xu, Y. Tong, Q. Tang, Y. Liu, *J. Mater. Chem. C* **2020**, *8*, 16542.

Fabrizio Torricelli received a D.Eng. degree with honors and a Ph.D. degree in Electronics Engineering from the University of Brescia (Italy) in 2006 and 2010, respectively. From 2010 to 2012, he was a Post-Doctoral Fellow at the Eindhoven University of Technology, Netherlands. He was a consultant of ST-Microelectronics. Since 2019, he is Associate Professor at the Department of Information Engineering, University of Brescia. His research interests include device modeling, design of new memory and transistor architectures in silicon, metal-oxide and organic emerging technologies, development of green and sustainable (bio)electronics and design and development of bioelectronic sensors.

Ivano Alessandri received his Master's in Chemistry from the University of Pavia (Pavia, Italy) and his Ph.D. in Materials Science and Engineering from the University of Brescia (Brescia, Italy). Since 2015, he has been Associate Professor of Chemistry at the same university. His research interests include the development of new materials for energy conversion and advanced diagnostics. In the past few years, he has been working on all-dielectric and hybrid metal/dielectric nanoarchitectures for light-trapping, SERS and catalysis.

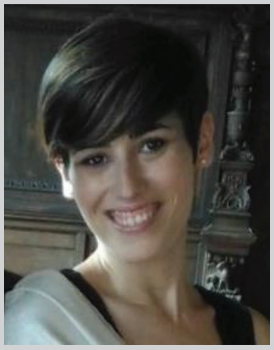

Eleonora Macchia is senior researcher at Åbo Akademi as PI of the project ProSiT-Protein Detection at the Single Molecule Limit with a Self-powered Organic Transistor for HIV early diagnosis, funded by Academy of Finland. She has been Postdoctoral fellow at University of Bari. She received her PhD in Chemical Sciences in 2018 from the University of Bari and her Master's degree in Physics in 2014.

Irene Vassalini is a researcher at the Department of Information Engineering at University of Brescia (Italy). She received a Master's in Chemistry, in 2013, from University of Pavia (Italy) and a Ph.D. in Mechanical and Industrial Engineering in 2017, from University of Brescia. Her research interests are related to the study of unconventional non-polymeric stimuli-responsive materials, optical antennas and nanosensors and photo-catalysts for the removal of pollutants from water, paying particular attention to the environmental sustainability of the developed systems.

Marina Maddaloni is a Ph.D. student at Department of Mechanical and Industrial Engineering at University of Brescia, Italy. She received a Bachelor's in Chemistry, in 2015, and a Master's in Chemical Science, in 2018, from University of Naples "Federico II" (Naples, Italy). At present, her research interests lie in the green production of waste-based nanostructured systems for sensing and removal of micro-pollutants in waters and soil and phytochemicals delivery, and development of nanostructured catalyst for the conversion of agricultural processing wastes into energy carriers and materials with high added value.

Luisa Torsi is professor of chemistry at the University of Bari and adjunct professor at Abo Academy University. She was post-doctoral fellow at Bell Labs in USA and was the first woman awarded with the H.E. Merck prize. Lately, she was awarded also with the Wilhelm Exner Medal 2021. Torsi has authored almost 200 papers, including some published in Science, and Nature Materials. Torsi is committed to the role-modeling for female scientists. She was featured in a story of the Italian comic series of Disney comics, as "Louise Torduck", a successful female scientist of the Calisota valley.